SCUOLA NORMALE SUPERIORE

PISA

STUDIES ON THE ASSEMBLY OF ROTAVIRUS' VIROPLASMS

(Thesis submitted for the degree of Doctor Philosophiae)

(Perfezionamento in Genetica Molecolare e Biotecnologie)

Academic Year 2008-2009

Candidate: **Roberta Contin**

Supervisor: **Dr. Oscar R. Burrone**

CONTENTS

LIST OF ABBREVIATIONS

3D	three-dimensional
aa	amino acids
ATP	adenosine triphosphate
bp	base pair
CPE	cytopathic effect
C-terminal	carboxy-terminal
DLP	double-layered particle
DMEM	Dulbecco's modified Eagle's medium
DMSO	dimethylsulfoxide
DSP	Dithiobis(succinimidylpropionate)
dsRNA	double-strand RNA
EDTA	ethylenediamine tetraacetic acid
EGFP	enhanced green fluorescent protein
EM	electron microscopy
ER	endoplasmic reticulum
ERGIC	ER-Golgi Intermediate Compartment
FCS	foetal calf serum
FITC	fluorescein isothiocyanate
GST	glutathione-S-transferase
HA	hemagglutinin
HIT	histidine triad
HRP	horseradish peroxidase
IFN	interferon
IPTG	isopropyl-β-D-thiogalactopyranoside
IRF3	Interferone regulatory factor 3
λ-PPase	lambda-phosphatase
MOI	multiplicity of infection
NSP	nonstructural protein
nt	nucleotides
N-terminal	amino-terminal
ORF	open reading frame

PAGE	polyacrylamide gel electrophoresis
PBS	Phosphate buffered saline
h.p.i.	Hours post infection
p.t.	post transfection
RdRp	RNA-dependent RNA polymerase
RITC	rhodamine isothiocianate
RNase	Ribonuclease
siRNA	small interfering RNA
sn	supernatant
ssRNA	single-strand RNA
TBS	Tris buffered saline
TLP	triple-layered particle
UTR	untranslated region
UV	ultraviolet
VLP	virus-like particle
VLS	viroplasm-like structures

ABSTRACT (1)

The processes that regulate Rotavirus replication are not fully understood and the lack of a reverse genetic approach represent an obstacle for the investigations in Rotavirus biology.
Viroplasms are cytoplasmic structures that form soon after infection, and constitute the site of virus replication. Structural proteins like the viral RNA-dependent RNA -polymerase VP1, the capping enzyme VP3, the scaffolding protein VP2,and the middle layer VP6 localize in viroplasms; in addition, also the non-structural proteins NSP5 and NSP2 have been demonstrated to be essential components for viroplasm formation. Following the characterization of the interaction between NSP5 and VP1, we characterized the relationships between NSP5 and the structural protein VP2.
In this work, interaction of NSP5 with VP2 was investigated by coexpression of the two proteins in uninfected cells, which resulted in a strong hyperphosphorylation of NSP5 and in the formation of viroplasm like structures (VLS). The behaviour of NSP5 in the presence of VP2 is very similar to that induced by NSP2 and already described (1), (60). Therefore, a comparison between the phosphorylation degree of NSP5 and VLS formation induced either by VP2 or by NSP2 was conducted.
In both cases VLS formation was shown to assemble independently of the phosphorylation degree of NSP5, and to recruit the viroplasm-resident proteins VP1. However, VP6 (the protein forming the middle layer of the virion) was shown to be recruited only into VLS induced by VP2 (VLS(VP2i)), while it remains organized in tubular structures when VLSinduced by NSP2 (VLS(NSP2i)) were formed. Attempts to coimmunoprecipitate NSP5 and VP2 failed both from infected and co-transfected cells. However, promising preliminary results were obtained with a recently isolated monoclonal Ab specific for NSP5.
Altogether, these data showed that two different viral proteins induced the same kind of modifications in NSP5, suggesting that these modifications may have a fundamental role for virus replication. Moreover, these data suggest that NSP5 plays a key role in architectural assembly of viroplasms and in recruitment of the other viroplasmic proteins.

1 INTRODUCTION (1)

In the 1960s Rotavirus was discovered in animals, and in 1973 was first described in humans, when electron microscopy images reveal its presence in duodenal biopsies of children with acute gastroenteritis (19). Subsequently it was recognized as the most important cause of severe, dehydrating gastroenteritis in infant and young children worldwide. About 600.000 children die every year from Rotavirus, with more than 80% of all rotavirus related deaths occurring in resource-poor countries in south Asia and sub-Saharan Africa. Rotavirus related deaths represent approximately 5% of all deaths in children younger than 5 years of age worldwide. Furthermore, recent studies indicate that rotavirus causes approximately 39% of childhood diarrhea hospitalizations worldwide. The burden of rotavirus infection is not limited to the less-developed countries. Studies from the western European found that 50% of cases of gastroenteritis in children younger than 5 years old that were hospitalized were caused by Rotavirus infection, and, moreover, that these infections caused 230 deaths per year. In the United States Rotavirus is estimated to cause 20-60 deaths, and 55.000-70.000 hospitalizations per years, with very high health and social costs consequences (75).

According to all these statistical studies on Rotavirus infection, an effective vaccine program is necessary. Fortunately, following initials problems with the first attempts to develop a vaccine, in 2006 two new Rotavirus vaccine were licensed in the United States, the Europe Union and in many countries in Central and South America. The effectiveness of these two vaccines is well documented and still under investigation, in particular postmarketing surveillance studies are monitoring the impact of vaccine on different circulating strains of rotavirus, according to geographic distribution and selection pressure (75).

Rotavirus biology has been extensively studied in these past decades, and some infection mecchanisms have been elucidated, however much need to be learned in Rotavirus replication. In particular the goal of a reverse genetic system would answer to different questions related to rotavirus replication and to the role of different viral proteins during rotavirus infection, in order to identify a unique viral target that might be useful in developing therapies.

1.1 VIRUS CLASSIFICATION

Rotavirus is a non-envelope double stranded RNA virus that belong to the family of *Reoviridae.* The term Rotavirus derived from latin word *rota*, which means wheel, according to the distinctive morphologic appearance at electron microscopic analysis (58).

The viral particle is large (1000 Å) and complex, it consists of three concentric protein layers (outer, intermediate, inner layer) surrounding the viral genome of 11 double strand RNA segments. The genome segments encode for 6 structural proteins (viral proteins, VPs VP1-4, VP6-7), that make up the virus particles, and 5 (or 6, depending on the strain) non structural viral proteins (NSPs, NSP1-5, NSP6) (58).

Rotaviruses are classified according to antigenic specificity. They are classified in groups, viruses of the same group share cross-reacting antigens serologically detected using monoclonal and polyclonal antibodies against VP6 (intermediate layer protein). Groups A-E have been clearly identified, two more groups F,G are likely to exist. VP6 mediates also subgroups specificity according to the exclusive reactivity of two VP6 specific monoclonal antibodies (subgroup I, and subgroup II).

The structural protein VP7 is the main component of outer layer, and it is associated with VP4, a structural protein that forms spikes that emerge from the VP7 shell. This particular organization induces neutralizing antibody responses that are the basis for the binary classification in serotypes mapping VP4, or VP7, and genotypes by sequence comparison, within each group. Serotypes determined by the glycoprotein VP7 are termed **G** (which stands for **g**lycoprotein) and those defined by VP4 are named **P** (which stands for **p**rotease-sensitive protein, which is the case for VP4). For VP7 classification, neutralization assays and sequencing yeld to concordant results, so viruses are refer to their G serotype alone (G1, G2, G3 and so forth). On the contrary, for VP4 classification, serotypes do not correspond to genotypes and a dual system for P typing is used. P serotype are referred to by their serotype number (P1, P2, P3 ecc) while P genotypes are denoted in brackets (P[1], P[2] ecc). P genotyping is the most widely used method, since it is difficult to standardize VP4 neutralization assays. Currently, 19G and 24[P] types are known.(57, 58, 75).

Recently, it has been proposed a rotavirus classification system for all the rotavirus genes that recognizes phylogenetic relationships and defines genotypes based on percentage identity cutoff values for each of the genes, which may have followed separate evolutionary paths. Such a classification system could be an important tool to elucidate how rotaviruses

evolve over time, to identify reassortment events and gene constellations shared by human and animal rotaviruses.(122)

1.2 VIRION STRUCTURE

The morphology of the complete rotavirus infective particle is peculiar, and by electron microscopy analysis it is possible to observe three types of particles in the cytoplasm of infected cells. The first type of particle is a triple-layered particle (TLP) that is the complete infective particle of about 100 nm in diameter and present a triple-layerd icosahedral protein capsid composed of an outer layer, an intermediate layer, and a inner core layer. The second type is the double-layered particle (DLP) formed when the outer layer of the TLP is missing, while the third type is the single-layered particle (or core) composed only by the innermost layer and seen infrequently, it lacks the genome and aggregates in the cytoplasm with other single-layerd particles (160) (210).

A particular characteristic of the virus structure is the presence of 132 large channels that extend over the two shells and link the outer surface with the inner core. Three types of channels (type I-III) can be distinguished based on their position and size (160).

The viral genome is packaged inside the inner core together with two viral proteins essential for viral transcription and replication: the viral RNA-dependent RNA-polymerase VP1 and the capping enzyme VP3 (140).

Herein a detailed description of virus structure is reported:

The outermost layer : the outer layer is mainly composed by the structural protein VP7 that is uniformly distributed and forms a smooth surface from which sixty spikes of VP4 hemagglutinin protein extend. VP7 is organized in trimers, with a total number of 780 VP7 molecules forming the outer shell organized in a T=13l (levo) icosahedral surface. The VP4 spikes is multi-domained with a radial length of about 200Å, and extend about 120Å from the surface of the virus. It interacts with two molecules of VP7 by extending inwards about 80Å into the virion outer layer, and inside it appears that VP4 interacts with six VP6 molecules that surround type II channel (209). The interaction between VP4-VP7 and VP4-VP6 implies that VP4 has a relevant role in maintaining the precise geometric organization between outer and middle capsids (210) (Fig.1A).

The intermediate layer : VP6 is the only component of the intermediate layer. 760 molecules of VP6 are arranged in trimers and localized in the local threefold axis of the

T=13 icosahedral lattice. VP6 trimers lie below VP7 trimers, so that the aqueous channel in the two T=13 layers are in register, and above the inner layer of VP2 (160). The VP6 molecule has two domains: the distal eight-stranded β-sheet domain core makes contact with the VP7 layer, and the lower α-elical domain that makes contact with the inner VP2 layer. The interacting surfaces (VP6-VP7 and VP6-VP2) expose the most conserved residues of VP6, suggesting that VP6 may play a major role in providing structural integrity to the rotavirus capsid. However, the lateral interactions between trimers that form the T=13 icosahedral organization, are not sufficient per sè to allow the closed shell. On the contrary, VP2 is able to form native like icosahedral shell, suggesting that VP2 layer provides a proper scaffold for the assembly of VP6 trimer into a T=13 icosahedral organization (210) (Fig.1A).

The innermost layer : the single layerd particle posses a T=1 symmetry and is composed of 120 VP2 molecules, arranged in dimers that surround the viral genome. VP2 protein interacts with both VP6 of the middle layer and the RNA genome, through the N-terminal residues that have RNA binding ability. N-terminal residues of VP2 are also involved in the anchoring to the inside surface of the VP2 layer, at the vertices of the icosahedral structure, heterodimer of RNA-dependent RNA-polymerase (RdRp) VP1 and capping enzyme VP3 (159). The RNA genome is well organized inside the core, as well. In particular the 25% of genome made internal dodecahedral structure in which the RNA double helices, interact closely with VP2 and are packed around the transcription complexes located at the vertices of the icosahedral structure. (Fig1B) (89)

The aqueous channels : in the mature infective particle there are three types of channels classified on the basis of positions and size. There are twelve type I channels located in the five-fold axes, sixty channels of type II at the six-coordinated position surrounding the fivefold axes, and sixty type III channels on the six-coordinated positions around the icosahedral three-fold axes. All three channels type are about 140Å in depth, and differ in width since type II and III reach 55Å in width at the outer surface of the virus, while type I channels are narrower (about 40Å) at the outer surface of the virus. In entering the viral particles, these channels constraints before to reach the maximum width, which is close to the surface of the inner shell. These channels are involved in importing the metabolites required for RNA transcription, and in particular type I channel in exporting the viral mRNA transcripts into the cytosol of the cells for subsequent viral replication processes (89).

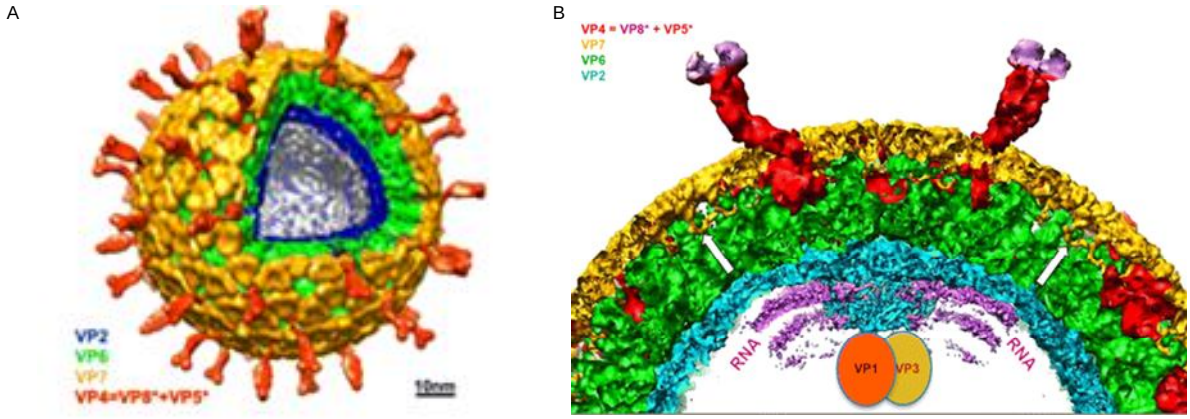

Figure 1: **Rotavirus structure determined by cryo-EM.** A) Cut-away view of the rotavirus TLP showing the outer layer (VP7 in yellow and VP4 in red), the middle layer (VP6 in green) and the inner layer (VP2 in blu). B) Cross-section of a rotavirus particle. The various protein components are colored as indicated in A). VP1 and VP3, the polymerase and mRNA capping enzyme, respectively, are anchored to the inside of the VP2 layer at the five-fold. White arrows show where the N-terminal arms of the outer-layer protein, VP7, clamp onto the underlying VP6. surrounding the enzymes VP1 and VP3 (in red), which (From Chen et al. PNAS 2009).

1.3 GENOME STRUCTURE AND ORGANIZATION

The viral genome consists of 11 segments of double stranded RNA, that range in size from 0.7 to 3.1 kB, and is enclosed inside the inner core of the virus. The viral segments are thought to be organized in the core with a dodecahedral symmetry: one copy of each segment interacts with one replication complex constituted by one molecule of RdRp VP1 and one of capping enzyme VP3 (159) (49).

The sequences from different rotavirus strains show common features in the structure of each segments (58):

- ✓ Segments are A+U rich (58% to 67%).
- ✓ 5'-methylated cap sequences $m^7GpppG^{(m)}GPy$, uncapped minus strand lacking a γ-phosphate.
- ✓ An open reading frame (ORF) that encodes the protein product of the gene, flanked by untranslated ragions (UTRs).
- ✓ A set of conserved consensus sequences (CS) at the 5'-3' UTRs.
- ✓ The last four to five nucleotides of the 3'CS[(U)GACC] can function as translation enhancer.
- ✓ There is no polyadenylation signal at the 3'-end of the mRNA segments.

The 5’ and 3’ UTRs of the 11 genome segments show considerable variation in length and sequence, this suggest that they are needed for their own translation and packaging. In contrast the UTRs of homologous segments are highly conserved among viruses belonging to the same group, in some cases more than the sequence of the ORF (142) (144).

In the case of group A rotavirus, that is the most important in term of human morbidity and mortality, the (+)strand RNAs of genome segments typically end with 5’CS, 5’–GGC(U/A)$_7$-3’, and the 3’CS, 5’-UGUGACC-3’ (49).

Computer modelling proposed that base-pairing in *cis* between 5’ and 3’ regions of mRNA, leads to the formation of panhandle structure from which the 3’CC extends in an un-paired tail (142),(34),(33). This stable structure allows the recognition by the viral RdRp that interacts with the 3’-CC and induces the formation of (–) strand initiation complex (145),(144). Indeed, the 3’-terminal CC have been shown to be crucial for the formation of the initiation complex of RNA replication (30),(32).

The 3’CS not only includes sequences that promote genome replication but also contains a determinant sequence required for efficient translation of rotavirus (+)RNAs. In particular the last four nucleotide of 3’CS [(U)GACC] are recognised by a dimer of the non-structural protein NSP3 (155),(154), that in turn is recognise by the eukaryotic translation initiation factor, eIF4GI (152),(151). This however, has been described below (see page 22).

Sequences enhancing replication are localized also in the 5’CS of the genome segments (145); however attempts to identify 5’-sequences recognised by the RdRp VP1 have been unsuccessful. It cannot be excluded that the 5’-recognition signals interact with VP1 or the core protein VP2, despite evidences from replication studies that the synthesis of (-)RNA depends on the interactions with viral protein of the replicase complex with both ends of viral segment (197). (Fig. 2)

The most interesting, and still obscure, aspect of rotavirus genome organization is related to the mechanisms that control replication and packaging of the 11 segments. Indeed the 11 segments should share similar cis-acting signals to be recognise and replicated by the same polymerase; moreover each segment should have a unique sequence signal in order to be distinguished from one another during the packaging. The packaging of the 11 dsRNA segments is mediated by a deep interaction between RNA and viral proteins. The viral proteins that participate in the encapsidation of the viral genome are still under identification. Obviously an important role is played by VP1, VP3 and VP2, but involvement of non-structural proteins is not to excluded (126), (58).

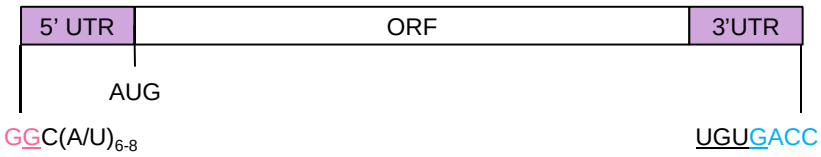

Figure 2: Schematic representation of a group A rotavirus plus-strand RNA. The conserved sequences at the 5' and 3' ends are indicated. Both sequences were shown to be essential for the formation of the minus-strand initiation complex. They are predicted to stably base-pair forming a panhandle structure. The dinucleotide GG indicated in purple is conserved within all groups of rotaviruses and the second G was shown to be essential for specific recognition by the polymerase VP1. Another recognition signal for VP1 is at the 3'UTR. Both signals are underlined. The sequence indicated in blue is a translation enhancer.

1.4 VIRAL PROTEIN

Although new functions for the different rotaviral proteins are continuously identified, their assignment with the 11 genome segments has been well established. The Rotavirus genome encodes for 6 structural proteins, that make up the viral particles, and 6 non-structural proteins, with exception of some strains that have 5 non-structural proteins, that are produced during the infection to maintain infective status.

The proteins of SA11, a simian strain, have been studied more thoroughly, since it was completed first and for this reason it is considered the strain of reference. The migration order/pattern of RNA segments could differ among different strain.

In figure 3 is reported the protein assignment to the different RNA segments of SA11 strain: RNA segments 1, 2, 3 encode for the core structural proteins VP1, VP2, and VP3; segment 6 encodes the middle layer viral protein VP6; segments 4 and 9 produce the outer layer proteins VP4, and VP7, respectively. The non-structural proteins NSP1, NSP2, NSP3, NSP4, are encoded respectively by segment 5, 8, 7, 10; while segment 11 encodes for NSP5, and in some strain in a different ORF for NSP6 (58).

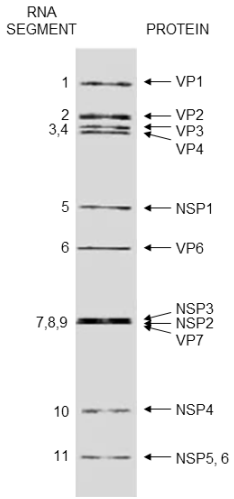

Figure 3: Gel PAGE of the 11 dsRNA segments of Roatvirus SA11. Genome segments are indicated on the left and the encoded proteins on the right.

Table 1 summerizes and describes all Rotavirus proteins with their functions and properties.

Genome Segment † Size [bp]	Gene Product(s)	Protein Size aa (Da)	Location in Virus Particle	Functions and Properties
1 (3302)	VP1 (Pol)	1088 (125005)	Inner capsid, 5-fold axis	RNA-dependent RNA polymerase ; Part of minimal replication complex ;Virus specific 3'-mRNA binding ;Part of virion transcription complex with VP3
2 (2690)	VP2 (T1)	881 (102431)	Inner capsid	Inner capsid structural protein;Non-specific ss & dsRNA-binding activity; Myristoylated;Cleaved; Part of minimal replication complex;Leucine zipper Interacts with VP5
3 (2591)	VP3 (Cap)	835 (98120)	Inner capsid, 5-fold axis	Guanylyltransferase ;Methyltransferase Basic Protein ;Part of virion transcription complex with VP1 ;Non-specific ssRNA binding
4 (2362)	VP4	776 (86782)	Outer capsid spike	VP4 Dimers form outer capsid spike;Interacts with VP6 ;Virus infectivity enhanced by trypsin cleavage of VP4 into VP5* and VP8* ;Hemagglutinin;Cell attachment protein ;P-type neutralization antigen ;VP5* permeabilizes membranes ,Crystal structure of VP8 fragment (galectin fold);TRAF2 signaling ;Protection
	VP5*	529 247-776 (60000)		
	VP8*	247 1-247 (28000)		
5 (1611)	NSP1	495 (58654)	Nonstructural	Associates with cytoskeleton;Extensive sequence diversity between strains Two conserved cysteine-rich zinc-finger motifs;Virus specific 5'-mRNA binding Interacts with host IFN regulatory factor 3
6 (1356)	VP6 (T13)	397 (4816)	Middle capsid	Major virion protein ;Middle capsid structural protein;Homotrimeric 4º structure Subgroup antigen ;Myristoylated ;Protection (? Mechanism) ;Crystal structure;Hydrophobic
7 (1105)	NSP3	315 (34600)	Nonstructural	Homodimer ;Virus-specific 3'- mRNA binding ;Binds eIF4G1 and circularizes mRNA on initiation complex;Involved in translational regulation and host shut-off ;Crystal structure: NSP3 NH_3 fragment with 3'- viral RNA and NSP3 COOH fragment with eIF4G fragment
8 (1059)	NSP2 (VIP)	317 (36700)	Nonstructural	Non-specific ssRNA-binding ;Accumulates in viroplasm ;Involved in viroplasm formation with NSP5 ;NTPase activity ;Helix destabilization activity ;Functional octamer ;Binds NSP5 and VP1;Regulates NSP5 autophosphorylation ;Crystal structure (HIT-like fold)
9 (1062)	VP7	326 [7368)	Outer capsid glycoprotein	Outer capsid structural glycoprotein;G-type neutralization antigen ;N-linked high mannose glycosylation and trimming ;RER transmembrane protein, cleaved signal sequence ;Ca^{2+} binding ;Protection ;
10 (751)	NSP4	175 (20290)	Nonstructural	Enterotoxin ;Receptor for budding of double-layer particle through ER membrane RER transmembrane glycoprotein ;Ca++/ Sr++ binding site ;N-linked high mannose glycosylation ;Protection ;Host cell $[Ca^{2+}]_i$ mobilization
11 (667)	NSP5	198 (21725)	Nonstructural	Interacts with VP2, NSP2 and NSP6;Homomultimerizes;O-linked glycosylation (Hyper-) Phosphorylated ;Autocatalytic kinase activity enhanced by NSP2 interaction Non-specific ssRNA binding
	NSP6	92 (11012)	Nonstructural	Product of second, out-of-frame ORF ;Interacts with NSP5 ;Localizes to viroplasm

Table 1: List of Rotavirus genes, relative proteins, functions and properties.

In the follow paragraphs, the viral proteins are described more in detail starting from the structural proteins that form the viral particle, in particular from the proteins inside the core in contact with the viral genome, towards those forming the middle and the outer layer. Subsequently the non-structural proteins are taken in consideration, classified in those involved in viral replication and those with different role in viral morphogenesis.

1.4.1 STRUCTURAL PROTEINS

The core:

VP1

VP1 is the viral RNA dependent RNA polymerase encoded by segment 1, and it functions as both, the transcriptase for mRNA synthesis, and the replicase for minus-strand RNA synthesis to generate genomic dsRNA.

VP1 crystal structure has been recently resolved, revealing that it is a compact protein of about 70 Å in diameter. Three distinct domains were identified: an N-teminal domain (aa 1-332); a polymerase domain consisting in finger, palm, and thumb subdomains (aa 333-778) and a C-terminal "bracelet" domain (aa 779-1089) (118) (Fig.4).

N and C-terminal domains surround most of the polymerase domain creating a sort of cage with a large hollow center.

The polymerase domain has the six canonical motif A-F that are also present in RdRp of other viruses like reovirus λ3 (187), bacteriophage φ6 P2 (25), hepatitis C virus NS5B (3). The palm subdomain consists of three helices that support the four-stranded antiparallel β-sheet and includes the conserved residues of the active site.

The finger subdomain comprises one side of the template entry tunnel, and has a three dimensional arrangement that is different of that observed for *reovirus* polymerase λ3. The thumb subdomain consist of a β-strand followed by three α-helices, a loop at the tip of thumb interacts with the tip of finger domain enclosing the catalytic site on the palm of the polymerase domain, and maintaining VP1 in a closed conformation (118).

The closed conformation is reinforced by the N-terminal domain that covers one side of the active domain, while C-terminal domain is situated around the exit tunnel for the dsRNA product of replication and for the minus RNA template of transcription. In particular aa1072-1089 form a α-helical plug that extend into the template tunnel and reduces its diameter, so it is necessary to remove the plug for the exit of dsRNA (118).

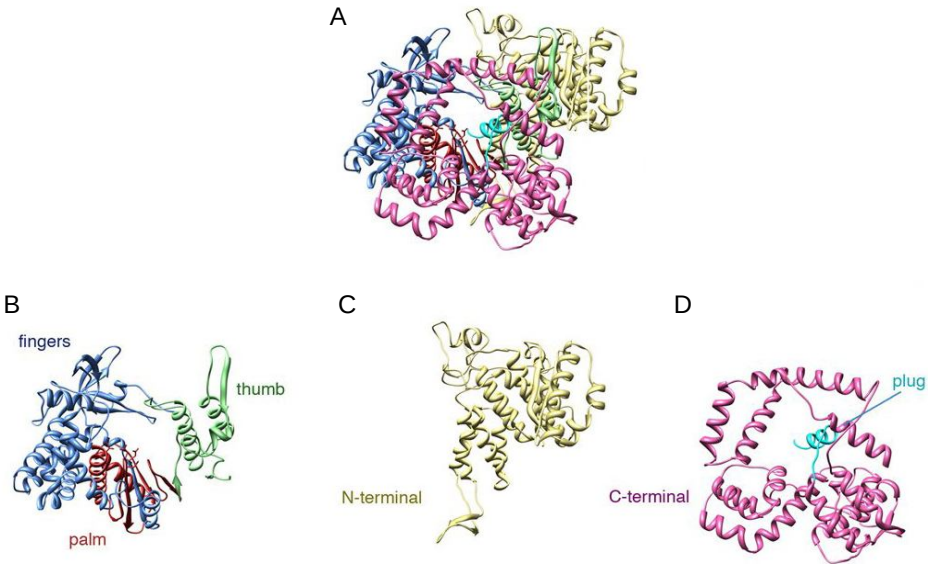

Figure 4: **Structure of the RdRp VP1.** A)Ribbon diagram of the entire polypeptide chain. B) The fingers, palm, and thumb subdomains of the polymerase in blue, red, and green, respectively. C)The N-terminal domain is in yellow. D) the C-terminal bracelet domain, in pink; the C-terminal plug, in cyan. (118)

VP1 polymerase (separated by gradient centrifugation from the other components of open cores VP2 and VP3), when incubated alone with plus strand RNA does not show any replicase activity, indicating that the enzyme alone is an inactive form of the viral RdRp. However, when VP1 is incubated with (+)RNA and the core protein VP2, the synthesis of dsRNA activity takes place, proving that VP2 induces the conversion to the active form of VP1 (136). The ratio between VP1 and VP2 is also critical to obtain the maximal replicase activity. Stoichiometric analysis have demonstrated that the optimal ratio VP1:VP2 is 1:10 which is the ratio present at the vertices of rotavirus core. This suggests that not only the presence of VP2 is required to have an active polymerase but also that VP1 has to be collocated into a precise structure that is the pentamer unit of the core (141).

Electrophoretic mobility shift assays have shown that VP1 has a strong affinity for viral (+)RNAs due to the recognition of sequence signals located near the 3-end of RNAs. According to these assays it has been proposed a multistep interaction between the polymerase and (+)strand RNA: VP1 recognises the UGUGA sequence at 3'CS of (+)RNA in a VP2-independent manner, then VP1/+RNA complex interacts with VP2, (involving its N-terminal domain) that induces a conformational change on VP1 leading to the interaction with 3'CC portion to form the initiation complex. This model however does not take in consideration the requirement of VP2 also during the elongation step of (-)RNA synthesis.

In addition, VP1 also interacts with other protein and in particular with the virus non-structural protein NSP5 and NSP2. (see NSP5 paragraph, page 25)

Interaction with NSP2 has been demonstrated by co-immunoprecipitation assays from infected and trancfected cells (96).

VP3

VP3 is the structural protein encoded by genome segment 3. It is the minor component of the virion core, there are 11-12 molecules per particle, and several studies provided evidences that VP3 is the viral guanylyltransferase, responsible for the capping of viral mRNAs. The protein has the intrinsic ability to bind GTP molecule in the absence of other viral proteins (31). Moreover, it has been demonstrated that VP3 has specific ability to bind ssRNA but no dsRNA, and also its 5' capping activity was also shown to be non specific (138). VP3 interacts with the N-terminal of VP2 together with VP1 and the RNA segment, and is an essential components of trascriptase complex, but not of the replicase one, since baculovirus expressed core like particles composed only by VP1 and VP2, still possess replicase activity (141).

In addition to the capping function, VP3 seems to have another distinct role in the formation of replication intermediates, revealed by the analysis of mutants with a *ts* lesion in VP3. Thus it is supposed that VP3 would increase the rate of VP1-VP2 complexes assembly into replicase particles (201),(141).

VP2

The structural protein VP2 is the main component of the inner core of the virus. The core is made up by 120 copies of VP2, with two molecules of VP2, named VP2A and VP2B, in the icosaedral asymmetric unit. A recent CryoEM analysis for the identification of secondary structures revealed the presence of 28 distinct α-helices and four β-sheet, where the α-helices are well distributed in the structure, while three of the four β-sheet are located in the lower part of the protein. VP2 shares common features in secondary structure with other viral inner core proteins like blutoungue VP3 (95). One characteristic feature of Rotavirus VP2 is helix 1, located at the the N-terminus, that is not present among other reovirus inner capsid proteins, and that extends towards the fivefold vertex and crosses over to an adjacent VP2 molecule. At the end of helix 1, another helix (helix 0) can be seen to cross underneath VP2, towards the fivefold vertex where it may interact with the transcription enzyme complex. However the resolution of this analysis does not permit to assign the helix to one or the other molecule of the dimer. Moreover interaction between

VP2 and VP6 layer has been resolved. Since there is a symmetry mismatch between VP2 and VP6 layers, different interactions between VP6 trimers and VP2 dimers have been described. In particular, the VP6 trimer that surround type I channel near the fivefold axes contacts the apical domain of both VP2A and VP2B; the VP6 trimer located at the threefold axes and near to type three channel makes contact only with VP2B; and other three VP6 trimers that surround the type II channels contact VP2A and/or VP2B. All these interactions strongly stabilize the double layer particle (112) (Fig.5).

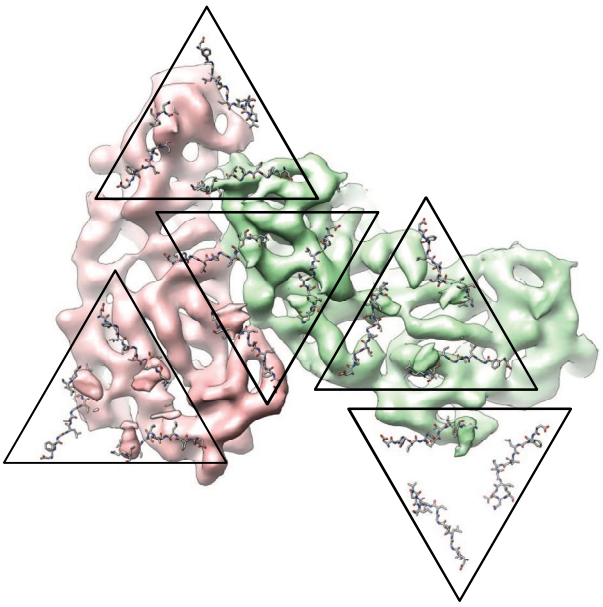

Figure 5: VP2 pentamer (A) VP2A (pink) and VP2B (light green) subunits in the icosahedral asymmetric unit are shown. The VP6 trimers that sit atop VP2 subunits are indicated by triangles. The VP6 residues, as deduced from fitting of the VP6 crystal structure, that interact with VP2
are shown (112).

By analsysis of baculovirus-expressed recombinant proteins, it has been demonstrated that N-terminus of VP2 is required for the binding of VP1 and VP3, however, the synthesis of rotavirus dsRNA *in vitro* is sufficiently supported by particles formed by VP1 and VP2 (141). The N-terminal domain of VP2, contains also the RNA-binding domain and binds ssRNA more efficiently than dsRNA. This difference would have an important role during transcription, allowing the dsRNA genome able to move and to be read from VP1. Moreover, the low affinity of VP2 for dsRNA reveals that VP2 does not have a dominant role in the packaging of viral genome and involvement of other viral protein occurs (105). The VP2 N-terminal domain has also a structural role (as already describe): it contains the α-helix1 that stabilizes the VP2 dimer allowing the pentamer organization (112).

A weak interaction between VP2 and NSP5 has been reported in both mammalian infected cells and in transfected insect cells (18). The description of the interaction between NSP5 and VP2 will be discussed in this thesis.

The middle layer:

VP6

VP6 is the most abundant protein of the viral particle. It is the main constituent of the intermediate layer of the triple layerd particle, in particular 780 molecules of VP6, organized in trimers surround the VP2 core with a icosahedral symmetry. VP6 integrates two principal functions of the virus: cell entry and transcription since it interacts with both, the components of the outer layer and with VP2, the core of the virus.

VP6 has two domains: an eight-stranded β-sheet domain that interacts with VP7 layer, and a cluster of α-helices that make contacts with the inner VP2 layer. The trimers of VP6 interact laterally to form the icosahedral structure and this contacts involved charged residues. The interacting surface with the other components of the triple layer particle involves conserved residues of VP6, the contacts with VP2 and VP7 involves principally hydrophobic residues. Although VP6 have the capacity to form trimers, stabilized by a Zn ion, it does not have the information to organize the different trimers into a closed shell. Indeed, when expressed alone VP6 easily forms helical tubes in the cytosol. So, the correct assembly of the middle layer is driven by the core, since VP2 alone has all the information to form native icosahedral shell around which VP6 trimers organize (Fig.5) (89).

Earlier biochemical studies revealed that none of the component of the DLPs are able to transcribe alone the viral genome, and that VP6, althought does not have any enzymatic activity, is essential for endogenous transcription. This hypothesis was confirmed using mutants, with an extra charge in the VP6-VP2 interface, that does not rescue the transcriptase activity of the reconstituted DLPs (29). Moreover, it has been observed that interfering with the conformational changes near the VP6-VP2 interface using monoclonal antibody (MAb) against VP6, affects viral transcription (192). A conserved β-hairpin motif of VP6 extends inside a type I channel, used by the newly transcribed mRNA to exit the DLPs, and may play a role in the translocation of the mRNA. This suggests that the dynamics of VP6 itself and in the VP2-interface have an important role in mRNA viral transcription.

During rotavirus replication, VP6 is found in viroplasms, that are electrondense structures that form soon after infection and are the putative site of viral replication and core assembly. VP6 has active role in virus assembly, probably through the interaction with

NSP4, which may facilitate association to core particles, to form DLPs, during the exit of core particles from viroplasm (117).

The outer layer:

VP7

VP7 is the main component of the outermost layer of rotavirus particles. It is a glycoprotein of about 38 KDa, that forms a smooth capsid where VP4 spikes associate. The shell has 760 copies of VP7 organized in 260 trimers with an icosahedral symmetry. The trimers are stabilized by two Ca^{2+} ions, bound at each subunit interface. The core of each subunit folds into two compact domains, a Rossmann fold domain (domain I) and a jelly-roll β sandwich (domain II), with disordered N and C-terminal arms. The arms extend away from the compact core; the N-terminal arm moves towards the centre along the surface of VP6 subunit, so that the three arms of the VP7 trimer grip the VP6 trimer (Fig.1), and it is also involved intra-trimer contacts. The C-terminal arm of one subunit interacts with its counterpart of the other subunit, but most of its contacts appear to be within its trimer of origin (4, 35).

VP7 is involved in the entry of the virus into the cell by modulating VP4 rearrangements during attachment and penetration of the viral particle. While the appropriate levels of calcium help in maintaining the structural integrity of the VP7 layer, low calcium concentrations trigger VP7 conformational changes and subsequent dissociation of VP7 trimers (51). Since VP7 shell stably locks the spikes in the assembled virion, VP7 trimers dissociation would precede VP5* rearrangements, in order to promote virus penetration into the host cell .

According to measurement by cryo-microscopy the VP4 spikes located inwards the type II channels, have a diameter of 70Å, that fits more with the diameter of type II channel at the surface of VP6 layer (78Å) respect to that of VP7 layer (54-58Å). This suggest that, during the assembly of the virus, the spikes should first anchor to the VP6 layer about at the type II channel and then VP7 trimers would subsequently arrange above VP6 trimers to form stable triple layer particle (112).

VP7 has been identify as the viral protein that interacts with integrins. In particular, after the initial binding mediated by VP4 with sialic acid and integrin $\alpha 2\beta 1$, VP7 is prompted to interacts with $\alpha X\beta 2$ and $\alpha v\beta 3$ integrins, and mediates the entry of the virus probably through an endocytic pathway (73). The low calcium concentration inside the endocytes may favour VP7 trimer dissociation and subsequent uncoating of TLPs to release DLPs.

During Rotavirus infection VP7 is localized in the ER where the virus morphogenesis is completed. It is found in the transient enveloped particle that the DLPs acquire in the budding process into the ER, together with NSP4 and VP4 (117). Silencing of VP7 induces accumulation of enveloped particles in the ER, a phenotype similar to depletion of calcium, suggesting that in order to displace the transient membrane surrounding the DLP, VP7 needs to trimerize (123).

VP4

VP4 is encoded by segment 4, and is one of the two constituents of the outermost layer. It has an important role in virus attachment and entry into the host cell. Association of two or three, molecules of VP4 forms spikes that protrude from the smooth VP7 shell, and are located at the level of type II channels.

VP4 spikes are characterized by a globular domain that forms the head of the spike, and a central domain that forms the central body of the spike. Moreover, the spikes are anchored to a globular base that has been demonstrated to be part of VP4, and is linked to the central bodies with an elongated bridging domain (158).

In order to induce the attachment and penetration into the host cell VP4 needs to be cleaved by trypsin. The cleavage products are the globular domain (VP8*) that is involved in virus attachment, and the central body (VP5*) that is thought to mediate cellular penetration. Both the cleavage products remain associated to the viral particles.

Recently cryo-EM analysis gave evidence that spikes have both dimeric and trimeric structures.

VP5* is a well-ordered homotrimer with a C-terminal α-helical triple coiled-coil, and a N-terminal globular domain. Each globular domain packs in a groove between the α-helices of the other two subunits. The globular domain of VP5* have a core of eight stranded anti-parallel β-sandwich, with two functional important β-hairpin: one stabilizes the globular structure, while the other is involved in the rotavirus binding to the $\alpha 2\beta 1$ integrins (52).

VP8* is the head of VP4 protein, and is attached to the central body by about 25 amino acidic residues non structurally defined. However, hydrophobic interaction between VP5* and VP8* are present, as well. The central structural feature of VP8* domain is an 11-stranded anti-parallel β-sandwich formed from a five-stranded β-sheet, and a six-stranded β-sheet with an interrupted top strand. The domain contained other structural elements like: intersheet loop containing a short α-helix, a longer α-helix at the c-terminus, and a β-

ribbon. All these elements with a dense hydrophobic core between major structural elements suggest a rigid structure that does not undergo structural rearrangements during virus entry. Between the two β-sheets lies the sialic acid bindig site, since rotavirus have a sialic acid-dependent mechanism to enter the host cell (53).

The spikes extend inward into the type II channels making contacts with VP7 trimers , and are anchored to the globular base located between the VP7 and VP6 layers. The base present a strong threefold symmetry with both α-helices and β-sheets secondary structures, and make symmetrical contacts with three trimers of VP6 (112).

Image reconstruction from electron cryomicroscopy of rotavirus particle have provided evidence that VP4 is subjected to a series of rearrangements, upon trypsin treatment, that allow the entry of the virus into the host cell. Before the processing by trypsin, the spikes are flexible structure visible by cryo-EM. Following trypsinization VP4 spikes are stabilized inducing a disorder-to-order transition, not shown for other viruses. The hypothesis is that, following trypsinization, they assume a dimeric appearance leaving the third subunit flexible, which, following an unknown triggering event, folds back to the dimer forming the trimeric structure and promoting cell membrane penetration and virus entry. VP8* is thought to dissociate from VP5* before o during the folding back rearrangment. (211). (Fig.6)

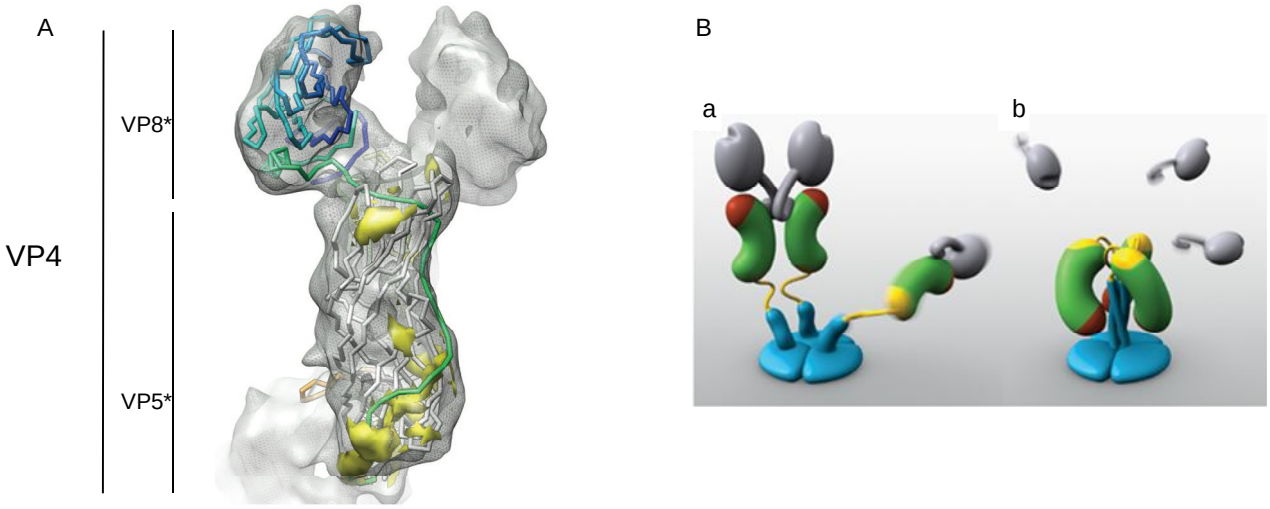

Figure 6: Structure of VP4 spike. A) Fitted VP8* and VP5*-t secondary structures are shown in the cryoEM density map of one of the dimeric subunits of the VP4 spike. The polypeptide chain is colored from the N (blue) to C (red) terminus. (112). B) Models of two VP4 conformations. (a)Two subunits form the spike visible in electron cryomicroscopy image reconstructions of trypsin-primed virions. A third subunit is flexible. VP8* is gray, the VP5* antigen domain is green bean-shape, with a red membrane interaction region and a yellow GH loop, the foot is blue, as is a protruding region that rearranges into the coiled-coil. Following trypsinization two of three spike dimerize living the third subunit flexible. (b)The putative post-membrane penetration state. Unknown trigger events induce VP8* released; the yellow parts of each subunit have joined in a -annulus; the -helical triple coiled-coil has zipped up; and the VP5* antigen domain has folded back. The models were produced by Digizyme, Inc. (211)

After the initial contact, which is mediated by VP8*, a second interaction with integrin $\alpha 2\beta 1$ occurs. This interaction is mediated by the integrin binding motif DGE present in the β-hairpin motif in the globular core of the VP5*. Moreover, VP5* is likely to be involved in binding to integrins $\alpha 4\beta 1$ and $\alpha 4\beta 7$ through its peptide sequence YGL (72, 74). Additional interactions in a post-attachment step, involving also VP7, occur and bind heat shock protein 70 (Hsc70) and other integrins $\alpha v\beta 3$ and $\alpha x\beta 2$ (76).

The role of VP4 during viral morphogenesis remains unclear. VP4 has been found at the plasma membrane associated to microtubules, and also detected in filamentous arrays. Infected cells treated with siRNA against gene4 still form viral particles, suggesting that VP4 is not essential for virus assembly or release of DLPs from the ER. More interestingly, the use of siRNA against gene 4 allowed to detect two different pools of newly synthetized VP4 inside the infected cells: one pool that rapidly associates with rafts at the plasma membrane and a second that associated with viral particle at the ER (45).

Within VP4 and in particular the N-terminal VP8* cleavage product, it has been identified a conserved TNFR-associated factor (TRAF) binding motif, that permits to bind TRAFs, a member of the family of adapter proteins involved in transducing signals generated by

ligands of Tumor Necrosis factor (TNF), and NF-κB transcription factor . This permit VP4 to direct NF-κB activation and the cellular response to viral invasion (106).

1.4.2 NON-STRUCTURAL PROTEINS

Essential role in virus replication cycle:

NSP2

NSP2 is protein of about 35KDa encoded by segment 8 of SA11 Rotavirus genome. Crystallographic analysis showed that the monomer consists of two domains, and it is organized in tetramer, that self-interact head-to-head to form a donut-shaped octamer with a central hole of about 35Å and deep grooves lined by basic residues at the periphery. NSP2 octamer possesses multiple activities: it binds ssRNA non-specifically and cooperatively, it has helix-destabilizing activity that is Mg^{2+} and ATP-independent (190); it has an associated Mg^{2+}-dependent nucleoside-triphosphate phosphoidrolase (NTPase) activity and hydrolizes all four NTPs to NDP and P_i (188). Interestingly the NTPase activity of NSP2 is associated to NSP2 phoshorylation transiently expresses *in vivo*. Since no phosphorylated NSP2 is found in infected cells, the phosphate group generated from hydrolysis of NTPs would rapidly transferred from NSP2 to another viral protein or removed by cellular phospahatases (191). The NSP2 monomer has two distinct domains (C-terminal, N-terminal domain) separated by a deep cleft involved in the biding and hydrolysis of NTPs. The C-terminal domain has a prominent twisted anti-parallel β-sheet flanked by α-helices that exhibits a HIT (histidine triad)-like motif, that is common among nucleotidyl hydrolases (90). In NSP2 the three histidine and a cluster of basic residues at the base of the cleft are probably involved in NTP binding and hydrolysis. In particular H225 was proposed as the catalytic residue of NSP2 since mutants H225A failed to promote dsRNA synthesis, without affecting viroplasm formation and the octameric structure of NSP2. This suggests that the triposphate activity is localized in the HIT motif and is involved in viral genome replication (104) (189) (Fig 7).

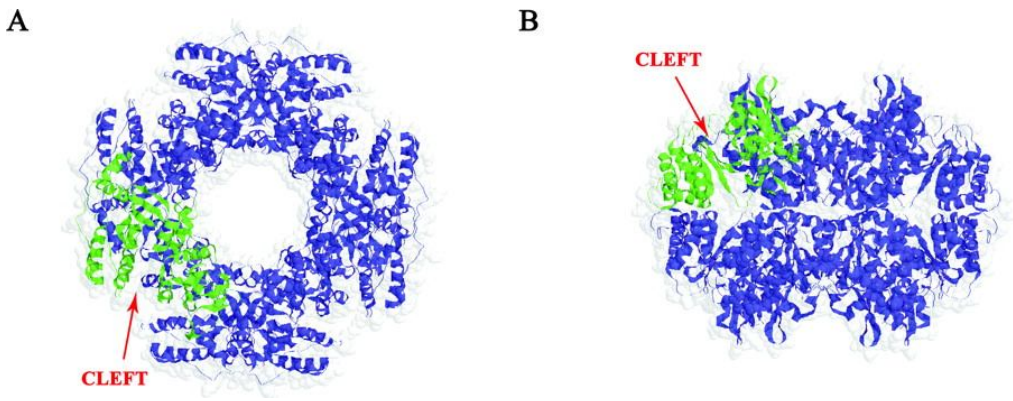

Figure 7: **NSP2 octamer**. *A)* and *B)*, ribbon representation of the NSP2 octamer superimposed on a space-filling model. The 25-Å-deep cleft between the C- and N-terminal domains of one NSP2 monomer (*green*) oriented along 4-fold (*A*) and 2-fold (*B*) axes is indicated. Three histidines and a cluster basic residues at the base of the cleft are probably involved in NTP binding and hydrolisis.(200)

The N-terminal domain of NSP2 is mainly composed of α-helices and it is possible to distinguish two sub-domains separated by a 24-residues basic loop. This loop lines the grooves that form on the surface of the octamer and, based to the concentration of charged residues at this level, they are supposed to be the site of ssRNA binding (191). At the same time, the loop exposed the electropositive residues at the entrance of the cleft that contains the HIT-like motif. The close proximity of grooves and clefts, allows the 5'-triphosphate end of the ssRNA, bound to the groove, to accommodate in the cleft where the HIT-like motif directs the cleavage of the γ-β phosphoanhyidride bond at the 5'end of ssRNA. Thus, NSP2 protein shows an additional activity that is the RNA triphosphatase activity (RTPase) that utilizes the same HIT-like motif of the NTPase activity producing indistinguishable phosphorylated intermediates (200).

The binding of ssRNA, the helix-destabilizing activity, and the NTPase activity suggest that NSP2 might function as a motor that uses the energy derived from NTP hydrolysis to drive rotavirus dsRNA replication and packaging. In fact, *in vivo* complementation experiments revealed that the synthesis of dsRNA does not proceed without the hydrolysis of NTPs, despite formation of viroplasms. Thus, once the sub-cellular sites for replication and virus assembly form, NTPase activity of NSP2 takes place. It is been proposed that binding of nucleic to the cleft of the protein induces a structural rearrangements of NSP2 octameric structure, from a relaxed conformation to a more compact one, involving the ssRNA binding groove that allows the interaction with the 5'γ-phosphate of mRNA, switching from NTPase to RTPase activity, and to initiate of viral replication (189),(200).

The localization of NSP2 in viroplasms, where the replication and the packaging take place, is not surprising since it accumulates in a environment that contains the substrates

for both NTPase and RTPase activities. In particular, in the presence of RNA substrates, as in viroplasms, the RTPase activity would be anticipated inducing the switch from NTPase to RTPase that is an activity directly link with genome replication, traslocation and packaging. Early studies demonstrated the interaction of NSP2 with the viral RdRp VP1, VP2 and with partially replicated RNA, suggesting the active role of this protein in viral replication. This was further confirmed using siRNA specific for NSP2, that causes a complete inhibition in viroplasms formation, viral protein production and viral genome replication (180).

Interestingly, experiments preformed in transfected cells, revelead that NSP2 interacts with NSP5, leading to the formation of structures that resemble viroplasms of infected cells, named viroplasms like structures (VLS) where both proteins co-localize (60). This interaction has been demonstrated also with co-immunoprecipitation assays from both infected and co-trasfected cells. Moreover NSP2 has been demonstrated to induce NSP5 hyperphosphorylation, however VLS formation and NSP5 hyperphosphorylation appear not related events (1). However, part of this aspect is discussed in this thesis.

NSP5

NSP5 is encoded by the segment 11 of Rotavirus genome. It is a protein of 196-198aa with a high content of serine (21%) and threonine (4.5%). The protein is produced soon after the viral infection and initially was described as a protein of 26 kDa. Further studies showed that it is subjected to different post-translational modifications that involved both O-glicosylation and hyperphosphorylation, that, following Western blot analysis, is possible to separate into different isoform with two main bands at 26 and 28 kDa and a series of higher molecular weight bands spanning from 30 to 34 kDa.

Cytoplasmic O-glycosylation occurs by the addition of O-linked monosaccharide residues of N-acetylgluocosamine (O-GlcNAc) to serine or threonine residues of cytoplasmic or nuclear proteins. In particular O-GlcNAc of NSP5 occurs in both the 26 and 28 kDa forms of the protein, since N-acetylglucosaminitol was released from both isoforms following β-elimination (67). The higher molecular weight isoforms showed almost no glycosylation. Indeed, in infected cells both the isoforms are labelled with [^{3}H]glucosamine that is released upon β-elimination, indicating that the 26 kDa isoform is not the first product of gene 11, and the protein is subjected to O-GlcNAc soon after its translation. This suggests that the O-Glcycosilation event would protect NSP5 from degradation and, since NSP5 is subjected to phosphorylation, it could also regulate the phosphorylation events (67).

The hyperphosphorilation events, involving NSP5, are not well clarified and still under investigation. Western blot analysis of extracts of infected cells treated with phospatases shows a disappearance of the higher molecular weight bands and the accumulation of the band at 26 kDa, confirming that the isoforms at higher molecular weight are due to hyperphosphorylation events during Rotavirus infection (2).

However the band at 26 kDa is still phosphorylated indicating that some of the phosphorylation sites are resistant to phosphatase treatment. The phosphorylation involved residues of serine and threonine as demonstrated by partial acid hydrolysis of NSP5 and a two-dimensional thin-layer electrophoresis of the obtained phospho-aminoacid (2). (Fig.8)

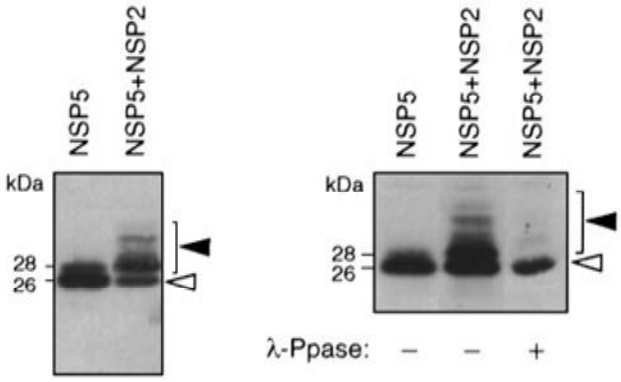

Figure 8: Hyperphosphorylation of NSP5 induced by NSP2. Anti-NSP5 Western immunoblot of cellular extracts of MA104 cellstransfected with pT7v-NSP5 or co-transfected with pT7v-NSP5 and pT7v-NSP2, as indicated. Where indicated, k-Ppase treatment of the extract was performed beforePAGE. Open and closed arrowheads indicate the NSP5 26 kDa precursor and phosphorylated forms, respectively (1).

NSP5 is able to multimerize, and the multimerization involved the C-terminal domain of the protein that have a predicted α-helical structure, since NSP5 deletion mutants lacking the last 10aa, or the last 18aa, are not able to multimerize (195).

Several studies report that NSP5 has a low level of autokinase activity (56), that in any case is not sufficient to produce the higher molecular weight isoforms of the protein. In particular, a Mg^{2+}-dependent triphosphatase activity of NSP5 has been identified and the N-terminal or C-terminal, or both, of NSP5 influence this activity. The triphospatase activity lead to the formation of γ-P_i products that could be released as free γ-P_i, or used to produce low-level of autophosphorylated protein as detected by in vitro phosphorylation assays in the presence of [γ-^{32}P] ATP (2), (12). These data suggest that other viral and/or cellular protein as phosphatases or kinases, would be necessary to obtain the hyperphosphorylated form of NSP5.

The NSP5 hyperphosphorylation has been proposed to be up-regulated by NSP2, an hypothesis supported by different observations: the *in vivo* hyperphosphorylation of NSP5 when it is co-expressed with NSP2 in uninfected cells (1); and the *in vitro* hyperphosphorylation when purified recombinant NSP5 and NSP2 are incubated in a phosphorylation assay. Moreover, it has been demonstrated a physical interaction between NSP5 and NSP2 by co-immunoprecipitation assays from both infected and co-trasfected cells. This interaction involves the N-terminal region of NSP5, and it is reinforced when both proteins are bound to RNA. This is suggested by UV treatment experiments, that allows RNA to crosslink to NSP2 (96) conferring a conformation that facilitate the interaction with NSP5 (1).

Recent studies have proved that NSP5 dimerized (in particular residues 66-188 are sufficient to drive the dimerization) and four dimers are able to interact with one NSP2 octamer, near the grooves, to form a stable complex detectable by cryoelectron microscopy (91). The mechanism that drive the hyperphosphorylation of NSP5 mediated by NSP2 is not known. One possibility is that the interaction between the two proteins induce conformational changes in NSP5 dimer that induce the activation of its (auto)-kinase activity. Alternatively, the fact that the dimer binds the groove of the NSP2 octamer, near its catalytic cleft, raised the hypothesis that the NTPase/NDP kinase activities of NSP2 could provide the phosphate moieties for NSP5 low (auto)-phophorilation (195) (202). This, however was not shown to be the case since NSP2 mutants that are NTPase defective induce NSP5 hyperphosphorylation (28).

Attempts to map the regions involved in the hyperphosphorylation of NSP5 led to the identification of Ser67 as the residue responsible for initiation event of hyperphosphorylation. In particular, phosphorylation of this residue, more likely due to a cellular kinase, is the first step of a hierarchical process that leads to NSP5 hyperphosphorylation. Moreover it has been observed that Ser67 is localized in a consensus region for casein kinase I α (CK1α) phosphorylation. Indeed, in vitro phosphorylation assays with recombinant CK1α, show phosphorylation of NSP5 wt, but no phosphorylation for a mutant NSP5, in which Ser 67 in mutated into Ala. (54).

The involvement of cellular CK1α in NSP5 hyperphosphorylation has been investigated using a small interference RNA specific for CKIα. In particular the role of this kinase has been studied in the contest of the infection and co-expression of NSP5 and NSP2. In both cases, silencing of CK1α affected NSP5 hyperphosphorylation (26).

NSP5 has shown to be localized in viroplasms during rotavirus infection. More interestingly, recombinant NSP5 expressed in cells together with NSP2 induce the formation of particular structures resembling viroplasm of infected cells and for this reason called viroplasm like structure VLS (60). NSP5 and NSP2 have been found co-localized into VLS, and, although the interactions between $NSP5_{66\text{-}188}$ and NSP2 has been characterized, the arrangements of the complex NSP5 dimer-NSP2 octamer to form VLS have not been identified, probably due to the lacking of NSP5 C-terminal region. However, it is has been proposed that C-terminal region of NSP5 in one NSP5-NSP2 complex may operate as a multimerizing domain, interacting with the C-terminal region of another NSP5-NSP2 complex. Since other reports show that also the N-terminal domain of NSP5 is involved (127), it is possible that a multi-step mechanism involving different regions of NSP5 controls NSP2-NSP5 interaction within VLS (195).(Fig 9)

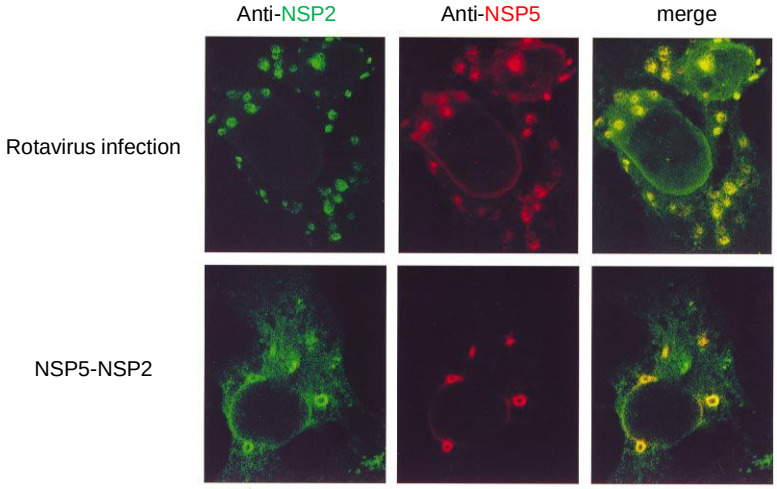

Figure 9: VLS formation. Confocal immunofluorescence microscopy of cells co-expressing NSP2 and NSP5. (*a)* MA104 cells, either infected with rotavirus SA11 or co-transfected with NSP2 and NSP5 as indicated, were reacted simultaneously with anti-NSP2 (green) and anti-NSP5 (red). The rightmost panel is a superimposition of the two independently acquired images.

Several evidences showed that hyperphosphorylation of NSP5 is not related to VLS formation: i) NSP5 mutants with Ser67 mutated into alanine, that are not phosphorylated when expressed with NSP2, still form VLS (54); ii) *in vivo* inhibition of phosphatases in cells transfected with an NSP5 encoding plasmid results in a fully phosphorylated NSP5, but not in VLS formation (20) ; iii) an siRNA against CK1α, the kinase involved in the phosphorylation of serine 67, inhibits NSP5 hyperphosphorylation, but not viroplasm formation (26). This observations are presented in results1 of this thesis.

Silencing the NSP5 expression in infected cells, with specific siRNA, abolishes viroplasms formation, indicating an important structural role of NSP5 during rotavirus infection.

Moreover, knocking down NSP5 in infected cells inhibits the accumulation of other viral proteins. Indeed the lack of viroplasms, as consequence of silencing NSP5, determines the inhibition of the assembly of new DLPs and the production of mRNA as a consequence of the secondary transcription. It has also been observed an inhibition of replication, revealing the relevant role of NSP5 in viral dsRNA production (27). This role was also supported by co-immunoprecipitation assays from infected and trasfected cells that showed that NSP5 strongly interacts with viral polymerase VP1. In particular, the last 48aa of NSP5 are involved in the interaction with VP1, and since the C-terminal region of NSP5 is also involved in dimerization, it is possible that a dimeric NSP5 is required for the association to VP1, with the binding region located just up-stream of the C-terminal tail. Moreover, this interaction is not weakened by the interaction of NSP5 with NSP2, since all three protein are co-immunoprecipitated in transfected cells and in particular they co-localized in VLS (6). On the contrary, VP1 impaired the ability of NSP2 to induce NSP5 hyperphosphorylation, probably sequestering NSP5, or blocking its conformational changing.

All the information collected about NSP5 features and functions in infected cells, provide new highlights to the important role of NSP5 during Rotavirus infection.

NSP4

The product of gene 10 is the non-structural protein NSP4, an ER-resident glycosylated protein that has been identified as the viral enterotoxin protein (216). The first protein product is a 20kDa protein, that upon glycosylation in the ER, becomes a polypepetide of about 28kDa.

NSP4 has two main domain: the N-terminal one that is anchored to the membrane of ER with three hydrophobic domains, and the C-terminal region, corresponding to the majority of the protein, that is oriented to the cytosol and exhibits all known NSP4 biological functions (44).

NSP4 has been extensively studied for its important role in virus morphogenesis and because it was first shown to be an enterotoxin that cause many symptoms of the viral infection (216).

A distinctive feature of NSP4 is its role as a receptor for DLP assembled into the viroplasms. About 20aa of the C-terminal region appear important for the binding of DLPs and their subsequent budding into the ER lumen (88). The receptor role of NSP4 is supported by the lower levels of TLP accumulated in cells treated with siRNA against NSP4 (117).

However knocking down NSP4 expression not only decreases the formation of triple layered particles as expected, but affects other Rotavirus activities: it induces increased levels of plus-strand RNAs, suggesting that NSP4 can be hypothesized to act as a feedback inhibitor in the infected cell and to signal to the viral transcription system, when adequate plus-strand RNAs have been generated to allow productive infection (181). Moreover, NSP4 silencing does not affect the synthesis of the other viral proteins, normal amount of viral proteins are synthesized, however it induces failure of viroplasms maturation since NSP4 silenced cells show small viroplasms. Thus, the effect of the lack of NSP4 on viroplasms is not associated to a low amount of viroplasmic proteins, but it is likely to a defect on the traslocation of viroplasmic protein to the viroplasms. In particular a redistribution of VP2 and VP6 has been observed in NSP4 silenced infected cells: VP2 is more diffused in the cytoplasm rather than concentrated around viroplasms, and also VP6, is redistributed from viroplasms to fibers. This redistribution is thought to be mediated by the interaction of NSP4 C-terminal with VP6. Upon these observations, NSP4 is thought to create a cytoplasmic environment that promote the association of the different structural or non-structural proteins to form viroplasms (117).

Besides VP6, NSP4 has been found in oligomeric complexes with VP7 and VP4 in enveloped particles. The association of VP4, NSP4, and VP7 may represent sites on the endoplasmic reticulum membrane that participate in the budding of the DLPs into the lumen of the ER, where maturation to TLPs occurs (120).

The enterotoxin property of NSP4 has been associated to a 66aa cleavage product of NSP4 ($NSP4_{112-175}$), that is secreted from infected cells early post infection. The trafficking pathway that lead to the secretion of NSP4 peptide has been indentified as a nonclassical vesicular transport that bypasses the Golgi apparatus and involves the microtubule network, since treatment with nocodazole and cytochalasin D, but not with brefaldin A, impaired its secretion. The production of the enterotoxin is due to protease activity, however the proteases responsible for the cleavage of NSP4 have not been yet identified (216).

The released cleavage product is available to bind to a putative receptor on the neighboring secretory cells to trigger the signal pathway that results in diarrhea (11),(131). Surface Plasmon resonance (SPR) associated to mass spectrometry identified two distinct functional domains on NSP4. In particular the $NSP4_{114-130}$ domain binds to the MIDAS motif on integrin I domain, involved in the binding of divalent cation, and the second

region, $NSP4_{131-140}$, interacts with other un-identified domain of $\alpha 2\beta 1$ or other surface molecules (179).

NSP4 was also found to be associated with cellular proteins: calnexin, that needs a glycosylated form of NSP4 for binding (125); caveolin, that induces destabilization of the plasma membrane and promotes secretion of NSP4 peptide (enterotoxin) (124, 134, 185); and tubulin that interferes with the transport of vesicles to the plasma membrane (207).

At least three pools of intracellular NSP4 exist in rotavirus infected cells: 1) NSP4 localized in the ER plasma membrane, to drive DLPs internalization into ER; 2) a minor pool in the ERGIC compartment that may be recycled back to the ER or use for a non-classical secretion of NSP4 peptides into the medium of infected cells; 3) NSP4 distributed in cytoplasmic structure associated with autophagosomal marker LC3 and viroplasms. The third pool appears in infected cells at 6h post infection, and it has been hypothesize that the association LC3 autophagosomes-NSP4 prevents the fusion of autophagosomes with lysosomes, which would affect virus replication (17).

Controversial role in virus replication cycle:

NSP3

NSP3 is the product of rotavirus gene 7, and it is a protein of about 35 kDa. Like NSP1, NSP3 has been found co-purified in cell-fractions containing cytoscheletal matrix. Indeed in IF analysis it has a diffuse to filamentous cytoplasmic distribution .

Crystallographic analysis revealed that NSP3 is organized in asymmetric homodimers, and each monomer is mainly composed of α-helices. The N-terminal has three α-helices, while the C-terminal includes both α-helices and β-sheet. Although the two monomers are identical in their secondary structure composition, they differ for their spatial positioning of N- and C-terminal, these lead to an asymmetry of the whole molecule (48). Poncet et al. demonstrated that monomers and multimeric species of NSP3 interact with 3' end of rotavirus mRNAs. Enzymatic sequencing of the RNA segments recognised by NSP3 revealed that the very last sequence UGACC of viral mRNA is the one bound to NSP3. Further analysis showed that only the last four nucleotide (GACC) are necessary for NSP3 recognition of viral mRNAs (155). The structural analysis demonstrated that the RNA binding doimain is localized at the N-terminal half of the monomer and in the homodimer the N-terminal are arranged in order to form a closed basic tunnel that preclude the possible recognition of internal GACC sequences (48). Extensive contacts between the two monomers and with the mRNA explain the high stability of the complex RNA-NSP3.

The evidences on the role of NSP3 in rotavirus infection were first highlighted with experiments of two hybrid screening systems, that identified NSP3 interactions with the cellular protein eIF4GI. This observation was also confirmed in vivo during rotavirus infection, by co-immunoprecipitation experiments (152).

eIF4GI is an eukaryotic translation initiation factor that usually interact with the poly-A binding protein (PABP), which recognises poly-A cellular mRNAs, and promotes synthesis of cellular proteins (110). The eIF4GI/PABP interaction involves the carboxy-terminal domain of eIF4GI, the same region involved in interaction with NSP3. Thus, it has been proposed that during infection NSP3 interacts with the C-terminal domain of eIF4GI, preventing association with PABP therefore affecting the cellular protein synthesis and dislocating the translation machinery towards non-polyadenylated viral mRNA (151, 152). Initially, the model, that propose NSP3 as a substitute factor for PABP to enhance translation of rotaviral mRNAs, while shutting off cellular protein synthesis, was widely accepted, supported by different experimental evidences. Even thought the interaction of the N-terminal domain of NSP3 with the 3'-end of a viral mRNA and of its C-terminal domain with eIF4GI have been clearly established, there are no clear evidences that these interactions occur simultaneously inducing circularization of the viral mRNA, favouring its translation (as it has been proposed by Piron et al.). In fact, recently observations of cells treated with an siRNA specific for NSP3 go against this model. Indeed, the synthesis of viral protein is not affected when the expression of NSP3 is knocking down, suggesting that binding of NSP3 to the viral mRNA is not necessary for its translation. Moreover, an increased level of viral mRNA and dsRNA has been found in NSP3 silenced cells, suggesting that, rather than promoting translation, NSP3 binds mRNAs to protect them from degradation and/or to keep a pool of mRNA available for translation. This results also indicates that it is not required for virus replication. However, the use of siRNA against NSP3 did confirm a role for NSP3 in shutting off cell protein synthesis since standard virus infected cells have an increased shut off of cellular protein synthesis with respect to cells treated with siRNA specific for NSP3. The studies with siRNA specific for NSP3 allow to proposed a modified model where the eIF4GF interaction domain and RNA binding domain of NSP3 have independent different functions. The binding of eIF4GI is responsible for affecting the synthesis of cellular proteins as it has previously suggest, while the binding of the RNA might have a role in protecting the mRNA from degradation or from VP1 polymerase binding to ensure a pool of mRNA available for translation (128).

Non essential for virus replication:

NSP1

NSP1 is the product of segment 5, and is 55 kDa protein that accumulates in the cytoplasm of infected cells. Among all different rotavirus strains, NSP1 has a conserved cystein-rich region and is involved in specific mRNA binding, since mutants lacking this region do not conserve this feature.

The distribution of NSP1 in infected cells is rather diffuse with slightly punctated and filamentous pattern consistent with results from cellular fractionation studies, indicating that some of the protein is associated to the cytoskeleton. The recruitment of mRNA to the cytoskeleton may only require transient interactions of NSP1 with the cytoskeleton and thus may explain why significant amounts of this protein are found both in the soluble and cytoskeletal fractions of infected cells. A possible role of NSP1 bound to the cytoskeleton may be to move mRNAs to the viroplasm where other RNA binding viral proteins accumulate to promote viral dsRNA synthesis and formation of new DLPs (82).

NSP1 is not an essential protein for viral replication, since rotavirus mutants with C-truncated forms of NSP1 are still able to replicate efficiently in infected cells (143). Moreover, infected cells treated with siRNAs against NSP1 actively support rotavirus replication (180). However, NSP1 silenced virus has a “very small plaque” phenotype suggesting that NSP1 may be involved in modulate cell immune response to viral infection. Indeed, it has been demonstrated that NSP1 interacts with Interferon Regulatory Factor 3 (IRF3) both *in vitro* and *in vivo* (70). IRF-3 is a 427-amino-acid transcription factor that is constitutively expressed in all cell types. IRF-3 resides latently in the cytoplasm, and upon activation is phosphorylated, dimerizes, and translocates to the nucleus, where it complexes with transcription coactivators such as CBP/p300 to induce stimulation the of interferon (IFN) response genes (10). It has been described that rotavirus NSP1 C-terminal deletion mutants have the ability to trigger IRF3 translocation to the nucleus and the expression of IFN, while Rotavirus with wild type NSP1 suppresses these mechanisms, indicating that the primary effect of NSP1 is to antagonize the immune cell response. NSP1 suppression of IFN response is not only due to binding IRF3 monomer and preventing its dimerization and traslocation, but is an inducer of the proteasome-dependent degradation of IRF3 (13). Recently, it has been demonstrated that NSP1 promotes proteasomal degradation of other IRF family members like IRF5 and IRF7, in this way NSP1 induce downregulation of proinflammatory cytokines, and type I interferon expression respectively (81),(9). However, the regulation of IRF3 amount is virus-strain

and cell-type specific (177). NSP1 of the porcine strain OSU is not able to induce proteasome-mediated degradation of IRF3, however it affects IFNβ expression. It has been recently demonstrated that OSU NSP1 represses induction of IFNβ by subverting the activation of NFκB transcription factor in MA104 cells. Indeed, it mediates the proteasomal degradation of β-TrCP, a protein of the $SCF\beta^{TrCP}$ E3 ligase complex, that regulates the degradation of IκBκ, that is stabilized and inhibits NFκB activation towards IFNβ genes (68). Thus NSP1 represents a broad-spectrum antagonist of immune cells response (14).

It has been proposed a putative function for NSP1 as an E3 ubiquitin-protein ligase, according to data on sequence analysis. Indeed, one of the prominent characteristic of NSP1 sequence is the conserved Cys-rich region at the N-terminus of the protein. This sequence fits with RING finger domains that are present in E3 ubiquitin-protein ligases, which promote transfer of ubiquitin, conjugated to enzyme E2, to the specific protein. Since it has been identified a proteasome degradation susceptibility of NSP1 that can be prevented by unidentified rotavirus protein(s) or viral mRNA, it is speculated that the presence of RING finger motif provides a means for self-ubiquitinilation (149). Mechanisms by which NSP1 functions in the ubiquitin-dependent proteasome system are still under investigation.

NSP6

NSP6 is a small protein of about 11kDa encoded by the alternative open reading frame of segment 11. It is not clear the function of this protein in the replicative cycle of Rotavirus, since in some strains it is not produced. However, it is thought to have a regulatory role during the infection. It seems to localize in viroplasms and to interact with the C-terminal region of NSP5 to form an heterocomplex. This interaction however, in infected cells has not been demonstrated, probably due to the low level of expression of NSP6 during infection, but it has been clearly characterized *in vitro* by two hybrid system and by *in vivo* expression of recombinant NSP5 and NSP6 (195).

Pulse–chase studies showed that, in contrast to other viral proteins like NSP5 that following post-translational modifications are stable, NSP6 has a high rate of turnover with the vast majority of the protein synthesized in a 5 h, pulsed with ^{35}S, being degraded after a 2 h chase period. Filter binding assays showed that, in common with NSP5 and most of the other proteins found in the viroplasm, NSP6 has an affinity for RNA, however it has a

broad nucleic acid binding capacity which does not exhibit any detectable sequence specificity (163).

1.5 ROTAVIRUS REPLICATIVE CYCLE

1.5.1 OVERVIEW

The general features of the rotavirus replicative cycle, based on studies in cultures of monkey kidney cells are:

- ✓ Replication of the virus is totally cytoplasmatic;
- ✓ DLPs are transcriptionally active producing mRNAs;
- ✓ Transcripts function both as a source of viral proteins and as template for synthesis of (-)strand to form the genomic dsRNA (replication);
- ✓ The replication machinery is totally viral; the cells do not contain enzymes to replicate dsRNA. Yet cell proteins could also be involved for instance in viroplasms formation;
- ✓ dsRNA synthesis and initial steps of assembly take place in specific cytoplasmic structures called viroplasms that formed soon after infection;
- ✓ No dsRNA, nor (-)ssRNA are found in the cytoplasm of infected cells;
- ✓ Subviral particles DLPs form within viroplasms and bud into the ER to complete their maturation;
- ✓ Levels of intracellular calcium are important for controlling virus assembly and integrity.

New insight about viral replication are coming from studies in polarized intestinal epithelial cells, or polarized differentiated enterocytes. In polarized intestinal cells, virus entry may occur mainly through the apical membrane, or even the basolateral one depending on the virus strain. In differentiated enterocytes the rotavirus infection alters different functions like cellular protein trafficking, cytosckeleton, and tight junctions, and finally the virus is released by a non-conventional vesicular transport that does not induce extensive cytophathic effect (58).

Several information collected nowadays lead to draw a general description of rotavirus cycle.

The entry of Rotavirus into the host cell is characterized by different interactions between the proteins of the outer layer, VP4 and VP7, with components of the cellular membrane. After the entry, Ca^{2+} concentration in the cytoplasm determine the disassociation of VP7

trimers, with the consequent disassembly of the outer layer capsid. The TLPs become transcriptionally active DLPs that start producing viral mRNA (primary transcription). The mRNA is extruded in the cytoplasm of the cells through type I channels and this has two main functions: to be translated to produce viral proteins, and to serve as a template for the synthesis of viral dsRNA (virus replication). After a critical amount of viral proteins accumulate in the cytosol, some of them are involved in the formation of viroplasms. It is within viroplasms that genome replication and new DLPs assembly occur. Newly formed DLPs, however, are transcriptionally active (secondary transcription) and produce mRNAs for the maintainment of the production of viral protein during the infective cycle. DLPs from viroplasms bud into the endoplasmic reticulum through the interaction with NSP4, where they acquire a transient envelope subsequently replaced by the assembly of VP7-VP4 outer layer. TLPs are released either by cell lysis or by a non-classical, Golgi-independent, vesicular transport involving interaction with lipid “rafts” near the plasma membrane and in this case resulting in extensive cytopathic effect (58). (Fig.10)

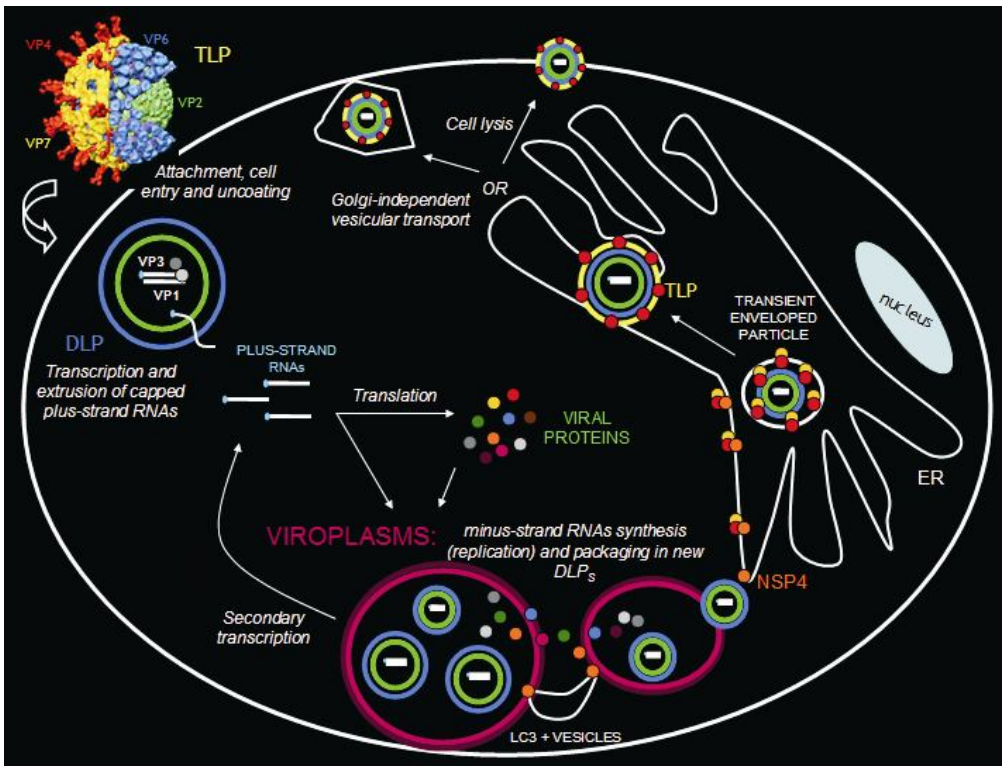

Figure 10: Schematic rappresentation of Rotavirus replicative cycle.

1.5.2 ATTACHMENT

The initial step of rotavirus infection is the binding of the virus to the membrane of the host cell.

The demonstration that the neuroaminidase (NA) treatment of red blood cells inhibits the attachment of Rotavirus on the cell surface indicated that sialic acid (SA) has an important role in virus binding. However, studies on rotavirus entry into the host cells reveal that the infectivity of many animal and human strains of rotavirus are not affected by the treatment with NA, and for this reason were named NA-resistant strains. Nevertheless this does not mean that these strains do not need SA to bind to the cell membrane. Indeed some NA–resistant strains are thought to bind to some internal NA-insensitive SA moieties on glycolipids or to modified SA-moieties on oligosaccharide structure on the cell surface (37). The SA binding domain is collocated in the VP8* cleavage product of the spike protein VP4, in particular between the two β-sheet of the β-sandwich, similar to that found in galectins, a family of sugar-binding proteins. X-ray crystallographic structures of both NA-sensitive and resistant strain confirm the occurrence of this interaction (53).

1.5.3 PENETRATION AND UNCOATING

The initial interaction with SA is generally followed by specific interaction with several other cell surface molecules as integrins and the heat shock cognate protein hsc70 (116) (5) (115) .

The initial interaction of VP8* with SA moieties is thought to induce conformational changes that favour the interaction of the VP5* cleavage product with integrin $\alpha 2\beta 1$ through its DGE sequence (73). Subsequently a series of post-attachment interactions that involve VP5* and VP7 take place:

1) VP5* interacts with heat shock cognate protein 70 (hsc70) that could induce a conformational changes in the virus particle to help the virus enter the cell (76);
2) VP7 interacts with $\alpha V\beta 3$ and $\alpha X\beta 2$ in an early stage of virus interaction (73) (77);
3) VP5* and VP7 interact with integrins $\alpha 4\beta 1$ and $\alpha 4\beta 7$ (72);
4) Ganglioside GM1 and GM3 have been suggested to play a role as possible receptors (79),(166);
5) infectious particles also associate with lipid rafts on cell membrane during early interactions (78),(5) (85);

The mechanism by which Rotavirus is internalized in infected cells is still under investigation, and till now two different models of viral particles entry have been proposed: a) non-classical endocytosis; and b) direct membrane penetration.

a) Early electron microscopy studies of rotavirus-infected cells suggested endocytosis as the virus internalization pathway, and suggested that uncoating might occur by the effect of acidification (146). However, rotavirus infectivity is not inhibited either by preventing the acidification of endosomes or by drugs that block the intracellular traffic of endocytic vesicles .

   However, since the model of a non classical endocytic-mediated entry is not to be excluded, it has been proposed that the solubilization of the outer layer would occur due to the low Ca^{2+} concentration within the endocytic particles (40). The low Ca^{2+} concentration would trigger conformational changes in the proteins of the outer capsid with their consequent solubilization. It has been observed that solubilized outer proteins are able to permeabilize cellular membranes. Thus disrupted VP4 and VP7 could permeabilize the vesicle's membrane to release the transcriptionally active double-layered particle into the cytosol (170).

b) On the other hand, different observation support the model of direct penetration of the viral particle (94),(132). It has been demonstrated that depletion of cholesterol inhibits rotavirus infection and that a functional dynamin, a protein associated in processes that involve membrane dynamics, is necessary for rotavirus infection. Moreover, it has been recently reported that drugs and dominant-negative mutants that are known to impair clathrin- and caveolae-mediated endocytosis did not affect rotavirus cell infection (171).

   Trypsin has been found associated to the outer capsid of the virus particles, and the hypothesis of the direct penetration would explain its role in rotavirus infection: VP7 and VP4 cleaved by trypsin would be capable to disrupt membranes and allow DLPs to gain access to the cytoplasm to begin the active transcription of the viral genome (169).

Therefore, rotavirus cell entry is a coordinated, multistep process that is not entirely elucidated and involves sequential interactions with several ligands. The results of this process is the release of transcriptionally active DLPs in the cytosol of infected cells, for the initial production of viral mRNA.

1.5.4 TRANSCRITPION

The transcription event consists in the production of positive sense RNAs from the dsRNA genome. It is possible to distinguish two events of transcription during rotavirus infection: primary transcription that occurs soon after the release of DLPs into the cytosol, and the secondary transcription performed by the newly synthesized DLPs within viroplasms.

The trascriptase complex consists of the polymerase VP1 associated to the capping enzyme VP3, that is attached to the inner surface of the VP2 layer at the fivefold axes (159). None of the viral proteins, by itself, demonstrate transcription activity, so the structural integrity of DLPs is necessary for the transcription to occur. TLPs are not transcriptionally active, the uncoating is necessary to trigger the transcriptional activity of DLPs, an observation supported by both *in vitro* assays and by liposome-mediated transcription of DLPs into cells, that is sufficient to initiate the transcription of viral genome (15),(38) .

In particular the whole process of transcription could be divided in three step: initiation, elongation, traslocation of the transcripts.

In the initiation step, the end of the dsRNA must be partially unwound (the helicase responsible of this process has not been identified) and then nucleotide transfer and the capping of the transcript occur. Two types of shorter particle-bound capped oligonucleotide (5-7 nucleotide in length) result from a brief pause in the transcription before it proceeds to the synthesis of full-length transcripts. These shorter oligonucleotides have been found associated to both TLP and DLP, in particular that associated to the TLPs become full length transcripts only when the outer layer is removed and the TLP is converted to a DLP. This indicates that VP7 inhibits the step elongation. Since the same observation was obtained when DLPs are coated with a monoclonal Ab anti-VP6, this suggests that both mAb anti-VP6 and VP7 confer conformational change in the structural integrity of DLPs that prevent elongation of the transcripts (107). The DLP structure has a rigid organization to permit the transcription of the viral genome. Indeed, the trascriptase activity results impaired if the hydrophobic interaction between VP2 and the layer of VP6 is perturbed, or with VP6 mutant that are not able to properly fold with the viral core (29). Since the short oligos are formed in the TLPs as well, this indicate that TLP are not transcripionally incompetent, and that the site of initiation and capping are closed within the core (108).

In vitro transcription studies have identified the different enzymatic activities of the transcriptase complex: trascriptase, nucleotide phosphohydrolase, guanyltransferase, and

methylase. Indeed viral mRNA are capped by the addition of $^{m7}GpppG^{m}$ at the 5' and do not contain poly-A tail. The process of capping proceeds in four step:

1. Phospho-hydrolysis at the 5' to remove the orthophosphate of the nascent mRNA
2. Attachment of guanine nucleotide to the 5'end
3. Attachment of a methyl group to the N^7 position of the G cap
4. Attachment of a second methyl group

Two of the four enzymatic activities are supported by the VP3 that is the methyl/guanyl transferase (31),(114),(138, 153). Since the template is a dsRNA, a helicase activity has been thought to be required to unwind the template, but that enzymatic property has so far not been demonstrated for any of the viral structural proteins.

Cryoelectron microscopy of in vitro transcription assays indicates that full-length transcripts are released through the type I channel, located at the fivefold axes of the icosahedral structure. Several mRNAs are released simultaneously from the same active particles, confirming that the transcription of the 11 segments occur simultaneously and in continuos (183). The mechanisms that allow repeated cycles of transcription remain unknown (109).

Viral mRNAs are extruded in the cytoplasm where are engaged by the cellular translation machinery to produce viral proteins, but viral mRNAs must also become available as templates for the replication of viral genome. This however takes place in viroplasms and not in the cytosol.

1.5.5 TRANSLATION

The viral protein synthesis is supported by the cellular translation machinery, that recognise capped and poly-adenilated mRNA. Since the viral mRNA is capped but non-polyadenilated, it is not recognisable by the poly(A) binding protein (PABP) and collocated in the right position of the initiation complex of translation. However the 3' end of viral mRNA presents the most conserved sequence, among all 11 segments, thus proposed that is recognised by the non-structural viral protein NSP3 (as describe before in page 32) (155).

Other viral proteins are involved in translation of viral mRNA: VP2 NSP2 and NSP5 seemed to be involved in inducing the phosphorylation status of the translation factor eIF2α, inhibiting in this way cellular protein synthesis, silencing the expression of each viral protein induce phosphorylation of eIF2α switching on cellular protein synthesis (129).

1.5.6 REPLICATION and PACKAGING

Several studies have defined the steps of viral replication and packaging using replication intermediates (RIs) purified from infected cells.

Kinetic studies revealed that positive and negative strand RNAs are present at 3 hours post infection and increasing between 9 and 12 hours, when the maximum level is reached (184).

Electron-dense cytoplasmic inclusions, termed viroplasms, function as sites of genome packaging and replication in the infected cell. Since in these structure localize both structural viral proteins, found in single shelled particles and DLP (VP1, VP2, VP3, VP6) and non-structural proteins NSP2 and NSP5, it is reasonable to assume that these protein have a role in virus replication and packaging (64). In vitro studies, however, revealed that VP1 and VP2 are the minimal proteins required for replication of mRNA but they are not sufficient to drive dsRNA packaging, suggesting the other proteins within viroplasms may have this role (141).

Different studies, both *in vitro* and *in vivo*, provide information about the mechanism of replication and the role of the different proteins.

Early analysis of replication intermediate (RI), recovered from infected cells, and revealed that the initial step of replication involves the interaction of VP1 and VP3 with (+)RNA to form pre-core RIs, and a second step involves the interaction with VP2 core to form core RIs that contain the full 11 (+)RNAs . Only the core RIs have replicase activity suggesting that the viral polymerase VP1 exists in an inactive form that the interaction with VP2 converts into an active one (141) (214). This was also confirmed using mutants that expressed a defective form of VP2 unable to assemble RIs with replicase activity (121). The intermediate layer of VP6 associates with the core RI to form DLP, that maintain the capacity to produce dsRNA (139),(64). Treatment of purified RIs with RNAse specific for ssRNA destroys their ability to synthesize dsRNA, while the treatment of in vitro replicating RIs with RNAase specific for dsRNA does not degrade the dsRNA produced. These observation suggest that positive ssRNAs move from the external into the RIs where they are replicated and they are protected from dsRNAase degradation (139) (137). Taken together all these observations suggest that packaging of (+)strand RNA and its replication are two related events that depend on the presence of the core protein VP2. The presence of VP2 ensures to gather the dsRNAs into the core, and to protect them from the dsRNA-dependent immune cell response. It has been observed that the packaging precedes the

replication events, and it does not finish before the initiation of replication, suggesting that the packaging signal must be present on the (+)RNAs and not in the dsRNA (142) (144).
NSP5 and NSP2 are components of RIs with replicase activity, and this is not surprising since the replication occurs within viroplasm. These proteins are able to bind to RNA and to the structural components of the RI (140).
In vitro replication assays performed with open cores were also a useful tool to study Rotavirus replication. Incubation of Rotavirus cores with low ionic strength buffers results in the disruption of the cores (open cores) and release of dsRNA . The polymerase of the open cores maintains its activity and was highly processive continuing the replication for hours, exclusively in the presence of VP2. Indeed, purified VP1 from open cores system does not show replicase activity, even incubated with (+)RNA. The open cores system was utilized to identify the *cis*-acting signals in (+)RNA. In particular it has been observed that open cores incubated with even small amount of salt have the synthesis of dsRNA impaired (32). The sensitivity to salt concentration is associated to the formation of initiation complex, since once it is formed, with a preincubation of RIs components without salt, the dsRNA synthesis occurs even at high salt concentration. In particular the formation of initiation complex required GTP, Mg^{2+}, (+)RNA, VP1, VP2, where the presence of $Mg^{2+}$is essential for the formation of the initiation complex (196). Through this method and RNA containing mutantions it has been possible to locate the regions and structures of RNA necessary for viral replication. Three region have been found to be important:

- ✓ The first signal is the 3’ consensus sequence (3’CS) 5’-UGUGACC-3’. It is a very conserved sequence among viruses of the same group, indicating its importance in replication. In particular the 5’-UGUGA-3’ sequence seems like to form a polymerase recognition signal, while the last two nucleotide CC-3’ are of primary importance for initiation of replication. In addition, the 3’CS signal must be single strand to function efficiently as replication signal (196).
- ✓ The second region lies upstream the 3’CS at the 3’ UTR of the viral mRNA; and seem to have an enhancing role on replication (145).
- ✓ The third region is located at the 5’ UTR and has been demonstrated to stimulate RNA replication (197)

Based on the location of the *cis*-acting sequences and computer modelling, it is hypothesized that the ends of the mRNA would interact in *cis* to form panhandle structure that promote the synthesis of dsRNA. Moreover, the predicted secondary structure present

some loop structure at the 3' and 5' of the mRNA that different among the 11 segments and would have role in packaging and assortment (145, 197),(144).

Using siRNA specific for different viral proteins, it was possible to characterize the role of the different viral proteins in viral replication. Affecting the expression of proteins not involved in virus replication, such as NSP1 and VP7, with siRNA against gene 5 and 9, it was observed that the synthesis of dsRNA segments was not affected. This confirm the presence of two pools of mRNA, one susceptible to siRNA treatment with a cytosolic localization and another, used as a tamplate of dsRNA, protected from siRNA recognition, more probably localized within viroplasms (180).

The role of VP1 and VP2 during replication has been widely demonstrated using in vitro systems. Additionally, the nonstructural proteins NSP5 and NSP2 have an important role in forming viroplasms, but they do not seem to be essential for the replicase activity. They might increase or regulate the replication process or have a role in genome packaging.

Although the role of the enzymatic activities of NSP2 (NTPase, RTPase, NDP kinase) is still unclear, it has been proposed that NSP2 acts as a molecular motor providing the energy deriving from hydrolysis of NTPs for genome replication and/or packaging and maintaining a pool of nucleotides in viroplasms for RNA synthesis and for processes requiring ATP (i.e. transcription or RNA packaging). Interestingly, an inhibitory role for NSP2 in the formation of the replication initiation complexes has been demonstrated in *in vitro* assays with recombinant VP1 and VP2. In detail, NSP2 was shown to interfere not with the binding of VP1 to the template, but with the function of VP2, possibly as a result of competition for RNA binding (188),(90) (96).

The role of NSP5 in viral replication is even more obscure than that of NSP2. Indeed, different studies demonstrates the relations of NSP5 with different components of replication complex:

- ✓ NSP5 interacts with NSP2 forming VLS in cytoplasm of transfected cells. Moreover, it competes with NSP2 in RNA binding, suggesting a regulatory role for NSP2-RNA interaction (60), (91).
- ✓ NSP5 interacts with VP2, functions as a physical adapter between NSP2 and VP2 (18).
- ✓ NSP5 strongly interacts with VP1 both in infected cells and in transfected cells in absence of other viral proteins (6).

All these observations, linked to the fact the NSP5 is indispensable for viroplasms formation, where replication occurs, suggest that, besides a structural role, it would have a more regulatory functions during viral replication.

The genome packaging is a selective mechanisms that lead to the encapsidation of equimolar genome segments within the core of the virus. The mechanism is still under investigation but different models have been proposed (142):

- ✓ The pre-core precursor complex: based on the characterization of replication intermediates the model proposes the organization and assembly of VP2 core protein around a nucleation site formed by the RdRp VP1, viral mRNA and VP3.
- ✓ Empty core precursor complex: based on the capacity of the capsid proteins to self assemble into VLPs it has been proposed that viral mRNA would be inserted in these cores.
- ✓ Encapsidation coincident with capsid assembly: this model is based on structural data, in which has been described that each VP1-VP3-mRNA complex is associated to a pentamer of VP2. Thus, each pentamer is associated to a specific mRNA, interactions between the different mRNAs would drive the assembly of the icosahedral structure, and the interaction between the different pentamers would confer conformational changes in the core lattice that activate the VP1 polymerase.

Further studies are needed to clarify which model is correct and if and how they may need to be modified. In particular none of these model take in concideration the strong interaction between NSP5 and VP1 (6).

1.5.7 VIRUS ASSEMBLY AND RELEASE

The virus morphogenesis is a process still under investigation since it differs from other members of *Reovirus* family, and from other viruses. The particular feature of the morphogenesis in Rotavirus system is that subviral particles, formed inside the viroplasm, bud through the membrane of the ER, acquiring a transient envelope, that is soon replaced by proteins that constitute the outer layer of the mature viral particle. Once the TLPs are formed, they are release from the cells with different mechanisms depending on cells type (58).

Both biochemical and morphological data support the idea that viroplasms are the site of virus replication and DLPs formation, since several proteins thought to be involved in viral

replication (NSP2, NSP5, NSP6) and structural elements of transcriptionally active DLPs (VP1, VP2, VP6) are found localized in these structures (140),. Moreover, structural protein VP4 was found distributed in the close periphery of viroplasms and outside the ER. The first step of virus morphogenesis occurs inside the viroplasms where viral structural proteins VP1 and VP3 interact with the 11 segments and pentamers of VP2 to form the core of the virus (140),(144). Subsequently, DLPs acquire the intermediate layer of VP6. VP6 is known to localize in the viroplasms in a distribution quite similar to that of NSP5 and NSP2. The assembly of the intermediate layer is thought to occur during the exit of the particle from the viroplasms. Since it has been observed that silencing of NSP4 impaired DLPs formation and VP6 distribution, it has been hypothesized that NSP4 interacts with unassembled VP6 driving its collocation in viroplasms, and consequently the formation of DLPs (181),(117).

Once DLPs are formed, the C-terminal region of NSP4 functions as a intracellular receptor on ER membranes and mediates the budding of newly formed DLPs into the ER by binding VP6. NSP4 does not need glycosylation to bind the DLPs and interacts with VP4 in the cytosolic side and VP7 in the ER lumen to form a heterotrimer with an unknown function (7),(8), (16).

The last steps of virus morphogenesis occur in the ER. The budding into the ER confers to the DLP a transient lipid envelope that is removed by VP7. Although VP4 and NSP4 were shown to have membrane destabilizing activity, the main role in removing the transient envelope is played by VP7, as demonstrated by siRNA experiments targeting VP7 mRNA. (117). It has been shown that this process is dependent on Ca^{2+} concentration since cells treated with thapsigargin or the calcium ionophore A23187, which decrease the Ca^{2+} concentration into the ER, virus morphogenensis is blocked at the stage of the enveloped particle (123), (156). VP7 trimer are stabilized by Ca^{2+} ions binding at the interface of the monomers, and trimerization is dependent on Ca^{2+} concentration (123),(157). Thus, it has been proposed that soon after budding of DLPs into the ER, VP7 that is embedded in the transiently enveloped layer surrounding DLP together with NSP4, VP4, assembles into trimers, with a process that is Ca^{2+} dependent, excludes the lipid enveloped from the virion, and associates with VP6 trimers (117). This model does not rule out that NSP4, as well as cellular protein, would be needed in this process (117).

The final step of virus morphogenesis is the association of VP4 spikes. Timing and location of VP4 assembly in infected cells is controversial.

Studies in non-polarized endothelial MA104 cells, suggest that VP4 binds DLPs before or during VP7 assembly in the ER. Evidences support the model of VP4 assembly to VP7 coated cores in the ER: immunoelectron microscopy analysis localizes VP4 in the cytoplasm between viroplasms and ER (147), immunofluorescence and biochemical analysis reveal VP4 localized in transient enveloped particles together with NSP4 (66),(120); cells treated with siRNA specific for VP4 accumulate spikeless particles in the ER (43),(41).

On the other hand, using one monoclonal antibody specific for VP4 in polarized intestinal epithelial Caco-2 cells, a pool of VP4 was detected in lipid rafts, suggesting the hypothesis that, in this cells, VP4 assembles after VP7 while the VP7 coated particle are transported from the ER to the cell surface within extrareticular compartments. (46),(42).

In vitro recoating experiments of DLP with recombinant outer proteins introduced the hypothesis that VP4 assembly precedes VP7 assembly *in vivo.* According to this model VP4 transiently oligomerize and bind weakly to the DLP, VP7 goes to Ca^{2+}–dependent trimerization and binds DLP tightly, locking VP4 in place. VP7 binding is independent from VP4 binding since triple layer spikeless particles are formed in cell treated with a siRNA specific of VP4 (198). This model is further supported by recent cryo-EM with subnanomolar resolution (112).

The release of mature viral particles occur with the lysis of non-polarized cell, following alteration in the permeability of the plasma membrane of infected cells. Despite cell lysis, most DLP ad TLP remain associated with cellular debris, suggesting interaction of the particles with some structures within the cells like cytoskeleton or cell membrane lipids (58).

Studies on Caco-2 gave different information about the release of mature viral particles. Caco-2 cells are human intestinal epithelial cells established from an adenocarcinoma that, after confluence, display many of the morphological and biochemical properties of mature enterocytes. These cells display an apical domain with a brush border and expression of intestinal hydrolases, and a basolateral domain (150). In this cell line release of virus has been demonstrated not to be mediated by cell lysis but by an atypical trafficking pathway bypassing the Golgi apparatus, that resembles more what happens in the natural rotavirus infection (92). In this mechanism, membrane raft microdomains are involved and in particular it has been demonstrated that VP4 is rapidly associated with these structures, and serve as a platform for the assembly of VP4 with the rest of the viral particle (172). Moreover VP4 located at the apical domain of Caco-2 cells creates

interaction with actin bodies, suggesting a role for raft and actin in Rotavirus final assembly and apical release (65).

VP4 associated to rafts microdomain has been found also in non-differentiated kidney epithelial cells, MA104. In this cell line siRNA specific for gene4 induce accumulation of viral particle into ER and prevent the targeting of TLPs to rafts, suggesting that in order to associate to raft viral particles need VP4 and its assembly with the viral particles occurs in the ER (41). Thus association of rotavirus particle into raft is a conserved process present in the two different polarized cells studied (45).

The association of rotavirus particle with lipid raft through VP4, is probably due to the galectin-like motive present in VP8* (172). However how the rotavirus particle translocate to lipid rafts remain an open question. Evidences suggest that VP7 and NSP4 are possible candidates for rafts targeting. However, in cells transfected with siRNA specific for VP7, the association with lipid rafts does not result impaired (41). In contrast, in cells treated with siRNA specific for NSP4, the association of viral particles with rafts does not occur. Indeed NSP4 is involved in different events during virus morphogenesis and release like the budding of DLP into ER working as a intracellular receptor (7),(8), (16); the removal of the transient enveloped, event that involved the interaction with VP4 (193), and interestingly the blockage of the transport of vesicles from the ER-Golgi intermediate compartment to the Golgi by NSP4 has been reported (207).

Generally the assembly of raft occur at the level of the Golgi apparatus, while the viral particles reach the apical surface with a non-conventional vesicular transport pathway, so it has been investigated at what level the association of lipid rafts with viral particle occurs. In the conventional secretion pathway the cargo proteins transit from the ER to the Golgi apparatus through a vesicle-mediated transport system that constitutes the so called ER-Golgi intermediate compartment (ERGIC) and can be visualized by two marker proteins usually recycling among ER, ERGIC and Golgi: ERGIC-53 and β-COP (207). Increasing evidence suggest participation of the ERGIC in rotavirus maturation:

- ✓ NSP4, VP4 and VP7 were all found in ERGIC, since co-localization with ERGIC-53 has been detected (41).
- ✓ Overexpression of NSP4 in transfected cells as well as natural rotavirus infection changes the distribution of ERGIC-53 from a juxtanuclear vesicle-like pattern to a more dispersed one (41).

Upon these observations, it has then been proposed that at some stages organelles containing ERGIC-53 and rotavirus proteins exit the traditional secretory pathway and do not reach the cis-Golgi (41).
The presence of rotavirus particles in ERGIC raises several questions to be addressed in future studies to investigate which transport pathways are directly involved in Rotavirus maturation and release.

1.6 PATHOGENESIS AND IMMUNITY

The pathogenesis of rotavirus has been investigate first using animal models. In this way it was possible to characterize the virus and to observe virus replication in different tissues in order to obtain information about the sites of infection and the immune response against it.
Rotavirus infection can result in asymptomatic or symptomatic infections and the outcome of the infection is affected by both viral and host factors. The most prominent host factor that affects the clinical outcome of infection is age: neonates infected with Rotavirus rarely have symptomatic desease, due to the transplacental transfer of maternal antibodies. Between 3 months and 2 years of age the susceptibility of the infection increases, due to the reduced amount of maternal antibodies, causing severe Rotavirus induced desease. Rotavirus can also infect adults, but severe disease is uncommon (75). Diarrhea is the main clinical manifestation of rotavirus infection in infants and young children. The features that distinguish the viral diarreha from bacterial-induced one is that little inflammation or lesions are seen in infected intestine.
The virulence of the virus is multigenic and would be associated with several of the 11 genes of the genome, like gene 3,4,5,9, and 10, and the basis of the involvement of these gene is only partially understood. Through the use of virus reassortants, the correlation between virulence and viral protein has been characterized. In particular mutations of NSP4 have been associated with altered virus virulence supporting a role of NSP4 in viral pathogenesis (215). It has been described that NSP4 acts as an enterotoxin both at intra and extracellular level (50),(216). The intracellular expression of NSP4 causes a disruption of Ca^{2+} homeostasis and increase in Ca^{2+} permeability triggers several intracellular process such as disruption of cytoskeleton, inhibition of Na-solute co-transporter system, and lack of the expression of enzymes in the apical part of the cells necessary for digestion (194). Moreover a cleavage product, corresponding to residues 112 -175 is release from infected cells and has a paracrine effect on un-infected cells since it binds to

integrins proteins and triggers phospholipase C-inositol 1,3,5-triphosphate cascade that cause the release of Ca^{2+} from the ER (24) (179).

Concluding disease pathogenesis is due to the virus-mediated destruction of absorptive enterocytes, virus-induced down regulation of the expression of absorptive enzymes, and alteration of the functional thigh junctions between enterocytes that lead to paracellular leakage (75).

A role of the enteric nervous system (ENS) in rotavirus diarrhea has been shown using drugs that are able to inhibits this pathway and that reveals to attenuate rotavirus induced diarrea in mice and children. NSP4 or other factors release from virus-infected cells would mediate this effect (119).

Rotavirus infection is not limited to the intestine. Extraintestinal spread has been documented more that 45 years ago when virus was detected in multiple organs of mice. The clinical consequences of such systemic infection remains unclear (75).

Studies on Rotavirus infection in both animals and human first showed the existence of the acquired immunity to the recurrent disease and also to a lesser extend re-infection after primary infection.

Studies on mice showed that B cells were the primary determinant of protection from re-infection after natural infection, whereas $CD8^+$ T cells were responsible to shortening the course of primary infection. $CD4^+$ T cells are involved in Rotavirus infection to mediate the active protection via interferon γ-dependent pathway. The regulatory T cells do not appear to modulate rotavirus infection, while lymphocyte homing is critical in regulating the rotavirus immunity and B cells trafficking to the intestine (75).

The role of immune response in the rotavirus infected cell and the effect of IFN induced antiviral effect has been examined both *in vivo* and *in vitro.* Levels of INF type I and II increase in rotavirus infected animals and children (204). It has been shown that INF I and II are able to inhibit the infection of rotavirus in vitro, and in early studies in pig and cattle administration of IFNα reduced rotavirus-associated diarrhea . Additionally, *in vitro* studies showed the link of Rotavirus infection to innate immunity, since Rotavirus NSP1 was demonstrated to regulate IFN response in infected cell by proteasome degradation of interferon regulatory factor 3 (IRF3) and 7 (IRF7), and inducing activation of nuclear factor-κB (68),(14).

1.7 VACCINES

Attempts to develop a vaccine against human rotavirus began in the early 1980s. The first efforts used a Jennerian approach (in reference to Edward Jenner's cow-pox vaccine against smallpox) and children were vaccinated against rotavirus that normally infect animals. An attenuated bovine strain was the first candidate that showed protection of calves from subsequent challenge with human rotavirus strain. Despite the high effectiveness in preventing diarrhea in Finnish children, it was less effective in African and Latin-American children. Thus, because of the failure in clinical trials in Africa this candidate was not pursued. Another candidate was a monovalent simian rotavirus strain that shows effectiveness in the preliminary trials but in a subsequent study it lost its efficacy. This failure was likely due to the differences between the serotypes oh this candidate and the circulating rotavirus strains at that time. To circumvent serological problems a tetravalent vaccine, based on reassortant strains with serotypes (G1-G4), was developed. This vaccine called, RotaShield was evaluated in different countries and gave high results of efficacy. However, cases of intussusceptions occurred after the administration of the vaccine and RotaShield was judged not safe for routine use an was withdrawn from commercial manufactories (75).

Recently, in 2006 two new rotavirus vaccines were licensed in USA in Europe and many countries in Central and South America: RotaTeq® and Rotarix® .

Rotateq is a pentavalent bovine rotavirus strain (WC3)-based vaccine manufactured by Merk. In the first trials 70.000 infants were vaccinated and the vaccine showed highly efficacy protection. Moreover the RotaTeq efficacy rates did not appear to be affected by breast-feeding and administration of the vaccine did not interfere with immune response induced by other vaccine. The important aspect is that no intussusception was associated with this vaccine (75).

Rotarix is a live-attenuated human rotavirus vaccine. It was developed following multiple passages of human rotavirus strain in MA104 cells to achieve its attenuation, and the final product resulted in a very efficient vaccine. The molecular basis for the attenuation, as for the RotaTaq, are not known, but sequence comparison with wild-type parent could identify gene changes associated with attenuation. Recent reports showed that Rotarix does not interfere with other routine childhood vaccination (75).

Several third generation vaccines are under development in case these vaccines do not overcome safety issues. Several groups are pursuing inactivated virus or recombinant virus-like particle approaches. Parental and intranasal immunization with recombinant

nonreplicating virus-like particle have been effective in animals and is going to reach phase I testing in human being (47).

Vaccine safety in immunocompromised children are needed to be monitored, case of chronic infections occurs in babies with immunodeficiency that receive the vaccine before the disorder was diagnosed. (75)

1.8 ROTAVIRUS REVERSE GENETIC

The lack of a reverse genetic system applicable to Rotavirus, limits the investigation on rotavirus biology and on the role of the different viral proteins during infection. As described in the previous chapters, the observations collected till now are due to the use of different approaches: infection with reassortant viruses or *ts* mutants; expression of the viral proteins, alone or in different combination between each other, into mammalian and insect cells; *in vitro* replication/transcription assays; small interfering RNA (siRNA). In particular the last approach was most useful, till now, in order to identify the different functions of viral proteins during infection.

However, the real approach that would revolutionize Rotavirus studies, would be a reverse genetic technique. In the past twenty years, especially since the first infectious clone of a negative-stranded RNA virus was reported in the mid-1990's, the reverse genetics systems have been available for nearly all the major human and animal RNA virus groups. There are mainly four external expression systems for construction of the RNA virus reverse genetics systems based on the kind of RNA viruses:

1. in vitro RNA transcripts,
2. RNA polymerase I-driven expression plasmids,
3. RNA polymerase II-driven expression plasmids,
4. modified vaccinia virus/T7 RNA polymerase-driven expression system.

In particular, the viral nucleoprotein and polymerase proteins are required to assemble the viral ribonucleoprotein (RNP) complexes for the rescue of the negative-stranded RNA viruses (83).

For the dsRNA viruses, among the family of *Reoviridae,* a successful reverse genetic approach has been developed for reovirus (10 segments) and bluetongue virus (12 segments). In particular, for reovirus it has been used a plasmid-based reverse genetic approach. Each reovirus segment was engineered downstream to a T7 RNA polymerase promoter and a hepatitis delta virus ribozyme fused to the 3’ terminus. Following co-

infection with an attenuated T7 RNA polymerase recombinant vaccinia virus and transfection of the ten plasmid DNAs, transcripts are expressed and, with the activity of the ribozyme, processed at the 3' end generating an authentic viral genome. The virus is rescued from plaques. The accuracy of the process was confirmed with the identification of silent point mutations opportunely inserted into one of the segments (101).

The original system applied to Bluetongue virus (BTV) is different, since it is based on the transfection of *in vitro* synthesized viral RNA transcripts. Two different approaches have been developed: mixture of authentic viral transcripts derived from DLPs and T7 transcripts; or a complete set of T7 transcripts. These approaches take advantage on the discovery that the BTV transcripts are infectious once transfected on permissive cells (23). The recovery of authentic recombinant BTV was verified with the identification of mutantions opportunely inserted (22).

Concerning Rotavirus a first approach of reverse genetic was developed by Taniguchi and involves transfectionof DNA plasmid encoding one segment under the contro of the T7 polymerase and rybozime at the 3'end followed by infection with a recombinant vaccinia virus expressing T7 RNA polymerase and superinfection with a helper virus. In particular it was used a plasmid, encoding the sequence of VP4 a mAb with strong neutralizing activity against the helper virus P serotype. After several passages in the presence of the strong selective pressure of the mAb a recombinant rotavirus was obtained. However, this system is limited by the need of a helper virus and by strong selective pressure that make it impossible for non-structural proteins or other VP non directly targetable.(102).

The development of an improved reverse genetic approach for rotavirus remains a big challenge. It would be extremely useful to address several questions on the molecular biology still unresolved, and the mechanism of packaging, the reassortment of genome segments, the morphogenesis of the virus. Moreover, it would improve the design of vaccines and understand the mechanism that induce the immunity against different phenotypes.

2 MATERIAL AND METHODS

2.1 Cell culture

MA104 cells (embryonic African green monkey kidney cells) were grown as monolayers in Dulbecco's modified Eagle's medium (DMEM) containing 10% foetal calf serum (FCS) (Invitrogen), 2mM L-glutamine and 50µg/ml gentamicin (Invitrogen).

MA104 cells stably transfected with an NSP5-EGFP fusion gene were obtained by calcium phosphate procedure as described previously (55) and cultured in DMEM complete medium supplemented with 500µg/ml geneticin (G-418, Invitrogen).

For the experiment of Results2, the cells were treated with proteasome inhibitors MG132 (SIGMA),or Bortezomib (Sellek), or Epoxomicin (SIGMA) at different time point post infection with different concentration as indicated.

2.2 Virus propagation

The simian SA11 (G3, P6[1]), and porcine OSU (G5, P9[7]) strains of rotavirus were propagated in MA104 cells as described previously (59),(71).

T7-recombinant vaccinia virus (strain vTF7.3) was propagated in HeLa cells as described by Fuerst et al. (63).

Viral titres were determined by plaque assay (71) and with measurements of percentage of green cells with infection of NSP5-EGFP cells.

2.3 Construction of plasmids

pT_7v-NSP5 was obtained as previously described (60). The NSP5 gene was derived from the OSU rotavirus strain (Genbank accession number: D00474). The VP1 and VP2 genes (X16830 and L33364, respectively) were cloned from extracts of SA11 rotavirus-infected cells: viral RNA was extracted from 500µl of cell supernatant after complete cytopathic effect (CPE) had been reached. The cDNA was obtained by reverse transcription, using random hexamers (Sigma) and MuLV reverse transcriptase (Applied Biosystem) (87). The final constructs in pcDNA3 coding for VP1 and VP2 has been obtain as reported in Arnoldi et al.(6).

The constructs coding for the phosphorylation mutants of NSP5 pT_7v-NSP5/S67A and pT_7v-NSP5a were obtained as described by Eichwald et al. (54).

The pT_7v-NSP5 S42A mutant has been constructs by amplification of pT_7v-NSP5 OSU. pT_7v-NSP5 OSU was amplify by PCR with two set of primers (listed in table 1) carrying the

mutation. The two segments, NSP5 S42A I and II, were mix and amplified by PCR with specific primers to incorporate KpnI and BamHI restriction sites at the 5'and 3' ends of the NSP5 gene, respectively. The fragments was clone KpnI/BamHI into pcDNA3. The same strategy and primers were used to obtain pT_7v-NSP5-S42-67A and pT_7v-NSP5a-S42A using as DNA tamplate the pT_7v-NSP5 S67A and pT_7v-NSP5a, respectively.

To obtain pT_7v-NSP5c, pT_7v-NSP5 OSU was amplified with two set of primer listed in table 2. The segments obtained are annealed and amplified with primers containing KpnI and BamHI restriction sites to cloned the amplicon into pcDNA3. pT_7v-NSP5c was used as template DNA to construct pT_7v-NSP5c S137-142A. Primers used for this cloning are listed in table 2. All the mutants were cloned in pcDNA3 KpnI/BamHI

The pT_7v-VP6 vector was obtained by cloning the VP6 gene (L33365) from SA11 rotavirus-infected cells: the cDNA was obtained as described for VP1 and VP2 and the region spanning the open reading frame (ORF) of VP6 was amplified with primers VP6-for and VP6-rev listed in Table 2. The VP6 amplicon was cloned into the pGEM-T Easy vector, sequenced and cut with KpnI and EcoRV. It was then inserted into pT_7v-Δd81-130 [Δ3] vector previously digested with the same restriction enzymes in order to remove the insert Δ3 and allow the insertion of the VP6 amplicon.

The siRNA against the cellular kinase CK1α was as previously described by Campagna et al. (26).

The vector pcDNA3-HA-PP2A/Cα encoding the 35KDa catalytic subunit of PP2A was constructed by cloning an N-terminally HA-tagged cDNA encoding PP2A/Cα into plasmid pcDNA3, and was the kind gift of David Pim (148).

DNA TAMPLATE	PRIMER NAME	PRIMER SEQUENCE	FRAGMENT	PRIMER FINAL PCR	FINAL CONSTRUCT
pT_7vNSP5 OSU	S42A up	5'ATTGCACCAGATGCAAGAAGCATTCAATA AATACATGTTGTC3'	S42A I	KpnI ATG NSP5 NSP5StopBam HI	pT_7vNSP5 S42A
	NSP5Stop-Bam HI	5'GCGGGATCCTTACAAATCTTCGATC3'			
	S42A down	5'GACAACATGTATTTATTGAATGCTTCTGC ATCTGGTGCAAT3'	S42A II		
	KpnIATG-NSP5	5'CGGGGTACCATGTCTCTCAGC3'			
	S153-155Aup	5'GATGCTGACGCTGAAGATTATGTTTTAGA TGA3'	S153-155A BamHI		pT_7vNSP5c
	NSP5Stop-Bam HI	5'GCGGGATCCTTACAAATCTTCGATC3'			
	S163-165Adown	5'TCAGCATCTGCATCATCTAAAACATAATC TTC3'	KpnI S163-165A		
	KpnIATG-NSP5	5'CGGGGTACCATGTCTCTCAGC3'			
pT_7vNSP5 S67A pT_7vNSP5a	S42A up	5'ATTGCACCAGATGCAAGAAGCATTCAATA AATACATGTTGTC3'	S42-67A I S42Aa I		pT_7vNSP5 S42-67A
	NSP5Stop-Bam HI	5'GCGGGATCCTTACAAATCTTCGATC3'			
	S42A down	5'GACAACATGTATTTATTGAATGCTTCTGC ATCTGGTGCAAT3'	S42-67A II S42Aa II		pT_7vNSP5a S42A
	KpnIATG-NSP5	5'CGGGGTACCATGTCTCTCAGC3'			
pT_7vNSP5c	S137-142Aup	5'GATAATAAAAAGGAGAAAGCAAAGAAAGA TAAAGCTAGGAAACACTACCCGAGA3'	S137-142c I		pT_7vNSP5c S137-142A
	NSP5Stop-Bam HI	5'GCGGGATCCTTACAAATCTTCGATC3'			
	S137-142Adown	5'GTGTTTCCTAGCTTTATCTTTCTTTGCTTT CTC3'	S137-142c II		
	KpnIATG-NSP5	5'CGGGGTACCATGTCTCTCAGC3'			
	VP6-for	5'-tatcaggtaccATGGATGTCCTATACT- (KpnI)			pT_7vVP6
	VP6-rev	5'-taataagatatcTCATTTAATGAGCATGCTT- (EcoRV)			

Table 2: Primers used for the cloning of different NSP5 Ser mutants.

2.4 Productions of antibody

Anti-NSP5 and anti-NSP2 sera were produced by immunization of guinea pigs and mice (1, 6, 67). Anti-serum to VP2 was produced by immunization of guinea pigs and mice with the GST-tagged VP2/I protein fragment (amino acids 1-357). The protein was produced in the E. coli BL21 strain with a procedure similar to that used for histidine tagged VP1/I but with the following modifications: cultures were induced with 1mM IPTG for 4 hours at 25°C; the bacterial pellet was washed with ice-cold STE (10mM TrisHCl pH8, 100mM NaCl, 1mM EDTA pH8) and resuspended in STE supplemented with 0.1µg/µl lysozyme, 1X CLAP cocktail, 0.3-0.5% laurilsarcosine, and 2mM DTT for sonication; after addition of 1%

Triton X-100 in STE, GST-VP2(I) was purified from bacterial lysates by affinity chromatography using GSTrap™ HP columns prepacked with Glutathione Sepharose™ High Performance medium (GE Healthcare) and was eluted under mild, nondenaturing conditions using reduced glutathione, following manufacturer's instructions. Guinea pigs and mice were injected subcutaneously with 125µg and 40µg of protein, respectively, and boosted 3 times every 15 days (with 50µg and 40µg of protein, respectively). Sera of the immunized guinea pigs and mice were tested by Western blot on extracts of rotavirus-infected and uninfected cells.

2.5 Transient trasfction of MA104 cells

T7 RNA polymerase expressed from a vaccinia virus recombinant (63) is used to increase the expression level of proteins encoded by the transfected genes engineered downstream the T7 promoter. Since the vaccinia virus replication cycle is cytoplasmatic, exogenous gene transcription and translation are coupled in the cytoplasm of the transfected cells. For transfection experiments confluent monolayers of MA104 cells in 6-well plates (Falcon) were infected with T7-recombinant vaccinia virus [strain vTF7.3 (63)] at a multiplicity of infection (MOI) of 20 and 1 hour later transfected with a maximum total of 3µg/well of plasmid DNA (1µg of each plasmid in cotransfections) using 5µl of Lipofectamine 2000 (Invitrogen)/well and following the manufacturer's instructions. Transfected cells were harvested at 18 hours post-transfection (p.t.). For transfection of siRNAs, approximately 1.5 x 10^5 cells were transfected with 2µg of siRNAs in 1ml of serum free medium containing 5µl Transfectam reagent (Promega). After 6 hours at 37°C, cells were washed twice with serum free medium, incubated for additional 32-35 hours in medium supplemented with 10% foetal bovine serum (Invitrogen) and then infected with vaccinia virus and transfected as described above.

2.6 Cellular lysis

Lysates (corresponding to about 5x10^5 cells) were prepared in 100µl of TNN lysis buffer (100mM Tris-HCl pH8.0, 250mM NaCl, 0.5%NP40) at 4°C and were subsequently centrifuged at 2000g for 5 minutes at 4°C. Usually 10µl of supernatants were used in PAGE and Western immunoblot analyses, and 40-80µl were used for immunoprecipitation experiments. The pellets were washed 3 times with PBS (170mM NaCl, 10mM phosphate, 3mM KCl, pH 7.4) and resuspended in 20µl of loading buffer for PAGE and Western blot analyses.

Alternatively lysis was performed with hot Laemmli buffer, 100 µl of Laemmli buffer were added to the cells and the lysate were sonicated for 30" and centrifuged. Finally, 5µl of sample buffer with β-mercaptoEtOH were added to 10 µl of extract and loaded into a PA gel.

2.7 Chemical DSP crosslinkig

Dithiobis(succinimidylpropionate) (DSP) was purchased from Pierce. Monolayers of transfected cells were washed twice with PBS, overlaid with 1.5ml PBS containing 600µM DSP and incubated at 4°C for 30 minutes. After removing the reactant solution, the reaction was quenched twice with 2ml Tris Buffered Saline (TBS; 40mM TrisHCl pH8, 150mM NaCl) for 3 minutes at 4°C. Cellular extracts were prepared in 100µl TNN buffer as described above.
Cellular extracts were then prepared as described above.

2.8 Real-Time PCR

Total RNA from MA104 OSU infected cells untreated, or treated with Mg132 was extracted using phenol-cloroform exctraction, and reverse transcribed using specific primer for Rotavirus gene 11(5'-GACCGGTCACATAACTGGAGTGGGGA-3'). The cDNA was then used as a template for real-time PCR amplification to detect the expression levels rotavirus genes 11 (using SybrGreen® technology (Applied Biosystems) and specific primer sets (5'-GACCGGTCACATAACTGGAGTGGGGA-3' and 5'AGGTACCAATACGACTCACTATAGGGGGCTTTTAAAGCGCTACAG-3'). All the amplifications were performed on a 7000 ABI Prism Instrument (Applied Biosystems).

2.9 Immunoprecipitation, PAGE and Western Immunoblot analysis

Cellular extracts (usually 4/5 of the total extract, i.e. approx. 80µl) were immunoprecipitated for 2 hours at 4°C after addition of 1µl of undiluted antibody, 1µl of 100mM PMSF, 50µl of 50% protein A-Sepharose CL-4B beads (Amersham Biosciences) in TNN buffer, and 20µl of TNN buffer. Beads were then washed four times with TNN buffer, once with PBS and resuspended in 20µl of loading buffer. Sample components were separated by SDS-PAGE (using the Precision Plus Protein Standards molecular markers, Bio-Rad) and after electrophoresis transferred to polyvinylidene difluoride membranes (Millipore). The membranes were incubated with the antibodies listed in Table

3. Signals were detected by using the enhanced chemiluminescence (ECL) system (Pierce).

PRIMARY ANTIBODIES				HRP-CONJUGATED SECONDARY ANTIBODIES			
Anti:	Animal species:	Dilution used:	Source:	Anti:	Animal species:	Dilution used:	Source:
NSP5	guinea pig	1:10,000	O. Burrone	guinea pig IgG	goat	1:10,000	Jackson Immuno Research
NSP2	guinea pig	1: 3,000	O. Burrone				
NSP2	mouse	1:3,000	O.Burrone	Mouse IgG (H+L)	goat	1:5000	Jackson Immuno Research
VP2	mouse	1:5,000	O. Burrone				
SV5	mouse	1:10,000	O. Burrone				
p53	mouse	1:5,000	Santa Cruz Biotechnolog				
IRF3	mouse	1:200	Santa Cruz Biotechnolog				
Actin	rabbit	1:500	Sigma	rabbit IgG	goat	1:5,000	Thermo Scientific Pierce
GFP	rabbit	1:1,000	Santa Cruz Biotechnolog				
CK1α	rabbit	1:2,000	Santa Cruz Biotechnolog				

Table 3: List of antibody used in western blot analysis

2.10 λ-Phosphatase treatment of immunoprecipitates

70µl out of 100µl of a cellular extract obtained from transfection/infection of about $5x10^5$ cells were immunoprecipitated over night with anti-NSP5 serum and then divided in two aliquots to be incubated with or without 2µl of λ-phosphatase (400U/µl, BioLabs) in buffer for λ-phosphatase treatment (50mM Tris-HCl pH 7.5, 100mM NaCl, 0.1mM EGTA, 2mM DTT, 0.01% Brij 35) (BioLabs) supplemented by 2mM $MnCl_2$. The reaction was incubated for 2 hours at 30°C and was stopped with 10µl of PAGE loading buffer (40% glycerol, 6% SDS, 125mM Tris-HCl pH 6.8, 0.04% bromo phenol blue, 5% β-mercaptoethanol).

2.11 Indirect immunofluorescence mycroscopy

For indirect immunofluorescence microscopy, cells were fixed in 3,7% paraformaldehyde in PBS for 10 minutes at room temperature. Cover slips were washed in PBS and blocked with 1% BSA in PBS for 30 minutes and incubated with primary antibody at room temperature. After three washing in PBS, slides were incubated either with another primary antibody for double staining or directly for 45 minutes with RITC- or FITC-conjugated secondary antibodies. After three washings, nuclei were stained with Hoechst dye 2µg/ml for 10 min, washed and mounted with ProLong mounting medium (Molecular Probes). Samples were analysed by confocal microscopy (Axiovert; Carl Zeiss). The antibodies used in immunofluorescence are listed in Table 4.

The quantitative immunofluorescence was performed directly on NSP5-EGFP cells plated on 96 multiwell plate, infected, fixed with paraformaldheyde 1.8%, and stained with Hoechst at different time post infection as indicated. 16 images for each well were acquired with a molecular devices ImageXpress high-content microscope and quantification of viroplasms was performed with MetaXpress software.

PRIMARY ANTIBODIES				SECONDARY ANTIBODIES				
Anti:	Animal Species:	Dilution used:	Source:	Anti:	Conjugated with:	Animal species:	Dilution used:	Source:
NSP5	guinea pig	1:1,000	O. R. Burrone	guinea pig	RITC	goat	1:200	KPL
NSP2	guinea pig	1:200	O. R. Burrone		Alexa 647	goat	1:1000	Molecular Probes
VP2	guinea pig	1:200	O. R. Burrone					
SV5	mouse (monoclonal)	1:300	O. R. Burrone	mouse	FITC	goat	1:200	Jackson Immuno Research
VP2	mouse	1:200	O. R. Burrone		RITC	goat	1:200	Jackson Immuno Research
VP6	mouse (RV138, monoclonal)	1:50	D. Poncet					
HA	rat (monoclonal)	1:100	Roche	rat	FITC	goat	1:200	KPL

Table 4: List of antibody used for Immunofluorescence.

2.12 DLPs CsCl purification

Viral particles were purified from cell cultures after harvest at about 20 hours p.i. when almost complete CPE had been reached. Virus was pelleted by ultracentrifugation, the pellets extracted with Freon (trichloro-trifluoro-ethane, Sigma) and banded by equilibrium ultracentrifugation in CsCl gradient, essentially as described by Patton et al. (135). This allowed to obtain three well separated gradient bands containing empty particles (EPs), TLPs and DLPs. Empty particle, TLP and DLP suspensions were diluted in 20mM PIPES buffer pH6.6 containing 10mM $CaCl_2$ and pelleted by ultracentrifugation at 110,000g for 1 hour in a Beckman ultracentrifuge using an SW55 rotor. The pellets containing the different viral particles were resuspended in 35µl of water and used in *in vitro* transcription assays.

2.13 *In vitro* transcri ption assays

DLPs purified with CsCl gradient centrifugation were incubated with transcription buffer 5x (Promega); DTT (3µM); ATP, CTP, GTP 3 µM, UTP 0,3 µM (Fermentas) and UTP-[α-P^{32}] (Perkin Elmer), 40U RNAsin (Promega), DMSO or MG132 50 µM (SIGMA). The transcription mix was incubated 3-4 hours at 42°C, ultracentrifuged with Airfuge ultracentrifuge (Beckman Coulter) at 40.000 r.p.m for 1 hour. Supernatants were treated with Proteinase K 1 µg/µl for 30 min. at 37°C, spotted on a PVDF membrane, previously treated with TCA 10%, and washed several time with TCA 10%. Membranes were acquired with Instant Imager instrument (Packard) and quantification of CPM was performed with Imager software.

2.14 *In vivo* phosphorylation with ^{32}P

For in vivo phosphorylation assays, MA104 cells were infected, at 4 hours post infection were extensively washed and maintained with phosphate-free Dulbecco MEM (GIBCO) medium for one hour. The medium was adjust to 10 µg/ml with actinomicyn D, 50 µM of MG132, or DMSO, and 100 µCi of [^{32}P]orthophosphate (Perkin Elmer) per ml, at 5 h.p.i. and the lysis of the cells was performed at 6 h.p.i. The cell were lysed with TNN buffer to separate the cytoplasmic exctract from nuclei the lysate were centrifuged at low-speed. Supernatants were incubated for 30 min. with proteinase K (Invitrogen), and dsRNA was precipitated with phenol-cloroform and ethanol precipitation. Resuspeded dsRNA was electrophoresed in a 12% SDS-PAGE gel for 5 hours at 30mA.

3 RESULTS(1)

The characterization and description of the behavior of rotaviral structural and non-structural proteins during virus infection is an important goal in rotavirus studies. Different studies have revealed the relevant role of the non-structural protein NSP5 and NSP2 in Rotavirus infection, since silencing the expression of either of these proteins affects viroplasms formation, virus replication and virion production (27, 180). Furthermore, previous studies in our laboratory have characterized the interaction of NSP5 with two different viral proteins: the non-structural protein NSP2 and the viral polymerase VP1. In this section we describe the interaction of NSP5 with the structural protein VP2, that is very similar to NSP2-NSP5 interaction, and we analyze the biochemical and morphological modifications of NSP5 induced by VP2 in comparison with those induced by NSP2.
(Part of the results presented in this thesis were conducted in collaboration with Francesca Arnoldi and some experiments performed together.)

3.1 VP2 induces NSP5 to form VLS

Since the interaction between NSP5 and VP1 has been well characterized by Arnoldi et al., and VP1 and VP2 strongly interact to form the replication complex *in vitro*, we decided to better investigate the relation between NSP5 and VP2. Indeed, a weak interaction with NSP5 has been previously reported by co-immunoprecipitation of VP2 with an anti-NSP5 antibody from virus-infected cells (18). More clearly the scaffolding protein VP2 has been shown to localize in viroplasms of infected cells.
As shown by immunofluorescence analysis (Fig.11), NSP5 and VP2 expressed alone show a diffuse distribution in the cytoplasm of transfected cells, whereas cells co-transfected with NSP5 and VP2, reveal the formation of structures similar to viroplasm like structure (VLS) that are induced by co-transfection of NSP5 and NSP2. NSP5 and VP2 in VLS seem to colocalize very tightly suggesting a possible biochemical/physical interaction between these two proteins. However we observed some differences: the structures induced by VP2 are less numerous, are not uniformly distributed, have the tendency to form clusters in the cytoplasm, and are apparently larger compared to VLS induced by NSP2 (Fig.11). Based on the morphological similarity with VLS induced by NSP2, we

named these structures VLS as well, and in particular we define VLS(NSP2i) the structures induced by NSP2, and VLS(VP2i) those induced by VP2.

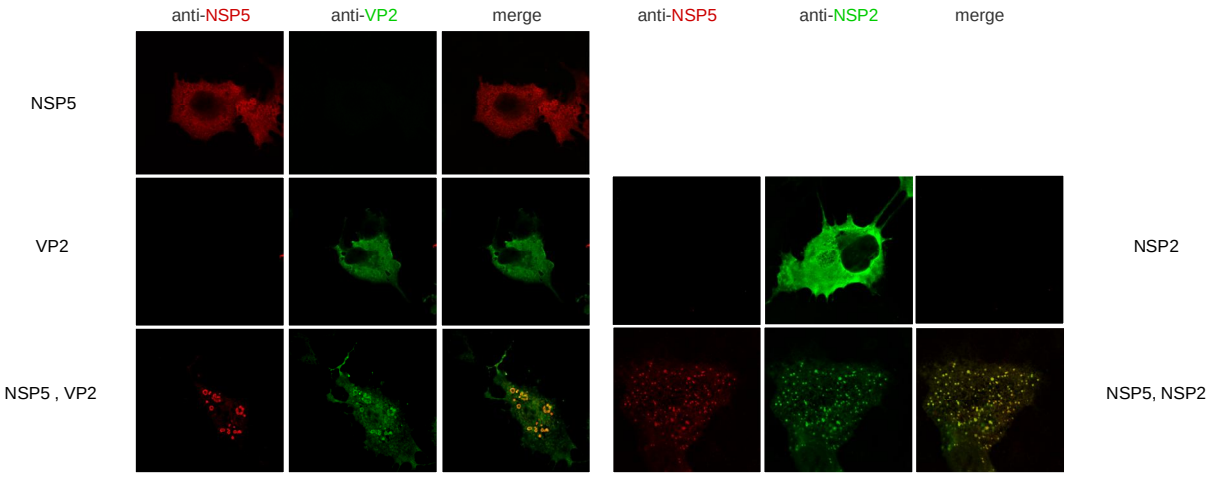

Figura 11: VLS formation. Immunofluorescence analysis of cells transfected with NSP5, NSP2, VP2 alone and co-transfected with NSP5 and VP2 or NSP2. NSP5 forms VLS, in the presence of VP2 (left panel) or NSP2 (right panel), where they co-localize. NSP5 protein is shown in red, VP2 and NSP2 in green.

Viroplasms formation teke place already at 3 hour post infection, and VP2 appears recruited in viroplasms since the very beginning of their formation. This is what happens also during VLS(VP2i) formation, since in cells co-trasfected with NSP5 and VP2 these two proteins soon interact to form VLS(VP2i) (already at 6 hour post transfection) suggesting that this interaction is not mediated by other viral protein (Fig 12).

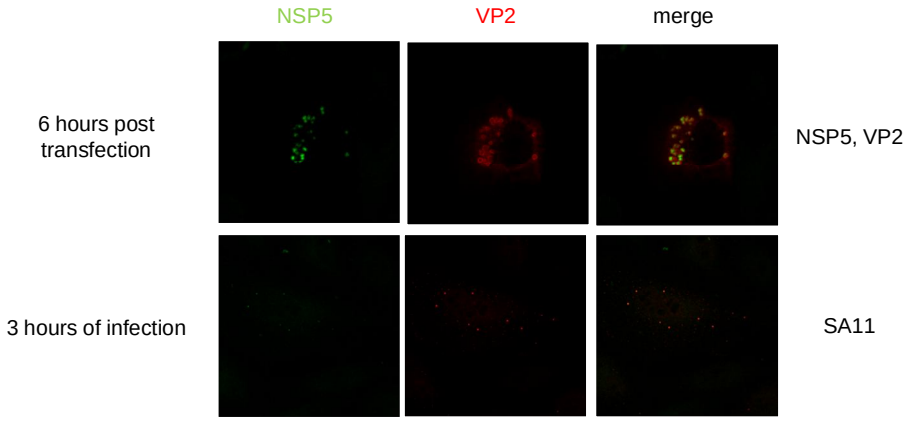

Figure 12: Timing of VLS formation. Immunofluorescence analysis of MA104 cells at 6 hours post transfection with NSP5 and VP2 (upper panel) or at 3 hours post infection with Rotavirus. NSP5 protein is shown in green, and VP2 in red.

3.2 VP2 induces NSP5 hyperphosphorylation

In order to characterize NSP5-VP2 interaction we performed biochemical analysis in both infected and trasfected cells. Western blot of extracts of cells transfected with plasmids encoding NSP5 and VP2 show a significant increase on NSP5 hyperphosphorylation. When plasmid encoding the viral protein NSP5 is transfected alone in uninfected cells, a single band at 26KDa and a weaker band at 28 KDa are visible in western blot analysis (Fig.13 lane 4), while when co-expressed with VP2 the pattern of NSP5 post-translational modifications highly resembles that found in infected cells: a weak band of 26 KDa is still present together with a very strong one of 28KDa, and a series of higher molecular weight bands ranging from 30 to 34 KDa (Fig.13 lane 5).

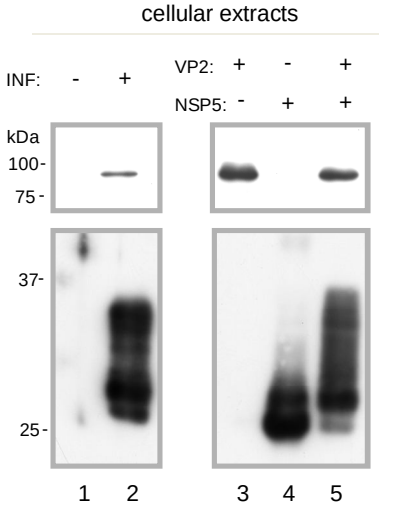

Figure 13: Hyperphosphorylation of NSP5 induced by VP2. Western blot analysis of extracts of MA104 cells infected with Rotavirus or transfected with NSP5 or/and VP2. The hyperphosphorylation of NSP5 induced by VP2 resembles that observed during normal infection.

To confirm that the NSP5 modifications is due to an increased hyperphosporylation, we performed both *in vitro* and *in vivo* phospatase assays. Extracts immunoprecipited with anti-NSP5 serum were incubated with lambda-phospatase at 37°C for 30 minutes. Western blot analysis of NSP5 clearly revealed that the NSP5 profile was reduced to a band of 26 KDa in correspondence to the sample of cells co-transfected with NSP5 and VP2 (Fig.14A).

To investigate the hyperphosphorilation induced by VP2 *in vivo,* NSP5 and VP2 were co-transfected with a plasmid encoding the catalityc subunit of PP2A phosphatase, a serine/threonine phosphatase with a broad substrate specificity. The presence of PP2A phosphatase induced a decrease in NSP5 hyperphosphorylation, in particular the isoforms of higher molecular weight which seem to disappear, and an inversion of the relative intensity of the bands of 26KDa and 28KDa (Fig.14B). All these observations confirmed

that NSP5 modifications induced by VP2 were the conseguence of hyperphosphorylation event.

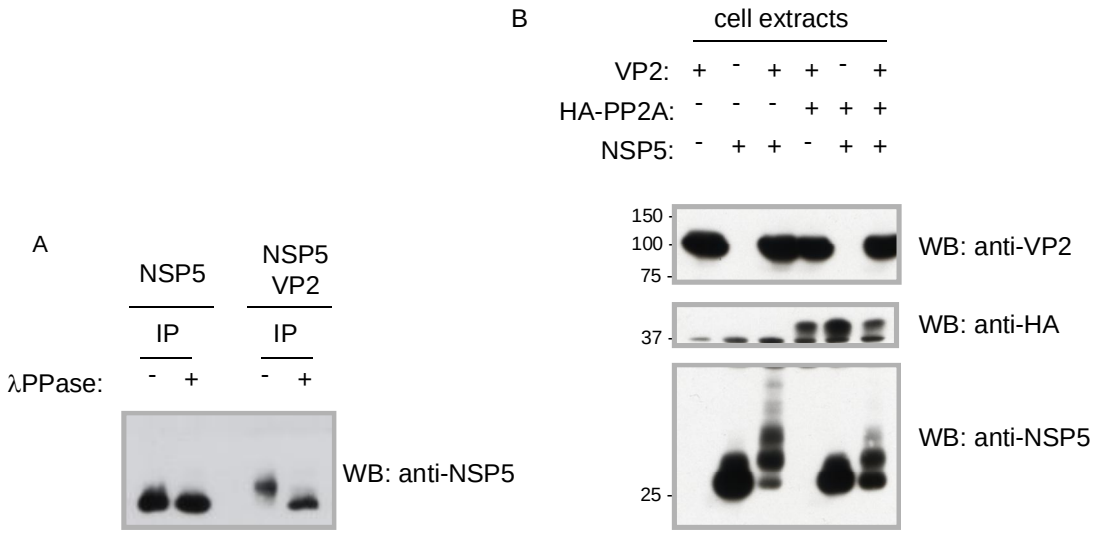

Figure 14: *In vitro* and *in vivo* phosphatase assays. A) Western blot analisys of NSP5 immunoprecipitated extracts, of MA104 cells transfected with NSP5 and NSP5, VP2. Immunoprecipitates are treated or not with λ-phosphatase before loading. **B)** Western blot analysis of extracts of cells transfected with different combination of NSP5 and VP2, in the presence, or not, of the tagged catalytic subunit of PP2A phosphatase. The expression of the phosphatase change the pattern of NSP5 hyperphosphorylation induced by VP2.

The cellular kinases involved in this process are still unknown. According to previous studies in our laboratory in which an involvement of the kinase CK1α on the initiation of NSP5 hyperphosphorylation during rotavirus infection was demonstrated (26), we investigated the possible involvement of this kinase on NSP5 hyperphosphorylation induced by VP2. For this purpose cells were transfected with an RNAi to specifically silence CK1α, and then transfected with plasmids encoding NSP5 and VP2. As shown in figure 15, despite efficient silencing of CK1α, NSP5 hyperphosphorylation induced by VP2 was not impaired and the electrophoretic mobility of NSP5 was similar to that found in cells treated with an irrelevant siRNA (Fig.15). These observations suggest that the kinase CK1α is not involved in the NSP5 hyperphosphorylation induced by VP2 and other kinases would be involved in this process.

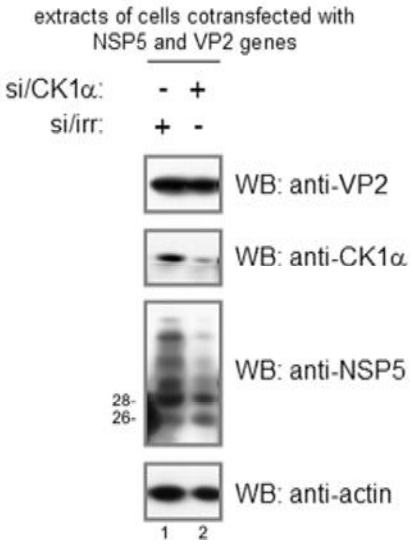

Figure 15: Involvment of CK1α on NSP5 hyperphosphorylation induced by VP2. Western blot analysis of cells transfected with NSP5 and VP2 and treated with a siRNA specific for CK1α or an irrelevant siRNA. Silencing the expression of CK1α does not impaired NSP5 hyperphosphorylation induced by VP2.

3.3 Mapping NSP5 hyperphosphorylation induced by VP2

NSP5 is rich in serine and threonine residues, that are good targets for phosphorylation events. We constructed a series of serine mutants in order to characterize the main residues involved in the hyperphosphorylation induced by VP2. Previous studies in our laboratory attempted to identify the serine residues involved in NSP5 hyperphosphorylation induced by NSP2, using both deletion mutants and Ser to Ala mutants in defined positions (54),(56). In particular NSP5 has been arbitrarily devided in five regions (1-4 and the tail T) and deletion mutants for all single regions have been constructed. These mutants were tested for their ability to be hyperphosphorilated in the presence of NSP2. From those studies, it was observed that the mutants lacking the region between residues 30-81 (region2) and the one lacking residues 131-181 (region 4) were not hyperphosphylated in vivo when expressed with NSP2. One particular residue (Ser67) was identified as the responsible for the initiation of a hyperphosphorilation cascade induced by NSP2 (54). Some of these mutants were also tested in the VP2 induced hyperphosphorylation.

Figure 16 shows a schematic representation of the NSP5 serine mutants used in these experiments.

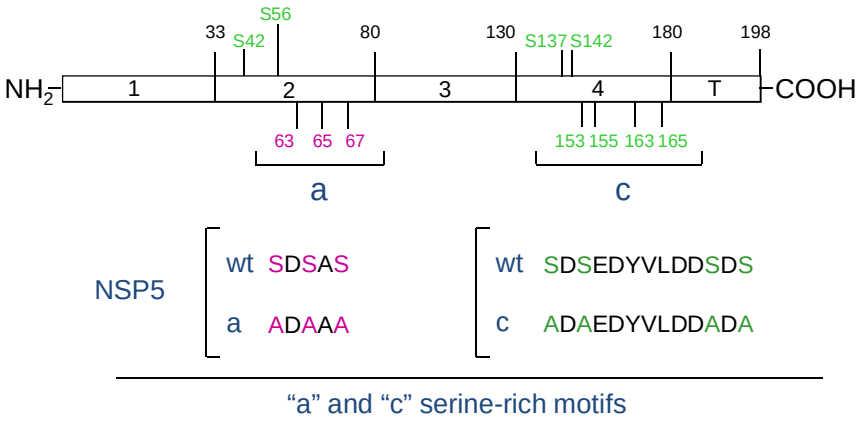

Figure 16: Schematic rappresentation of NSP5 Ser mutants. NSP5 has been arbitrarily devided in five regions (1-4 and the tail T) and deletion mutants for all single regions have been constructed

The first class of mutants we took into consideration was the one involving Ser67 residue, that is inserted in a serine rich motif. We analysed two different mutants: NSP5-S67A where the serine in position 67 was mutated into alanine preventing in this way NSP5 hyperphosphorylation, and NSP5-S67D with Ser67 mutated into aspartic acid, and two other serines of the motif mutated into Asp, to mimic a phosphorylated serine, resembling in this way the phosphorylated protein (54). By WB analysis, NSP5-S67A, that is not phosphorylated when expressed alone, becomes only partially phosphorylated, in a clearly distinct way as compared to the wt protein, when co-expressed with VP2 (Fig.17 lane11). In particular the 26KDa isoform was the main band observed together with a weaker band of 28 KDa. This result confirms the important role of Ser67 in initiating hyperphosphorylation, but suggesting that other residues could also be involved in the initiation events induced by VP2. On the other hand, mutant NSP5-S67D was already phosphorylated when expressed alone (Fig.17 lane 9) and when co-expressed with VP2 its phosphorylation profile increased producing a pattern similar to the wt protein in the presence of VP2 (Fig.17, lane 18). Together with serine 63 and serine 65, serine 67 forms one of the serine rich motif present in NSP5 that we named motif "*a*" (**S**D**S**A**S**). The mutant with all the serines in motif *a* mutated into alanine (named NSP5a) upon co-transfection with VP2 presented a pattern of phosphorylation very similar to mutant S67A, confirming the dominant role of serine 67 in promoting the formation of higher molecular weight NSP5 isoforms (Fig.17, lane 12). These observations suggest that the mechanisms of initiation of NSP5 hyperphosphorylation are similar regardless the inducer of hyperphosphorylation is NSP2 or VP2.

Following preliminary mass spectrometry analysis of different NSP5 isoforms from infected cells (F.Rossi graduation thesis), we observed that residue Ser42 was phosphorylated as well. To investigate the possible involvement of this residue in the hyperphosphorylation induced by VP2 we constructed Ser 42 to Ala mutant and analysed by western blot the effect of co-expression with VP2. As showed in figure 17 (lane13) the same pattern as the wild type protein co-expressed with VP2 was observed, so this mutant does not produce a particular phenotype, different from the wild type protein, when expressed with VP2 suggesting that this residue is not critical for the initiation of hyperphosphorilation induced by VP2. Furthermore we constructed the double mutant NSP5 S42-67A and the quadruple mutant NSP5a-S42A, in order to investigate the role of Ser67 in the context of mutated Ser42. Both these mutant upon co-expression with VP2 showed a similar pattern: a strong band at 26KDa with a minor band at 28KDa. The insertion of S67A mutation into NSP5 S42A mutant, promotes more accumulation of the 26KDa isoform respect to the 28 KDa one, and does not allow the appearance of higher molecular weight NSP5 isoforms (Fig17 lanes 14,15). All these data confirm the dominant role of Ser67 in initiating NSP5 hyperphosphorylation induced by VP2, as it happens for hyperphosphorylation induced by NSP2.

Based on previous studies, we took into consideration another serine rich motif, named motif "*c*", present in a particular acidic context (AD**S**D**S**EDYVLDD**S**D**S**DDG) located towards the C-terminal of NSP5 protein.(The region of NSP5 that we named tail does not contain any Ser residues.) The mutant with all the serine in motif *c* mutated into alanine, is indicated as NSP5c and it was tested for the ability to be hyperphosphorylated in the presence of VP2, as well.

When NSP5c is co-expressed with VP2, it is hyperphosphorylated in a way similar to the wt protein, confirming that even if these mutated residues are involved in the hyperphosphorylation induced by VP2, they do not induce a change in NSP5 pattern (Fig 17, lane 16). Furthermore we mutated two other serine residues (Ser 137, Ser 142) situated in the proximity of motif c, creating the mutant NSP5c S137/142A. It is important to note that in this way region 4 has all the serine mutated into alanine. Anyway, neither this mutant has its hyperposphorylation impaired when co-expressed with VP2 (Fig. 17 lane 17).

Taken together all these results, we can summarize that the phosphorylation of residues situated in region 4 of NSP5, are not involved in the initialization of NSP5 hyperphosphorylation induced by VP2. In contrast mutants with serine 67 mutated into

alanine are the only ones that present impaired hyperphosphorylation when co-expressed with VP2, although we never observed a complete non-phosphorylated protein. Once more, this confirm the relevant role of Ser67 in the initialization of NSP5 hypersphorylation, and moreover that other serine residues could be involved in this event.

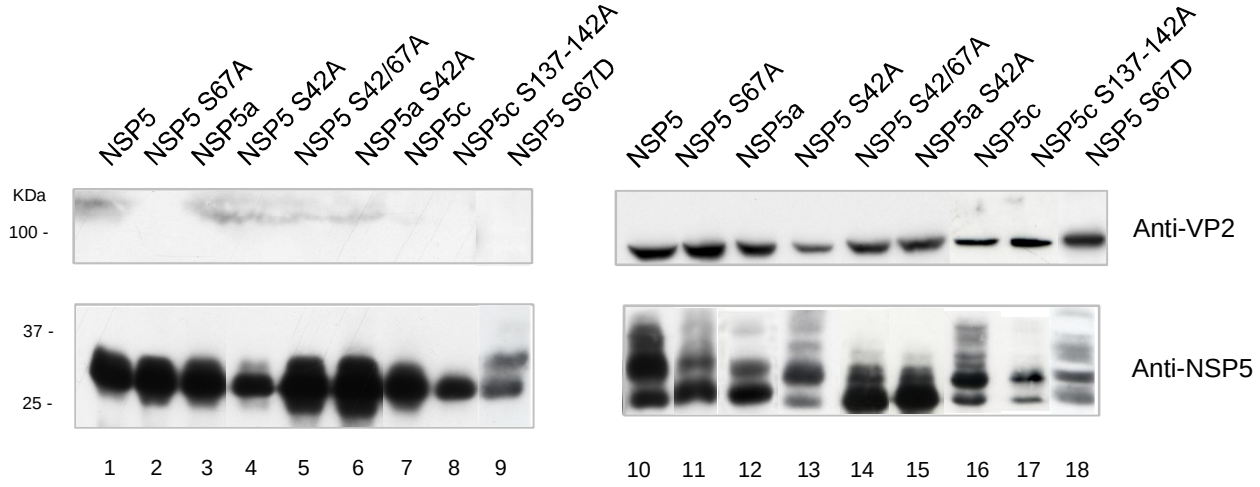

Figure 17: Hyperphosphoryation NSP5 Ser mutants induced by VP2. Western blot analysis of extracts of cells transfected with NSP5 and NSP5 Ser mutants alone (left panel) or in the presence of viral core protein VP2 (right panel). None of the NSP5 Ser mutants shows a complete non-phosphorylated phenotype, however mutants with Ser67 mutated into alanine show the more impaired phosphorylation confirming the important role of Ser67 in the initiation of hyperphosphorylation events.

3.4 Correlation between NSP5 hyperphosphorylation and VLS

As previously described, VP2 induces both VLS formation and NSP5 hyperphosphorylation. Moreover, NSP2 was first seen to induce VLS when co-transfected with NSP5, and it was demonstrated that this event is independent from NSP5 hyperphosphorylation induced by NSP2, using serine 67 mutants (54).

We investigated the possible correlation between VLS formation and hyperohosphorylation induced both by VP2 and NSP2. For this purpose, we performed immunofluorescence assays to follow VLS formation when NSP5 hyperphosphorylation was impaired.

Hereafter we indicate different methods we have used to impaired NSP5 hyperphosphorylation.

1. Since NSP5 hyperphosphorylation induced by VP2 is affected by the co-expression of the catalytic subunit of PP2A phosphatese (Fig 14), we characterized the effect on VLS formation in the same conditions. As shown in figure 18A, when NSP5 and

PP2A were co-expressed in uninfected cells, they both presented a diffuse distribution, while in the cytoplasm of cells co-transfected with NSP5,VP2 and PP2A, we observed the typical VLS formation. The same happens when we co-transfected NSP5 and NSP2 with PP2A: we observed a reduction of NSP5 hyperphosphorylation induced by NSP2 (Fig.18B) and, despite the inhibition of NSP5 hyperphosphorilation, in immunofluorescence assays we can still observed the typical formation of VLS (Fig.18C). This means that the reduction of NSP5 hyperphosphorylation due to the presence of PP2A in both cases does not influence VLS formation. Alternatively since the inhibition of NSP5 hyperphosphorylation by PP2A was not complete, it is possible that small amounts of phosphorylated NSP5 are sufficient to induce the formation of VLS.

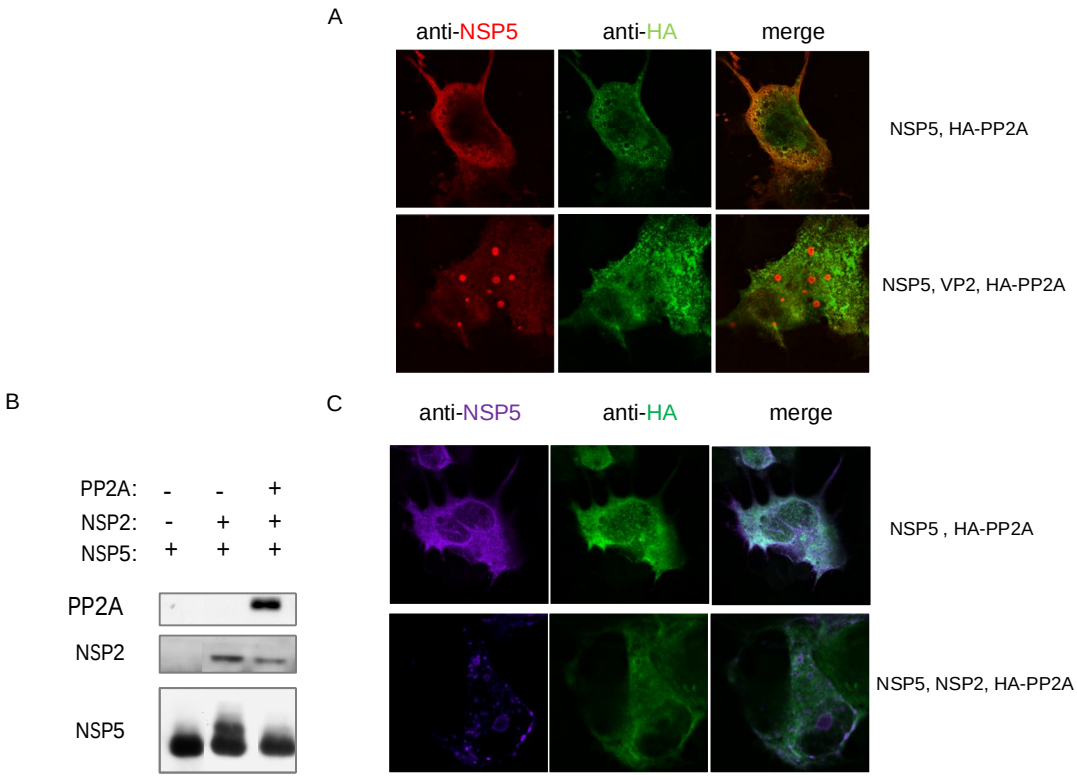

Figure 18: **VLS formation and NSP5 hyperphosphorylation.** B) Western blot analysis of extracts of cells transfected with NSP5 alone or co-trasfected with NSP2, in the presence, or not, of tagged catalytic subunit of PP2A phosphatase. A), C) Immunofluorescence analyisis of cells transfected with NSP5 alone (shown in red B) or in purple C)) or co-transfected with NSP5 and VLS inducers in the presence of tagged PP2A (shown in green in borh B) and C)). Despite the presence of the catalytic subunit of PP2A, there is still formation of VLS.

2. We had observed, not without surprise, that the expression of the viral polymerase VP1, together with NSP5 and VP2, affects NSP5 hyperphosphorylation induced by

VP2 (Fig.19A). This particular effect of VP1 polymerase is evident in the contest of NSP5 hyperphosphorylation induced by NSP2, as well. (Fig.19B), and is still under investigation. Since it has been demonstrated a strong interaction between NSP5 and VP1 (6), it is possible that the polymerase sequesters NSP5 to the effect of cellular kinase and/or VP2 and NSP2. It has been demonstrated that co-transfection of NSP5 with VP1 leads to a diffuse distribution of both proteins. However, the co-expression of NSP5 and VP1 with VP2 or NSP2, not only does not inhibit VLS formation, but induces recruitment of VP1 with a clear co-localization in VLS together with NSP5 and VP2 or NSP2 (Fig.19D).

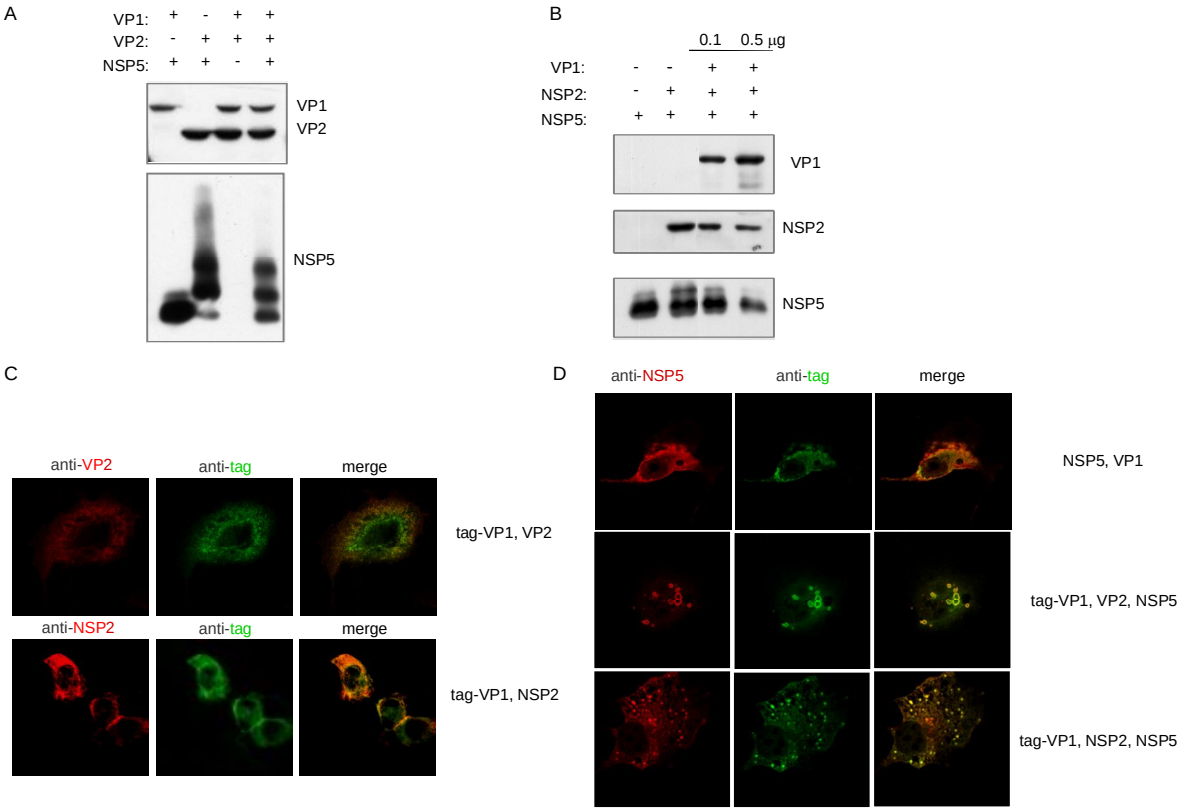

Figure 19: VLS formation and NSP5 hyperphosphorylation. A), B) Western blot analysis of extracts of cells transfected with different combinations or rotavirus proteins NSP5, VP2, NSP2 and tag-VP1,as indicated. VP1 affects NSP5 hyperphosphorylation induced by both VP2 or NSP2. **C) D)** Immunofluorescence analysis of cells transfected as indicated. VLS still form in the presence of VP1. Tag-VP1 is shown in green, VP2, NSP2 and NSP5 were labeled in red in C) and D) respectively.

3. The different NSP5 serine mutants, previously analysed with impaired VP2 induced hyperphosphorylation, were tested for their ability to form VLS (VP2i). Immunofluorescence experiments revealed that none of them have affected their

capacity to form VLS (VP2i). In particular, all the mutants that present the mutation in Ser67, that in co-expression with VP2 presented a more affected hyperphosphorylation pattern with respect to the others, still formed VLS in the cytoplasm of cells co-transfected with VP2.(Fig.21A). According to the data obtained for hyperphosphorylation induced by VP2, we analysed whether the same serine mutants would affect NSP5 hyperphosphorilation induced by NSP2, and the formation of VLS(NSP2i). As shown in figure 20, NSP5 S67A, NSP5a an NSP5c are the only serine mutants that have their hyperphosphorylation impaired when co-expressed with NSP2, as expected from previous studies (54). Whereas NSP5 S42A , NSP5 S42/67A, and NSP5a-S42A mutants when co-trasfected with NSP2 show the same pattern as they are co-transfected with VP2. Despite the different degree of hyperphosphorylation, all these mutants when express with NSP2 still form VLS(NSP2i). (Fig.21B)

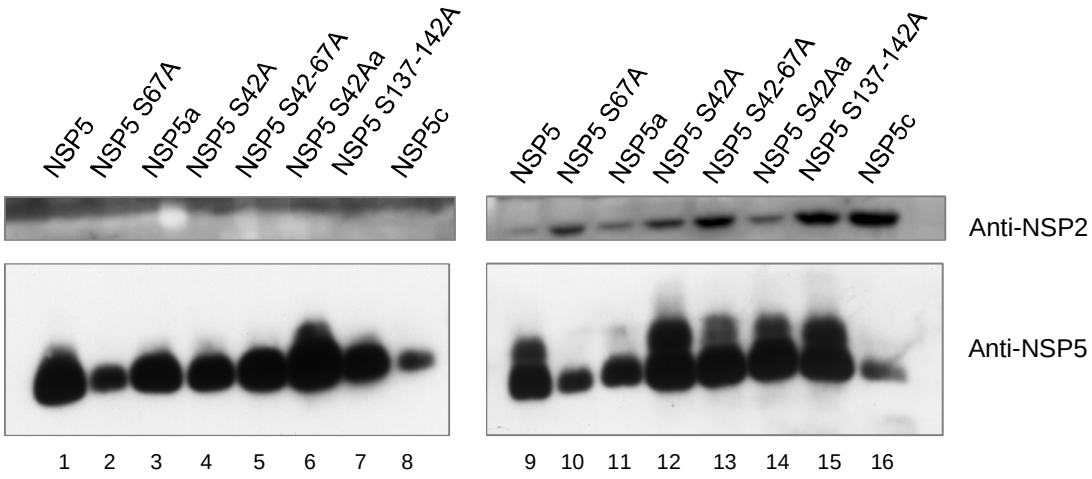

Figure 20: Hyperphosphorylation of Ser mutants induced by NSP2. Western blot analysis of NSP5 Ser mutants expressed with NSP2. As expected from previous data, only mutants with Ser67 mutated into alanine present a non-phosphorylated pattern. In addition NSP5c appears not to be phosphorylated in the presence of NSP2.

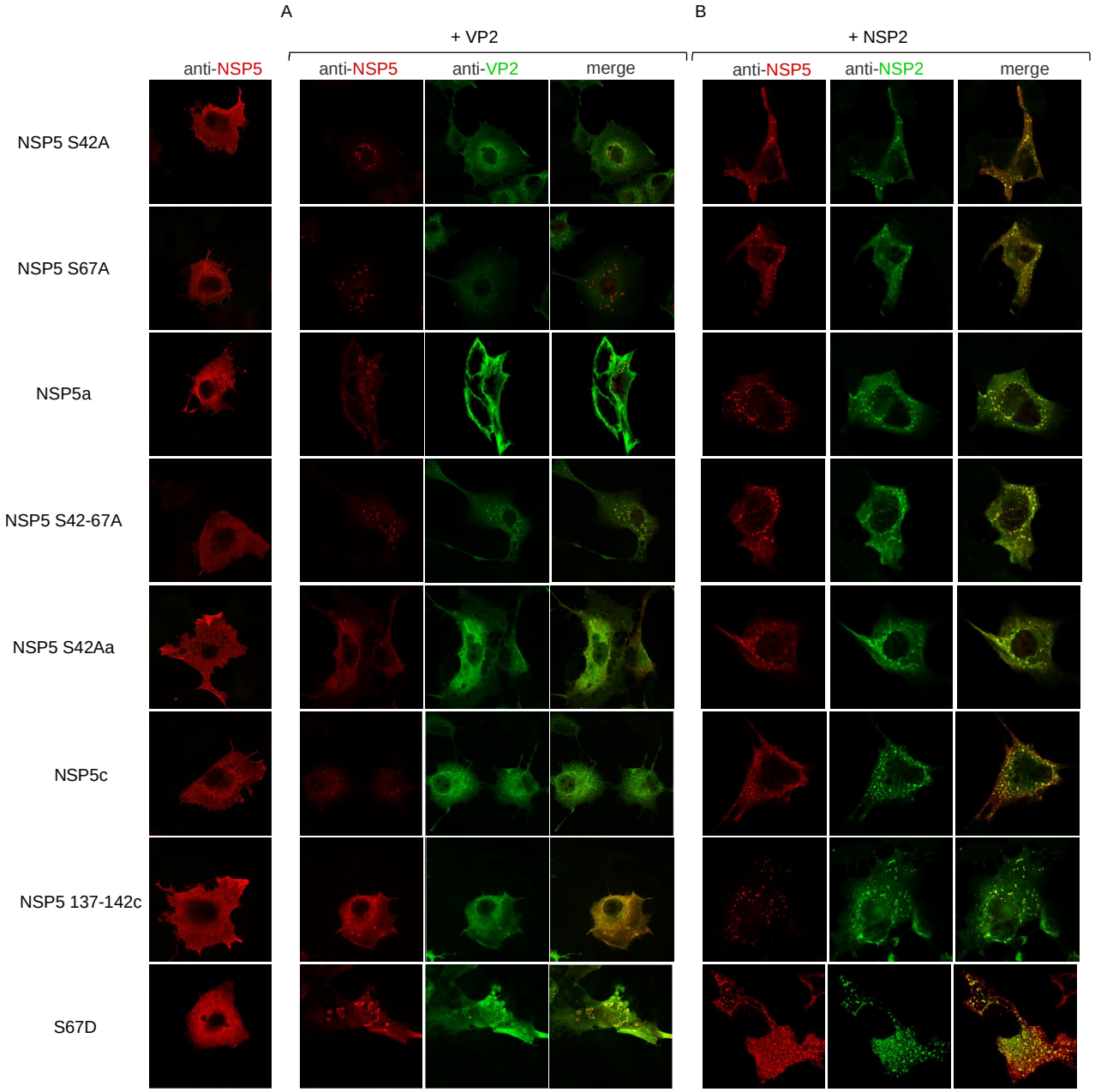

Figure 21: VLS formation of NSP5 Ser mutants. Immunofluorescence analysis of different NSP5 Ser mutants expressed alone (left column) or in the presence of VLS inducers. All Ser NSP5 mutants form VLS when expressed with VP2 or NSP2. NSP5 is shown in red, VLS inducers are shown in green.

Following these analyses, we can conclude that VLS(VP2i) and VLS(NSP2i) are similar, not only from a morphological point of view, but even they behave in the same way when subjected to treatments that impared NSP5 hyperphosphorylation, suggesting their independence from hyperphosphorylation degree of NSP5. In all the conditions analysed, NSP5 hyperphosphorylation was differently affected but we have not observed impaired VLS formation. This suggests that these two events are not strictly correlated. However we cannot draw a definitive conclusion since we never had a complete inhibition of NSP5

hyperphosphorylation in all the examples described, and it is therefore still possible that a weak phosphorylation is sufficient to drive VLS formation.

3.5 Towards viroplasms re-building:recruitment of different viral proteins into VLS

Viroplasms formation during infection is an event not entirely elucidated. It is known that within these structures both structural (VP1, VP2, VP3, VP6) and non-structural proteins (NSP2, NSP5) localize, but the mechanism underlining recruitment of the different components for viroplams assembly and the single protein function inside viroplasms is still an open question. Following the observations presented till here, VLS represent, from a morphological point of view, the more similar structures to viroplasms so far described. They could be consider as empty viroplasms in the sense that they would not contain the dsRNA viral genome. For this reason they could be studied as a valid model to investigate recruitment of viral proteins and viroplasm assembly, with the final aim to understand the role of different viral proteins within viroplasms, and to investigate the recruitment of viral mRNA, which in viroplasm functions as templates for the polymerase to produce the dsRNA of the viral progeny.

Since we have identified two different types of VLS, produced by two different inducers NSP2 and VP2, we investigated whether there are differences between VLS(VP2i) and VLS(NSP2i) in their ability to recruit other viral proteins. For this analysis we used a stable cell line (MA104 NSP5-EGFP) expressing the fusion protein NSP5-EGFP. The fluorescence of NSP5-EGFP becomes visible clearly upon rotaviral infection, when NSP5-EGFP, which has an otherwise diffuse distribution, concentrates in viroplasms (Fig.22A). We also tested this cell line for the ability to form VLS when co-transfected with one of the VLS-inducers. As shown in figure 22B, both VLS(NSP2i) and VLS(VP2i) are formed when either NSP2 or VP2 are expressed in the NSP5EGFP stable cell line. It is important to note that, although NSP5-EGFP protein is sufficient to form VLS when co-expressed with VLS inducers, in trasfection experiment it was preferable to co-transfect also the NSP5 wild type protein to improve the visualization and formation of VLS.

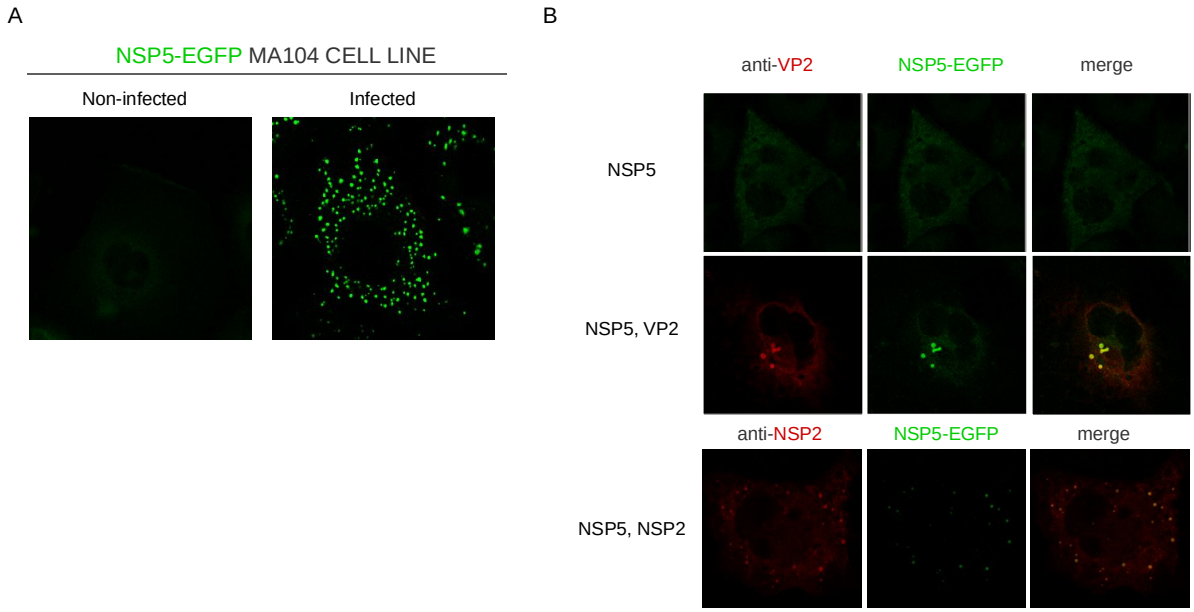

Figure 22: NSP5-EGFP cell line. A) Immunofluorescence images of infected NSP5-EGFP cell line, the NSP5-EGFP protein stably expressed concentrates into viroplasm of infected cells. **B)** Immunofluorescence of NSP5-EGFP cells transfected with NSP5 alone or in the presence of VLS inducers. NSP5-EGFP protein concentrates into VLS.

As expected, the two inducers, NSP2 and VP2 co-localized within VLS. Moreover, when both NSP2 and VP2 were co-transfected into the NSP5-EGFP cell line, VLS were formed with the co-localization of the three components. This indicate that both NSP2 and VP2 collaborate in VLS formation, and that neither of the two inducers inhibits the recruitment of the other into VLS (Fig.23).

We have already demonstrated that tag-VP1 is recruited in VLS (NSP2i), co-localizing with NSP5 and NSP2 (6). Previous data showed that the same happens when tag-VP1 is co-expressed with NSP5 and VP2 in VLS(VP2i), despite the inhibitory effect upon NSP5 hyperphosphorilation induced by NSP2 and VP2 (as shown previously in Fig.19) Figure 23 shows the co-localization of tag-VP1 in both VLS(VP2i) and VLS(NSP2i).

Since the middle layer protein VP6 localizes in viroplasms during infection, we investigated whether it was also recruited into VLS. It has been demonstrated that VP6 forms tubular structures when trasfected in cells (89) and this particular distribution is maintained when VP6 is co-expressed with NSP5. While, following co-transfection with NSP5 and VP2 (in NSP5-EGFP stable cell line) VP6 changes its tubular organization and it gets recruited into VLS(VP2i) (Fig.23). We analyse the distribution of VP6 in cells expressing NSP2 and NSP5, as well, and, differently from VLS(VP2i), VP6 remains organized in tubular structure and was not recruited into VLS(NSP2i) which were nevertheless formed (Fig.23). This is

not surprising since VP2 and VP6 physically interact to form DLPs and this interaction would be also present within VLS (VP2i), while no interaction has been described between NSP2 and VP6. This suggests that the structural protein VP2 is the driving force that lead to the recruitment of VP6 into VLS.

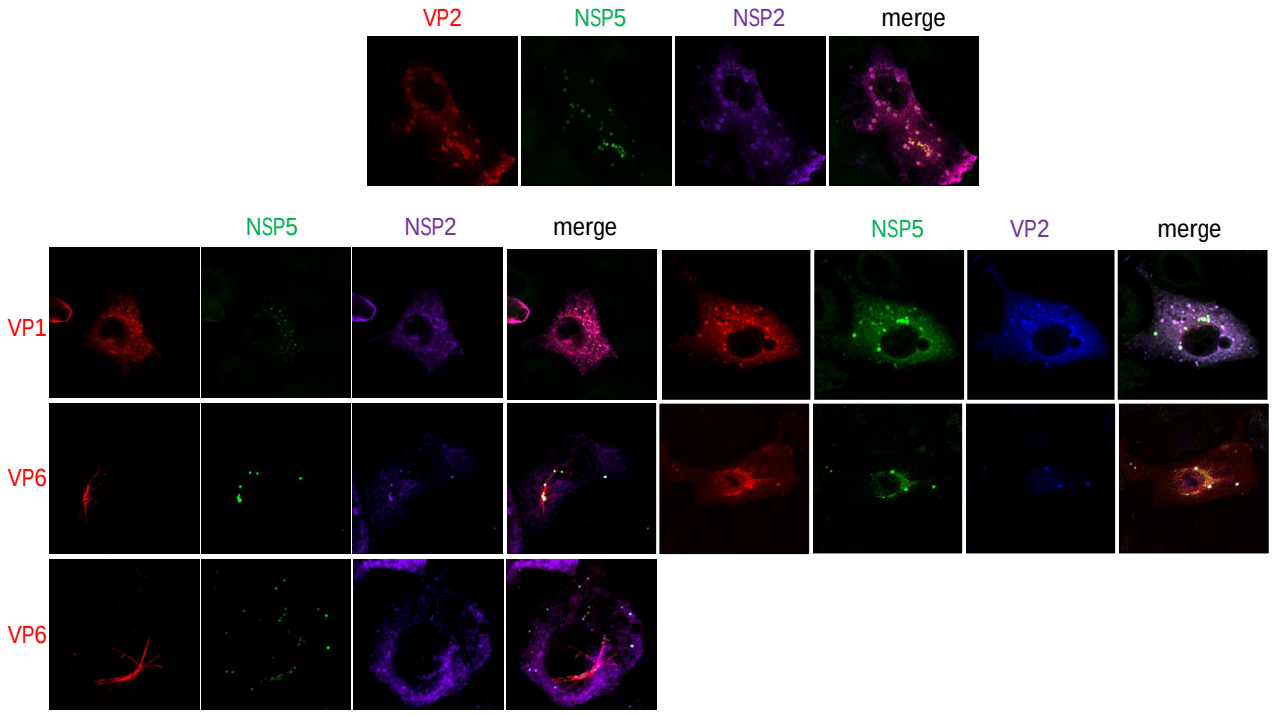

Figure 23: Recruitment of viral proteins into VLS. Immunofluorescence analysis of NSP5-EGFP cell line transfected with different combinations of viral proteins as indicated. NSP5-EGFP is shown in green, NSP2 in purple (left panel), VP2 in blu (right panel), tag-VP1 and VP6 are shown in red in both panels.

The immunofluorescence assays described indicated a complex macromolecular association among the different viral proteins within VLS. For this reason we wanted to verify these associations carring out co-immunoprecipatation experiments.

The interaction between NSP5 and NSP2 in infected cells is well documented in experiments of immmunoprecipitation with anti-NSP5 serum. (1)

The strong interaction between NSP5 and VP1 has been well described by Arnoldi et al. In some cases, in particular when using a polyclonal anti-NSP5 serum, co-immunoprecipitation of NSP5 and VP1 from co-transfected cell extracts was obtained only when cells were previously treated with the chemical crosslinker DSP. Immuniprecipitations performed on extracts cells co-transfected with NSP5 and VP2 genes, with both anti NSP5 or anti-VP2 sera, failed to co-immunoprecipate these proteins

in spite of good expression levels of both proteins, and regardless of the pretreatment with or without DSP crosslinker (Fig.24). As expected from control experiments from extracts of infected cells with anti-NSP5 serum did not succeed to co-immunoprecipitate VP2, even following DSP treatment (only NSP2 and VP1 are co-immunprecipitated in these conditions (not shown)) (6)(6).

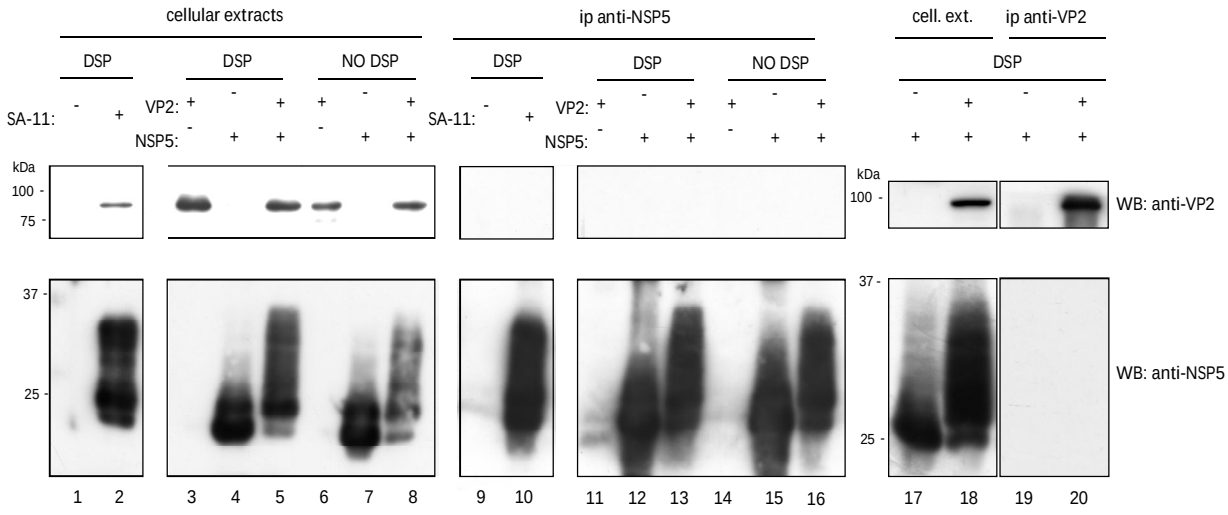

Figure 24: Interaction between NSP5 and VP2. Western blot analysis of immunoprecipitated extracts with both NSP5 serum and VP2 serum. Cells were infected or transfected with NSP5 and/or VP2, and treated, or not, with chemical crossliker DSP. Even the treatment with DSP does not elicit the co-immunoprecipitation of the two proteins.

The failure in our attempts of coimmunoprecipitating viroplasmic proteins might be due to methodological limitation such as lysis conditions, extraction, or most likely, the type of antibody used for immunoprecipation. For these reasons, we also performed co-immunoprecipitations with monoclonal antibodies against NSP5 recently isolated in our laboratory. One out of five monoclonal antibodies tested (mAb 1B7) gave promising results in co-immunoprepitating NSP5 with other viral proteins present in VLS, without any chemical crosslinking.

As shown in figure 25B, tag-VP1 is well co-immunoprecipitated, when co-trasfected with NSP5, (lane 17) and also when co-expressed with different combinations of NSP5 and VP2/NSP2/VP6 in comparable amount.

This antibody, however, does not have the same efficiency to co-immunoprecipitate VP2. Indeed only a faint band of immunoprecipitated VP2 is visible in correspondence of NSP5-VP2 co-trasfected cells (Fig.25B, lane 15). The co-expression of VP6 together with NSP5 and VP2 substantially increases the amount of VP2 protein co-immunoprecipitated,

suggesting that VP6 stabilizes VLS and the interaction between NSP5 and VP2 (Fig.25B lane 20). Importantly, we have excluded the possible unspecific interactions of VP6 trimers, or VP2-VP6 empty particles, with 1B7 antibody (not shown).

On the contrary, the co-expression of tag-VP1 with NSP5 and VP2 has the opposite effect. Indeed while an efficient immunoprecipitation of tag-VP1 takes place we can hardly appreciate the band corresponding to VP2 when all three proteins are co-expressed (fig.25B lane 19). This observation is in part consistent with the inhibitory effect of tag-VP1 on NSP5 hyperposphorylation induced by VP2, due to the strong interaction between NSP5 and the viral polymerase VP1. The dominant role of NSP5-VP1 interaction was also evident in the sample in which all the other viroplasmic components in different combination (VP2/NSP2/VP6) were also expressed (Fig.25B lane 25).

With respect to NSP2, its co-immunoprecipitation with mAb 1B7, was not very effective. Only a low amount of NSP2 was co-immunoprecipated when co-trasfected with NSP5 (Fig.25B lane 16). The amount of co-immunoprecipitated NSP2 does not change whether it is express with tag-VP1, but it shows a slight increase when express together with NSP5 and VP6 (Fig.25B lane 21-22).

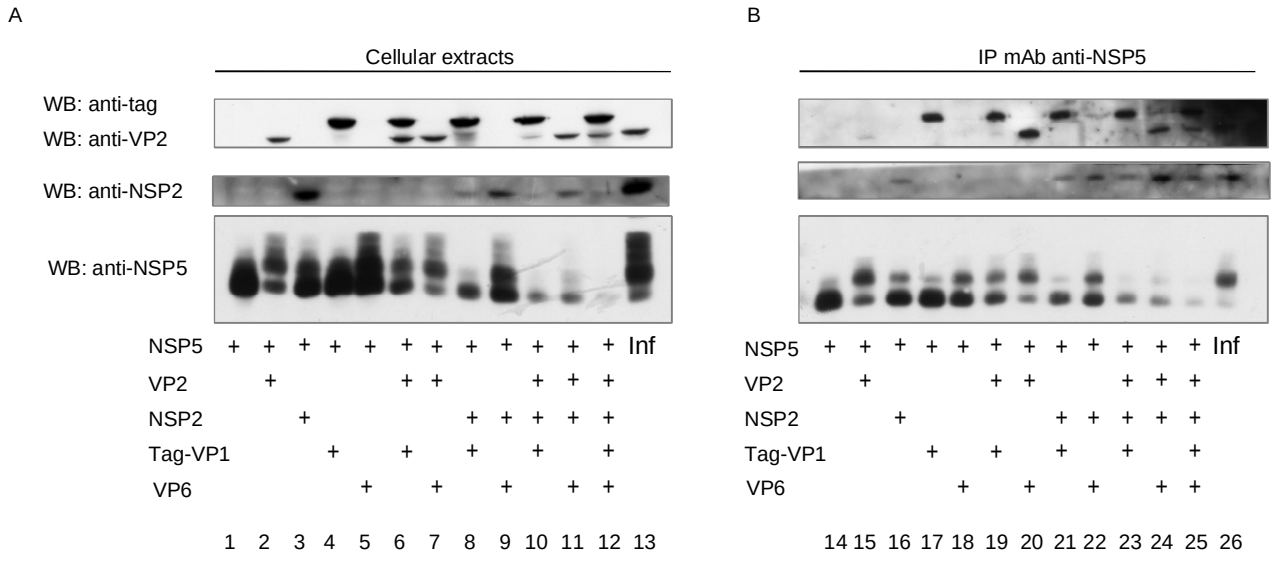

Figure 25: Interactions between VLS components. Western blot analysis of extracts (A) and immunoprecipitated (B) with mAb 1B7, of cells transfected with NSP5 and different combination of viral proteins.

We cannot exclude that the epitope, recognized by mAb 1B7, corresponds to the region of interaction between NSP5 and NSP2 or VP2 and, for this reason, 1B7 would have a dissociating function for these protein. However, it is clear that VP1 strongly interacts with NSP5 and function as a dissociating protein towards NSP2 and VP2. On the contrary, VP6

stabilized the interaction of NSP5 with both NSP2 and VP2, suggesting that one of the role of VP6 protein within viroplasms would be to stabilize the entire structure and to strongly associate all viroplasmic components.

4 DISCUSSION (1)

During Rotavirus infection the replication of viral genome occurs within viroplasms. In these structures different viral proteins converge to support viral replication and virus assembly. In particular, the localization of the two structural protein sufficient to support viral replication VP1 and VP2 has been demonstrated (141), and also of the two non-structural proteins NSP2 and NSP5, although their function at this level has not been completely characterized. NSP2 and NSP5, transiently transfected in the absence of other viral proteins, form cytoplasmic structures, similar to viroplasms, named VLS where they both localized (60). Moreover, the interaction between NSP5, NSP2 and VP1 has been recently described (6).

In this work we wanted to characterized the relationship between NSP5 and the structural protein VP2, comparing it with the very similar one of NSP5 and NSP2. The involvement and the influence of other viral proteins in these interactions have also been taken in consideration to better characterized the distribution and connection between the different viral proteins during infection.

We first observed that VLS formation takes place when NSP5 is co-expressed with the structural protein VP2, as well, and that, even in this case, both proteins localize in these structures. VLS formation in the presence of VP2 occurs soon after transfection, indicating that as soon as the proteins form they interact to form VLS (fig.12). Since the behavior of NSP5 in the presence of VP2 is very similar to that observed in the presence of NSP2 (60), we named the VLS formed by VP2 VLS(VP2i), where “i” stand form induced, and that formed by NSP2, VLS(NSP2i). Although the two type of VLS are very similar there are some differences regarding the dimension and distribution of these structures: VLS(VP2i) are larger respect to that formed by the interaction with NSP2, and they tend to cluster in a perinuclear localization while VLS(NSP2i) are diffused into the cytosol of transfected cells (fig.11).

These observations are particularly interesting in the context of NSP5 post-translational modifications. It has been demonstrated that NSP5 is hyperphosphorylated in infected cells (2), and when co-expressed with NSP2 in the absence of other viral proteins, NSP5 results hyperphosphorylated conferring to NSP2 a regulating role on NSP5 hyperphosphorylation (1). Recent results have shown that hyperphosphorylation of NSP5 occurs when it is expressed with VP2, as well (fig.13) (6). We further characterized this

modification. In particular, the hyperphosphorylation induced by VP2 resembles more the one observed in Rotavirus infected cells, since it gives arise to isoforms of higher molecular weight respect to that induced by NSP2. We confirm that the nature of this modification is hyperphosphorylation with treatment of the NSP5 immunoprecipitated extracts of transfected cells with lambda phosphatase, that converts the higher isoforms to the lower one at 26 kDa (fig.14). Moreover, the co-expression with the catalytical subunit of PP2A-phospatase contributes in part to reduce the hyperphosphorylion of NSP5 induced by VP2 in vivo, since we still observe the isoform at 28 kDa, even at low amount (fig.14). This is not the case of NSP2, indeed the co-expression of PP2A with NSP5 and NSP2 provokes an almost total de-phosphorylation of NSP5 that shows a pattern similar to the NSP5 expressed alone (fig.18). As it appears from the pattern shown in Western blot analysis, the two types of induced modifications are different and are differently sensitive to phosphatase treatment.

It has been demonstrated, with surprise, that VP1 co-expressed with NSP2 and NSP5 affects the up-regulation of NSP5 hyperposphorylation induced by NSP2. Indeed, NSP5 strongly interacts with VP1 and this interaction is not affected by the presence of NSP2, furthermore it seems to enhance VP1-NSP2 interaction. The region of interaction between NSP5 and VP1 has been mapped just upstream of the C-terminal tail, and since this region is involved in dimerization of NSP5, it is probable that dimers of NSP5 interact with VP1 (6). However by cryoEM analysis, it was demonstrated that four dimers of NSP5 interact with an octamer of NSP2, and that region proximal to the C-terminus of NSP5 are involved in this interaction. Thus, it is reasonable to suppose that the strong interaction between NSP5 and VP1 would interfere with the interaction of NSP2, dissecting, in this way, the up-regulation of the hyperphosphorylation of NSP5 induced by NSP2 (fig.19). Moreover, these observations suggest a possible coordinative role of NSP5 between NSP2 and VP1 interaction, that has already been proposed (96).

Upon this observations, and the interaction between VP1 and VP2 in forming the minimal replicase complex (141), we investigate if VP1 expression interferes with the NSP5 hyperphosphorylation induced by VP2. The pattern of hyperhosphorylation of NSP5 induced by VP2 changes in the presence of VP1, with the appearance of the 26 kDa isoform, and the inversion of the ratio between the 28 kDa and 26 kDa isoforms (fig.19). However, while it was possible to map the region of interaction between NSP5 and VP1 by co-immunoprecipitation experiments with anti NSP5 serum (6), the same approach was not useful to demonstrate the putative interaction between NSP5 and VP2, since we do

not succeed in the co-immunoprecipitation of VP2 with NSP5 in both infected and trasfected cells, and to map the NSP5 region(s) of interaction between them. In any case, it is evident that the strong interaction of NSP5 with VP1 interferes with the NSP5 hyperphosphorylation induced by VP2, as well (Fig 19).

NSP5 is a 198-aa protein with an high content of Ser, Thr residues that are good targets for the addition of phosphate groups. In order to identify the Ser residues involved in the hyperphosphorylation induced by VP2 we tested a series of Ser mutants. The first group that we take in consideration was that involving the Ser67 since they were already characterized by Eichwald et al. for their ability to get phosphorylated. Ser67 is inserted in a Ser rich motif (**S**D**S**A**S** named motif “a”) and was identified as the one responsible for the initiation of the NSP5 hyperphosphorylation. The point mutant has the Ser67 mutated into Ala (S67A) and it does not get phosphorylated in the presence of an activator of phosphorylation, while the mutant Ser67Asp (S67D), that mimics the phosphorylated protein, is sufficient alone to activate NSP5 hyperphosphorylation (54). In the presence of VP2, both S67A and NSP5a (whit all the Ser in motif “a” mutated into Ala) shows a low degree of phosphorylation: it is possible to appreciate a very weak band of 28 kDa band, but the main isoform expressed is the lower one of 26 kDa (fig.17 lane 11,12). Thus, the NSP5 hyperphospohorylation induced by VP2 is partially inhibited when S67 is mutated indicating that S67 maintains its important role in initiating the hyperphosphorilation event also when induced by VP2. This is important because it indicates that the basic mechanism by which NSP5 hyperphsophorylation is triggered is common with the one occurring during virus infection. However, since we have still a low degree of hyperphosphorylation, we can conclude that there are other important NSP5 residues involved in its hyperphosphorylation. The mutant NSP5-S67D alone, which mimics the hyperphosphorylated protein (54), is regardless still sensitive to the effect triggered by VP2 (fig.17.lane 9-18)

The second group of mutants analyzed was the S42 mutants. Preliminary mass spectrometry analysis of NSP5 isoforms obtained from infected cell, revealed the clear presence of a phosphate group at the level of S42 (F.Rossi graduation thesis data). Upon these evidences we constructed the mutant NSP5-S42A, and we combined this mutation with the S67A mutant to obtain the double mutant NSP5-S42/67A and NSP5a-S42A. NSP5-S42A in the presence of VP2 behaves as the wild type protein with the accumulation of the 28 kDa isoform, suggesting that this residues is not significant in NSP5 hyperphosphorylation induced by VP2 (Fig.17 lane 13). On the other hand, both the

double mutant NSP5-S42/67A and the quadruple one NSP5a-S42A show a change in the phenotype expressed in the presence of VP2 with respect to the wild type protein, that is an accumulation of 26 kDa isoform and a weak band at 28kDa (Fig.17 lane 14,15). This results confirm the critical role of S67 in the initiation of the hyperphosphorylation of NSP5, since all the mutants containing the Ser 67 mutated into an Ala show a phenotype that promotes the accumulation of the 26 kDa isoform with respect to the 28 kDa one.

In our studies on NSP5 hyperphosphorylation, another Ser rich motif (AD**S**D**S**EDYVLDD**S**D**S**DDG), located towards the C-terminal of NSP5 protein and named motif “c”, was studied. A mutants with all the serine in motif c mutated into alanine, NSP5c, and a second mutant, that present all the serine of region 4 mutated into alanine (the tail does not contain Ser residues) and named NSP5c-S137/142A, was expressed together with VP2. Both these mutants showed an unchanged pattern of phosphorylation compared to the wild type protein (fig.17, lane 16,17), suggesting that neither motif c, nor all the serine in region 4 are critical in providing residues for the generation of the isoforms with lower mobility in the presence of VP2.

This analysis with all NSP5 Ser mutants does not identify fundamental residues or motif in NSP5 protein that, once mutated, inhibits completely the hyperposphorylation induced by VP2, but we did confirm the role of S67 in initiating the phosphorylation cascade event as it happens when induced by NSP2. However, in this latter case the role of S67 is more critical respect to the that observed hyperphosphorylation induced by VP2. An important differences reside in region 4. Indeed, NSP5c together with NSP2 shows a phenotype similar to that of S67A, indicating that, the motif c does plays, in this case, an important role (fig.20 lanes 10,11,16). Since a big portion of NSP5, between residues 66-188, is able to bind to the groove of NSP2, as revealed by cryoEM microscopy (91), it could be supposed that the phosphate groups present in S67 and in motif c, would be an important signal in triggering the NSP5 hyperphosphorilation induced by NSP2.

Moreover, since the NSP5 hyperphosphorylation induced by NSP2 is more sensitive to the treatment with phosphatase, and to the mutation of certain Ser residues respect to that induced by VP2, we can argue that the two type of induced hyperphosphorylation are different and maybe complementary. It also suggests that the reduction in PAGE mobility of hyperphosphorylated isoforms can be obtained involving different residues.

According to the studies performed by Campagna et al. on CK1α kinase involved in NSP5 hyperphosphorylation in infected cells (26), we investigate if it is also involved in initiating NSP5 hyperphosphorylation induced by VP2. Treatment with siRNA specific for CK1α in

cells transfected with NSP5 and VP2 did not impaired the hyperphosphorylation mediated by VP2. Thus CK1α appears not to be involved in the mechanism of VP2 induced NSP5 hyperphosphorylation (fig.15). indicating that other kinases can efficiently participate and suggesting that the process is not tightly controlled , since alternative kinases can have similar consequences.

VP2 and NSP2 are able to induce both VLS formation and NSP5 hyperophosphorylation, however the two events are not necessarily correlated. Indeed, in all the cases analyzed in which NSP5 hyperphosphorylation results impaired (co-trasfection with PP2A, or with VP1, or NSP5 Ser mutants), we still observe formation of VLS in the cytosol of cells co-transfected with NSP5 and VP2, or NSP2 (fig.18, 19, 21). In particular, in the presence of VP1 polymerase, we still observe VLS formation, despite impaired NSP5 phosphorylation, and VP1 recruitment (fig.19) in these structures. In addition, all NSP5 Ser mutants, that we analyzed for their ability to get hyperphosphorylated, form VLS when express with NSP2 or VP2, even those that show a more affected hyperphosphorylation with NSP2 (Fig.21). However, in the case of co-expression with VP2, none of the NSP5 Ser mutants has a completely abolished phosphorylation. It is possible that a basal phosphorylation status is sufficient to drive the formation of VLS. However, this appears not to be the case since the NSP5 S67D mutant that is already phosphorylated when expressed alone, has a diffuse distribution in the cytosol of transfected cells, and only upon co-transfection with VP2 or NSP2 the rearrangement into VLS occurs (Fig 21). This is a very strong evidence that it is not the hyperphosphorylation status that leads to the formation of VLS, but rather the particular interaction with NSP2, (probably through dimerization), or with VP2 that regulate VLS formation.

To better characterize the two types of VLS, we investigate their ability to recruit other viral proteins. We first analyzed the recruitment of both NSP2 and VP2 into VLS. VLS inducers collaborate in the arrangement of VLS, they do not interfere between each other in the formation of these structures and they both co-localized there. As already discussed VP1 polymerase is recruited in both VLS(NSP2i) and (VP2i), and its recruitment is likely to be due to the strong interaction with NSP5 (fig.23). Moreover, NSP2 and VP2 have been demonstrated to interact with VP1, interactions that have functional roles during viral replication to synthesized the dsRNA genome (141), (96). Therefore, the localization of VP1 into VLS is not surprising and indicates that these structures may be considered as valid models of viroplasms.

This interpretation is consistent with the results obtained with VP6, which was clearly recruited into VLS with a very distinct distribution compared to when it was expressed alone (that showed formation of tubular structures (trimers) in the cytosol) (89). This change was particularly evident in VLS(VP2i), most likely because of the interaction with the core protein VP2. In contrast, VP6 does not localize into VLS(NSP2i) and remains organized in filamentous structure into the cytoplasm of transfected cells (fig.23). This observation is interesting since first reveals that VLS are not simple aggregate/random structures able to recruit whatever viral protein, but they represent, at least from a structural point of view, a real intermediate structure of viroplasms. It is, in this context, very interesting to characterize in the future VLS from a functional point of view, considering recruitment of viral RNA and formation of DLPs.

In contrast to the deep description of the interaction between NSP5, NSP2 and VP1, in both infected and transfected cells by Arnoldi et al., we failed in all our attempts to demonstrate a direct physical interaction between NSP5 and VP2, which was suggested by the co-localization of these proteins into VLS. Immunoprecipitation experiments of extracts of transfected cells with NSP5 and VP2, and of infected cells, with anti-NSP5 and anti-VP2 sera, did not succeed in co-immunoprecipitating the two proteins, even with DSP crosslinking. Moreover, neither the co-expression of NSP5, VP2 with NSP2 or VP1 triggers the interaction between NSP5 and VP2 (data not shown). The failure of co-immunoprecipitating NSP5 and VP2 was probably due to methodological limitations such as lysis condition or, most likely, the high-affinity hyperimmune polyclonal antibody used for the immunoprecipitation, that gives already evidences of dissociating activity (6). In fact, recently, in our laboratory a series of monoclonal Ab (mAb) specific for NSP5 have been isolated (G.Petris graduation thesis), that were tested for their ability to immunoprecipitate NSP5 with other viroplasmic components from both infected and co-trasfected cells. All the mAb isolated were able to recognize and immunoprecipitate NSP5 from infected cells (not shown), however only one mAb, named 1B7, gave promising results in co-immunoprecipitation of other viroplasmic components (Fig.25). The first attempts of immunoprecipitation assays with mAb 1B7 confirmed the strong interaction of VP1 with NSP5, since the polymerase immunoprecipitates without the necessity of chemical crosslinking (Fig 25B, lanes 17, 19, 21, 23, 25).

MAb 1B7, however, was not able to efficiently co-immunoprecipitate neither NSP2 nor VP2, unless VP6 was also present. It is possible that the epitope recognize by 1B7 overlaps with the region of interaction of the two viral proteins (fig.25 lanes 15, 16) with a

consequent dissociating activity. However, in the presence of VP6 both proteins could be co-immunoprecipitate with 1B7.(fig.25 lanes 20, 22) suggesting that VP6 probably through its strong interaction with VP2 stabilizes the structure of VLS(VP2i). On the contrary, VP6 is not recruited into VLS(NSP2i) and remains organized in tubular structure, a result somehow expected since there is not a protein able to drive its localization (VP6 does not interact with NSP2 nor with NSP5). However, VLS (NSP2i), was observed in some cases, aligned along VP6 tubes, suggesting a possible interaction between this two structures, that could explain the increased amount of co-immunoprecipiteted NSP2, when VP6 was also expressed.

NSP5, NSP2, VP2 and VP1,together with VP3 are the components of replication intermediates with replicase activity (RI). However, the temporal order that lead to the interaction of these proteins with viral mRNA and the consequent formation of RI is still under investigation.

Upon these observations, we could suppose a possible mechanism of viroplasms assembly during Rotavirus infection. Soon after virus penetration and uncoating, the synthesis of viral proteins take place. According to the characterization of RI from infected cells (64), VP1 and VP3 precede the other RI proteins in the interaction with mRNA. Moreover, the interaction between NSP5-VP1 (originally described by Arnoldi et al. and also briefly described in this thesis) indicates that these proteins interacts independently from other viral proteins. Thus, it is allowed to assume that NSP5 interacts with VP1 that is already in contact with VP3 and the viral mRNA.

It is difficult to describe the sequence of interaction of NSP2 and VP2 on NSP5-VP1-VP3-mRNA complex from our observations. Indeed there are no evidences in favour of a particular preference in the association with NSP2 before VP2 or viceversa. I would therefore propose two alternative situations:

1. In this scenario,NSP2 first bind to the non-replicative NSP5-VP1-VP3-mRNA complex through its interactions with both NSP5 and VP1 (1), (91), (96), leading to the formation of an intermediate precursor of a viroplasm similar to VLS(NSP2i). This structure would protect the pre-replicase complex, and would probably be linked to upregulation of NSP5 hyperphosphorylation, for an as yet obscure function. Thus, in order to allow the association of VP2 to render the RI competent for the replication of viral RNA, the rearrangement of NSP2 is needed, since NSP2 interferes with VP2 binding to ssRNA and initiation of replication would be inhibited (203). This process were probably reflected in the structural changes that we

observed going from the small VLS(NSP2i), to the large VLS formed with both NSP2 and VP2.

2. Alternatively, VP2 binds first to the NSP5-VP1-VP3-mRNA complex. This interaction would be possible through VP2 binding to VP1 (141) that has already been demonstrated. In this case, (also suggested by Vende et al. (203)), VP2 interacts with the non-replicative RI, forming an intermediate similar to VLS(VP2i), making the precursor replicative-competent, and inducing also NSP5 hyperphosphorylation. Subsequent binding of NSP2 would contribute to the assembly of the viroplasm and the actual initiation of dsRNA synthesis.

In both cases the association of VP6 occurs as last event, and only when VP2 is recruited into viroplasms. The presence of VP6 allows the formation of DLPs, that because of this become transcriptionally active (29), and bud from the viroplasms through the ER for virus morphogenesis.

The role of NSP5 hyperphosphorylation upon Rotavirus infection is still obscure, it is possible that it might influence the polymerase activities, as it has been shown for phosphoprotein that regulate the polymerase of negative-strand RNA virus (84),(174).

Further experiments will validate one of the two proposed models, in order to assign a role to NSP5 in viral replication and as the organizer of viroplasms assembly and functionality.

ABSTRACT (2)

The ubiquitin–protesome system (UPS) is important for almost every aspect of cellular functions. Viruses, on their hand, prevalently depend on host machinery for replication, therefore it is not surprising that viruses manipulate the UPS at many levels to enhance viral replication.

In this study we characterized the effect of the proteasome inhibition on Rotavirus infection. We observed that addition of proteasome inhibitor MG132 in infected cells induces a strong decrease in the amount of structural and non structural viral protein production. Kinetics studies revealed that inhibition of proteasome activity strongly affects viral proteins accumulation when added at early time point post infection (from 1 hour till 5 hour post infection). Moreover, absorption in the presence of proteasome inhibitors does not affect penetration and, probably, uncoating of the virus. Furthermore, the inhibition is dependent on the concentration of the different proteasome inhibitors utilized. Quantitative RT-PCR from infected cells showed that in MG132 treated cells the level of viral RNA is also largely reduced, respect to the DMSO-treated cells, indicating that the effect of protesome inhibition involved also viral processes that produce RNA like transcription or replication.

In transfection experiments, proteasome inhibition did not affect the expression of viral proteins like NSP5, NSP2, and VP2, either when expressed alone or in different combination. Moreover, both the hyperphosphorylation of NSP5 and the VLS formation induced by VP2 or NSP2, did not change in the presence of MG132.

We have excluded a direct effect of the inhibitor MG132 on the VP1 polymerase activities (transcriptase and repicase activities). In i*n vitro* transcription assay in the presence of MG132, we did not observe any variation in the amount of transcribed mRNA; *in vivo* ^{32}P labeling of replicated dsRNA in infected cells, when the replicase activity of VP1 is at maximal level, showed no effect on dsRNA production in the presence of proteasome inhibitor.

NSP1 is the only known Rotaviral protein related to UPS, since it induces proteasomal-mediated degradation of IRF3 factor in order to inhibit IFNβ response. In this regard, we observed that the amounts of IRF3 are not related to the strong impairment of Rotavirus infection that occurs when proteaseome is inhibited.

In addition to the biochemical analyses, we assessed the effect of MG132 by immunofluorescence assays. We looked at viroplasms formation and, consistently with the biochemical data, we observed that MG132 added during the early phases of infection does reduce viroplasms formation and growth in an early phase of viroplasms assembly

5 INTRODUCTION (2)

Different cellular functions are finely regulated by the ubiquitin-proteasome system (UPS). This is not only a machinery used for the degradation of misfolded proteins, but is also a regulatory system of several cellular processes like gene transcription, signal transduction, apoptosis, DNA repair. Upon viral infection, several cellular functions are subjected to adaptations driven by the viruses for their own advantage or as a response of the cell against them. These adaptations evidently involve the UPS machinery, and viruses have developed means to use this regulatory complex to permit their replication.
In the follows paragraphs, it is described the UP system and some of the methods used by viruses to exploit it to enhance their replication, as it is the case for Rotavirus.

5.1 The Proteasome

The proteasome is a complex molecular machinery involved in protein degradation within the cells. The process consists in recognition of the opportunely ubiquitinated substrates, unfolding, de-ubiquitination, and traslocation of the substrate into a narrow channel, that is the proteolytic core of the machinery, where the proteins are hydrolyzed.
Structurally, the proteasome consists of two main complexes: the 20S proteolytic core (core particle CP) and the 19S regulatory particle (RP), together these subunits form the 26S proteasome. The association of the RP with the CP induces the activation of the proteolitical activity of the proteasome (62).
The 20S complex is made up of α and β subunits organized in rings: two rings of 7α subunits are separated by two stacked rings of 7β subunits, with a symmetry 7α7β7β7α. A narrow channel runs through the centre of these structures where the hydrolysis of the substrates takes place, due to the proteolytic activity of the β subunits (93).
The 19S regulatory complex is been subdivided into two assemblies, the base, proximal to the CP, and the lid, distal from the CP. However, the whole RP subunit carries out a lot of functions (62):

- ✓ It recognizes polyubiquitinated particles,
- ✓ It cleaves the polyuquitin chains to obtain ubiquitin monomers (de-ubiquitination activity)
- ✓ It binds to the 20S complex inducing the opening of the narrow channel

- ✓ It functions as a chaperone for the unfolding of the substrates and their traslocation into the proteolytic core for the degradation.

5.1.1 The core particle (CP)

The proteolytic core of the proteasome has 28 subunits arranged into four heteroheptameric rings. The external rings are made up of 7 α-type subunits, while the two internal ones are composed by 7 β-type subunits (199) (Fig 26).

The inner rings contains the enzymatic activity of the machinery, in particular three of the seven subunits present the proteolytic active sites: β1, β2, and β5. These subunit belongs to the N-terminal nucleophile (Ntn) hydrolase family with an unusual, single-residue active site, the N-terminal threonine. Each sites is able to cleave a broad range of peptide sequence: in particular β1 prefers to cleave on the C-terminal side of acidic residues, β2 cleaves after Arg and Lys residues, tryptic cleavage, and β5 cleaves after hydrophobic residues. For these differences in the cleavage, the sites of the subunits are classified as caspase-like site for β1, trypsin-like for β2 and chymotrypsin-like for β5. However, this classification is approximate since the cleavage specificity is not determined by the amino acid at the N-terminus of the cleaved bond. The combination of several active site, even with a low specificity, in a very narrow space, for an unfolded proteins with all the peptide bonds exposed guarantees its complete hydrolysis after the passage into the core particle.

In the inactive state the core particle has its channel closed by a well defined network made up by the N-terminus of the α-type subunits of the external ring. The activation of the core particle needs the disruption of this network, and this process is regulated by the association of the RP. At the interface of the α-subunits, a structural pocket is formed, thus a series of seven pockets are exposed to the RP-facing surface of the α-ring that are the binding site for RP. The binding of RP induces the opening of the CP channel, that results in register with the RP channel, where the substrates need to translocate before reaching the CP. The substrate translocation channel is very constricted even when it is in the open conformation. This prevents the spurious degradation of cytoplasmic proteins and, furthermore, it imposes the substrates to reach the channel in an unfolded conformation, that facilitates the rapid hydrolysis of the protein within the CP. The unfolding activity is supposed to be mediated by the ATPases subunits of the RP complex (62).

The interaction between the C-termini of RP with the α-pockets is sufficient to open the CP channel, and this is due to a sequence specificity. Indeed a hydrophobic residue followed

by a tyrosine and an unspecific C-terminal residue, HbYX motif, is able to open the gate (182).

In addition to the RP HbYX motif, another protein has been characterized to induce the activation of CP, the heteromeric 28αβ proteasome activator (PA28). Differently from RP, PA28 lacks the ATPases activity and the capacity to bind the ubiquitinated substrates, however it is able to bind to the CP cylinder and to open the channel. The mechanism was well described through studies on the PA28 homolog from trypanosomes, PA26. In particular, the PA26 C-terminal β-strand-like structure inserts into the α-pockets of the CP. This insertion brings an internal sequence of the PA26, known as activator loop, to interact sterically with the Pro17 loop of the α-subunit. Seven PA28 proteins interact simultaneously with the seven pockets of the α-ring, in this way the seven Pro17 loops move and cannot maintain the ordered state of the closed channel (205).

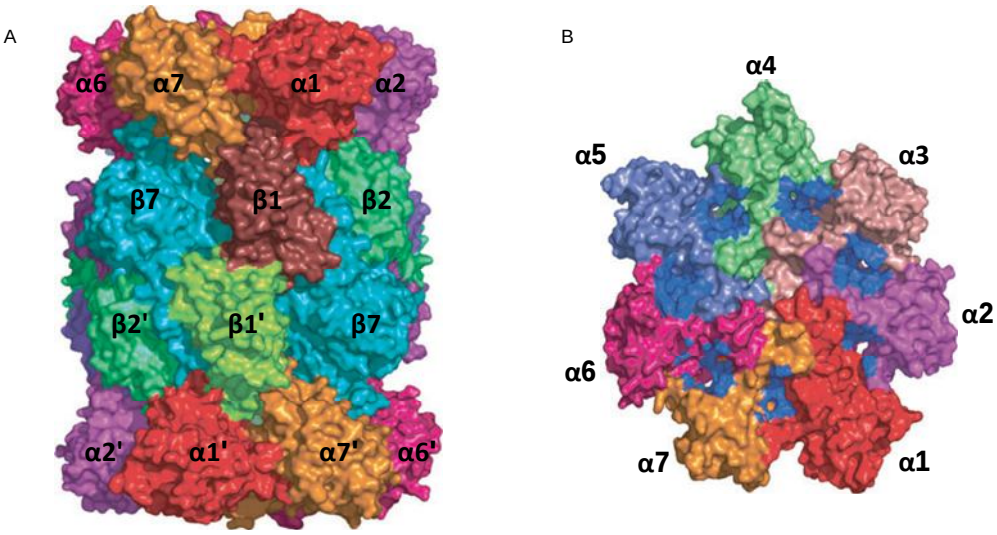

Figure 26: Core Particle. A) Medial section of the CP: it is organized in four heptameric rings of subunits. Two external rings of α-subunits and two internal rings of β-subunits.(left figure). B) Top view of the 20S subunit: dark blu color indicate the 7 α-pockets of the α-ring where regulatory particle and PA26 bind to open the channel. The channel is closed.

5.1.2 The regulatory particle (RP)

The base

The base consist of 10 subunits: six ATPases, that belong to the ATPases-associated-with-different-cellular-activities (AAA) family (also referred as Rpt, following the nomenclature for yeast); two scaffolding proteins Rpn1, Rpn2; and two ubiquitin receptors Rpn10, Rpn13 (61) (Fig 27).

The ATP-dependent proteases, that belong to the same family, are thought to form a pseudosymmetrical ring structure, within the highly assymetrical structure of the RP, forming a sort of translocation channel of the RP subunit. The substrate is retained within the ATPase ring where it is subjected to different processes. Indeed, the proteolysis of different substrates has been described to be ATP dependent, revealing a functional role of ATPases, moreover this subunits are thought to possess the unfoldase activity necessary to rapidly degrade the substrate (62).

ATPases ring have a structural function, as well. The C-termini of the ATPase subunits insert into the α-subunit cavities of the CP, and promote the formation of the RP-CP complex, favoring the alignment of the α-ring with ATPases rings.

The scaffolding subunits Rpn1, Rpn2 are the largest proteasome subunits and are characterized by the presence of tandem repeats elements that leads the formation of a particular secondary structure: a double-toroid. This toroid is able to attach to the CP, independently from ATPases subunits, and drives the alignment of the translocation channel of the RP with the channel of the CP. The model proposed is that the Rpn1/Rpn2 subunits form part of the translocation channel, inserted within the ATPases ring, and are situated between the CP and the ATPases ring (168).

Another function of Rpn1/Rpn2 complex is to function as a scaffolds for the binding of protesome subunits or proteasome-associated proteins. Indeed ubiquitin receptor Rpn13 binds to Rpn2, and other ubiquitin receptors bind to Rpn1. In addition, enzymes that disassembled or extend ubiquitin chains interact with Rpn1 and Rpn2 proteins .

Rpn10 and Rpn13 are the proteasome-associated ubiquitin receptors. They bind ubiquitinated substrates through different recognition motifs: Rpn10 has two ubiquitin interacting motif (UIMs), while Rpn13 has a pleckstrin-like ubiquitin receptor domain. In addition to these two subunits there are other ubiquitin receptors that are associated to the proteasome. They are called also “shuttle” receptors since recognize ubiquitinated substrate that are far from the proteasome and are able, through specific ubiquitin- like (UBL) or ubiquitin associate (UBA) domains, to engage and drive them towards the proteasome (186).

The lid

The lid consists of nine subunits, of which only one has been functionally characterized, Rpn11, as a de-ubiquitinated protein (DUB). Deubiquitination is an important step in proteasome activity, since before the degradation substrates need to be separated from

the ubiquitin groups. Ubiquitin is not degraded and is recycled within the cell. Rpn11 activity is finely controlled and exclusively directed towards proteolytic substrates. The mechanism of coupling degradation with deubiquitination is still under investigation, however the DUBs activity is inhibited in the absence of ATP, and since all the nine subuinits of the lid lack ATPases activity, it is likely that the nucleotide hydrolysis of the base ATPases allows the lid subunits to cleave ubiquitin from the substrate. In particular Rpn11 cleaves the whole ubiquitin chains and in the absence of this subunit the proteasome does not work, probably because the ubiquitinated substrate cannot fill the CP channel. In addition to Rpn11 there are other DUBs, that act before the substrate is committed to degradation and Rpn11 activity. These DUBs, Uch37 and Ubp6, do not completely eliminate ubiquitin chains from the substrates but they shorten them, decreasing the substrate affinity for the proteasome and slowing down its degradation. Uch37 and Ubp6 associated to the proteasome binding to the Rpn13 and to the Rpn1 respectevely.

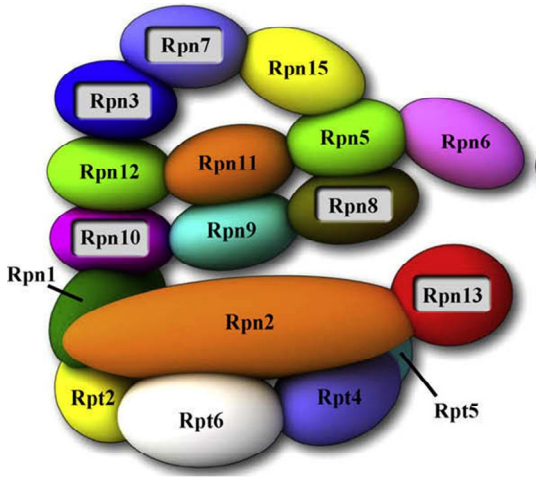

Figure 27: 19S Regulatory particle. Subunit arrangements of the 19S complex. The bottom part faces the α-ring of 20S complex.

5.2 The ubiquitin-proteasome system (UPS)

The UPS is the machinery involved in the regulation or life-span determination of intracellular proteins. In order to become proteasome substrates, the proteins need to be tagged with ubiquitin (Ub) molecules, even if there are rare examples of non-ubiquitinated substrates that are degraded by the proteasome. Ubiquitin is a small protein composed of 76aa, and the critical residue that permit the formation of ubiquitin chain is Lys 48. Mutation at the level of this residues prevents the formation of poly-ubiquitin chains and target to the proteasome. However, recently it has been demonstrated that other residues,

Lys11 and Lys63, have the ability to form chains that target the proteasome degradation of the substrates (208).

The process of ubiquitination consists in a very complicated mechanism, and involves different kind of enzymes (E1-E4). Herein the different steps of the process are described (93) (Fig.28):

1. *Ubiquitin activation by E1:* the initial step consists in the activation of ubiquitin and is an ATP dependent process. The enzyme involved in this process is the E1 “ubiquitin-activating enzyme”, that attaches to the Cys residue in its active centre the C-terminal end of the Ub. Different E1 enzyme are present in the cytosol and in the nucleus
2. *Ubiquitin-conjugation and E2 enzyme:* this is an intermediate step where the E1 enzyme transfers the activated Ub to a Cys residues of the “ubiquitin conjugation enzyme” E2. About several dozens of E2 enzyme exist, each interacting with a special set of E3 enzymes or substrates.
3. *Ubiquitin transfer to the substrate:* the process that promote the transfer of ubiquitin to the substrate involved a third class of enzymes: the “ubiquitin ligase”E3. E3 represent the largest group of enzymes involved in the UPS. It is supposed to exist at least several hundred of E3s in mammalian cells. The substrate ubiquitination could occur with two different ways depending on the type of E3 ligases:
    a. The E3 ligases characterized by the presence of the RING finger structure bind both the substrate and the Ub-E2 complex and catalyze the transfer of the Ub directly on the substrate.
    b. The E3ligases with the HECT structure bind both the substrate and the Ub-E2 as well but the Ub monomer is first transfered to the E3 enzyme,binding to a very conserved Cys residue, and then to the substrate protein.

How the Ub-molecules are attached to the first one to form poly-ubiquitinated chains is still unknown. There are models that propose repetitive cycles of ubiquitination involving E1-E3 enzymes. However, it has been observed in yeast the existence of a fourth enzyme: “ubiquitin-chain elongation factor” E4 enzyme, that has a still unknown mechanism of action (103).

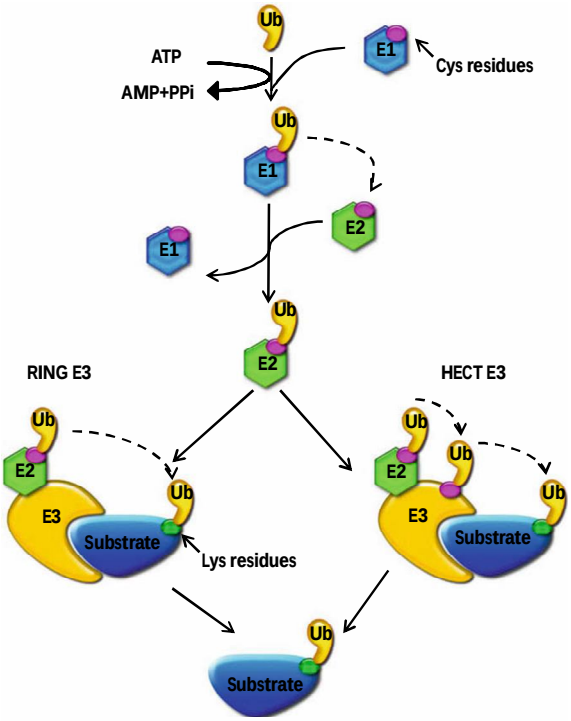

Figure 28: Schematic representation of substrate ubiquitination. Activation of the ubiquitin monomer occurs by E1 enzyme activity. The process need the hydrolysis of ATP and the ubiquitin monomer is transferred to a Cys residue of E1. Ubiquitin is then transfer to E2, binding to another Cys residues of this enzyme, and E1 is released. Ub-E2 complex binds the E3-substrate complex and, depending of the type of E3 ligase, the Ub molecule is transfered to the substrate. The transfer occurs directly to the Lys residues of the substate in the case of a RING E3 ligase (left) or throught a intermediate passage to the Cys residue of E3 and then to the substrate in the case of HECT-domain E3.

5.3 The degradation process

In order to be recognized for degradation, the substrates need to be tagged with at least four molecules of Ub. The recognition of the substrate is mediated by the subunit of the 19S complex, it involves subunit Rpn1, Rpn10 and one ATPases, Rpt5. Furthermore the subunit Rpn1 binds to the DUB enzyme Upb6, that may function as a regulator shortening the Ub chains of undegradable substrates and allowing their release from the proteasome. After the recognition, the substrate needs to be unfolded, and inserted into the traslocation channel, and the mechanism of this process is still under investigation. There are two proposed models:

1. *Unfolding of the substrate preceeds translocation:* this model proposes that the unfolding of the degradable substrate occurs at the surface of the ATPases ring of the 19S complex, and after the complete destabilization of the substrate it is translocated into the narrow channel of the CP (133).
2. *Unfolding occurs into the translocation channel:* this model propose the direct interaction between the substrate and the traslocation channel. So the unfolding of the substrate occurs consequently to its collision into the narrow channel and promotes its translocation, as well (98).

Once inside the CP the substrates is subjected to degradation by the β-subunits proteolytic activity, and heterogeneous mixture of peptides are released from the machinery. In mammals this subset of peptides are utilized for the adaptive cell-mediated immunity.
Ubiquitin are released during substrate degradation in the form of polyubiquitin chains that are subsequently decomposed in Ub monomer by the DUBs in the cytosol and recycled (62).

5.4 UPS and virus

The ubiquitin-proteasome system regulates different cellular process through the more rapid and easy degradation of cellular proteins. Indeed, apart from the elimination of misfolded, damaged, or unneeded proteins the UPS is involved in cell cycle regulation, apoptosis, antigen processing, transcriptional regulation, signals transduction, and other several cellular functions. Since virus replication is dependent on the activity of different host factors, it is not surprising that viruses have developed mechanisms to direct the cellular UPS activity to their own needs. A lot of studies have demonstrated that different type of viruses manipulate ubiquitin-proteasome pathway evading cellular response.
Herein, are reported examples of different virus strategies in manipulating UPS.

Viral proteins direct ubiquitination of cellular factors

This mechanism is used mostly among DNA tumor virus that target cell cycle regulation proteins to the proteasome inducing cell transformation. This was first observed in papilloma virus HPV, that induces the degradation of p53 protein through the viral protein E6. The mechanism of HPV E6 mediated degradation consists in the recruitment and redirection of one cellular E3 ligase to ubiquitinate p53 (173).
Adenovirus expresses two proteins, E1B-55K and E4orf6, able to engage another cellular E3 ligase in order to target p53 to proteasome degradation, as well (162).
On the other hand, HIV-Vif protein is an important regulator of HIV infection since it drives the polyubiquitination and the following degradation of APOBEC3G, a potent cellular antiviral factor (213).
In order to shut down the interferon response, several viruses take advantage of the proteasome activity and direct the degradation of cellular proteins involved in interferon signaling. This is the case of several paramoxyviruses, human parainfluenza virus

(HPIV2), and simian virus (SV5) that target to proteasome degradation STAT (signal trasducer and activator of transcription) proteins (164).

And this is also the case of Rotavirus that, through its NSP1 protein, mediates the degradation of IRF3 protein via proteasome, preventing the activation of interferon β response (this mechanism is extensively describe in introduction 1 page 34) (13), (14).

Another strategy of several virus is to interfere with the retrograde translocation through the ER. This is a process that normally occurs in cells for misfolded proteins that enter the secretory pathway. These protein are finely controlled into the ER and the misfolded or damaged one are rapidly retrotraslocated into the cytosol for rapid proteasomal degradation. Some viruses express proteins able to address into this secretory pathway, host proteins and to induce their degradation. Citomegalovirus, US2 and US11, mediate the degradation of MHC class I protein using this method, which serves as an immune evasion mechanism (206). In the same way HIV-Vpu induces degradation of the cell surface receptor CD4 (175).

Virus encoded ubiquitin-ligase

Virus may encode their own E3 ligase and almost all the viral E3 ligases identified were classified into the RING family.

In this classification is involved the herpes simplex virus type 1, with its ICP0 (infected cell protein 0). ICP0 has a RING domain with a E3 ligase activity that directs the ubiquitynilation and degradation of PML and SUMO-modified forms of Sp100, causing degradation of PML nuclear bodies and other substrates (21).

Among the viral RING E3 ligase family, there is the RING-CH sub-family that was first identified in murine and human γ-herpesvirus and characterized by the presence of C4HC3 Cys-His configuration in the RING (165). These are integral membrane proteins that act inducing ubiquitynilation and degradation of receptors. The degradation occurs both with the internalization of the receptor into a endolysosomal compartment, but also through proteasome-mediate degradation using the ERAD pathway. RING-CH ligases are involved in the degradation of MHC class I molecules in order to evading the viral immune response of the cells (165).

For Rotavirus, it has been identified a RING structure within NSP1, that suggests a possible role of this protein as a E3 ligase inducing directly its own, or IRF3, ubiquitination and consequently proteasome degradation. (This was already discussed in introduction page 34) (149).

In addition viruses have developed different mechanisms to take advantage from the cellular UPS (165),(86):

- ✓ Encode for viral ubiquitin,
- ✓ Encode viral DUBs,
- ✓ Interacts with cellular DUBs,
- ✓ Interacts with ubiquitin-like modifier like SUMO, ISG15.

All these strategies represent different ways that viruses have developed to avoid viral cellular responses and to enhance their own replication.

6 RESULTS (2)

6.1 Intro

The ubiquitin proteasome system, in addition to control several cellular functions, has been shown to be involved in different aspects of virus replication into host cells. In this study, which originated following an unexpected observation, we wanted to address the involvment of the proteasome activity during Rotavirus infection.

6.2 The striking observation

During our studies on Rotavirus, and in particular on the expression of NSP5 protein, we observed a particular effect on MG132 treated cells infected with Rotavirus. MG132 is a peptide aldehyde that functions as a reversible potent transition-state inhibitor of the chemotrypsin-like activity of the proteasome CP (111).

The biochemical analysis performed on infected cells treated with MG132 revealed that it causes a decrease in the amount of rotaviral proteins that accumulate during virus replication. As shown in figure 29, when infected cells were treated with MG132 from the beginning of the infection till hour 7 post infection the accumulation of both structural (VP2) and non-structural (NSP5) rotaviral proteins was strongly affected. The effectiveness of MG132 treatment on proteasome activity was always assessed by analysis of the levels of p53, which increases upon proteasome inhibition.(Fig.29B)

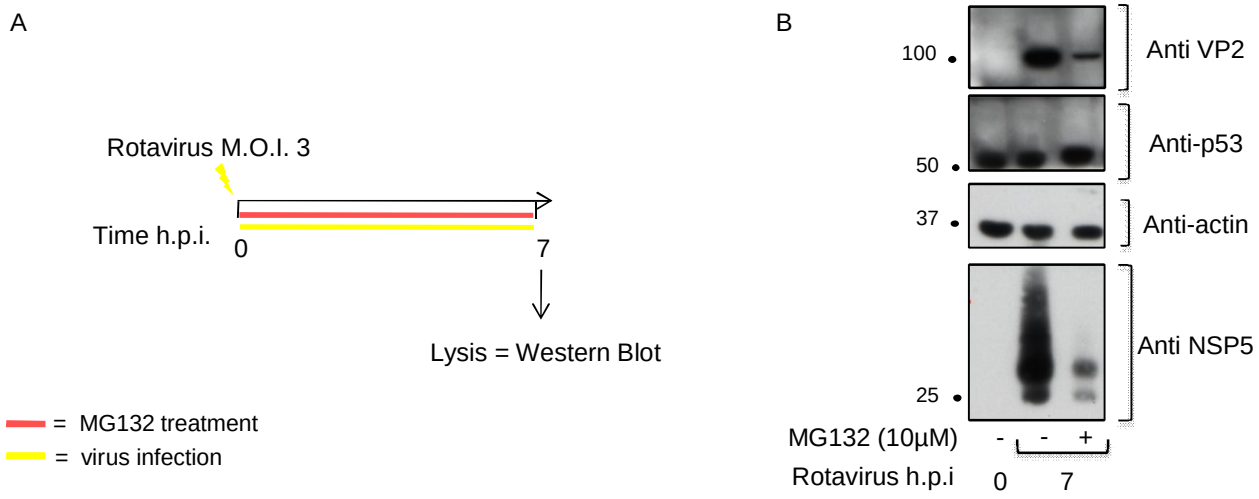

Figure 29: Effect of MG132 on Rotavirus infection. A) Schematic representation of the experimental steps. **B)** Western blot analysis of extracts of treated and untreated infected cells. Upon MG132 treatment there is a decrease in both structural e non structural viral proteins production.

In order to verify whether the inhibition on protein accumulation by MG132 treatment is related to the impairment of the first events of viral infection, we further tested its effect by adding the drug at three hours post infection (Fig.30A). Even in this case, we observed a strong reduction in both the amount of structural (VP2) and non-structural (NSP2, NSP5) viral proteins amount (Fig.30B).

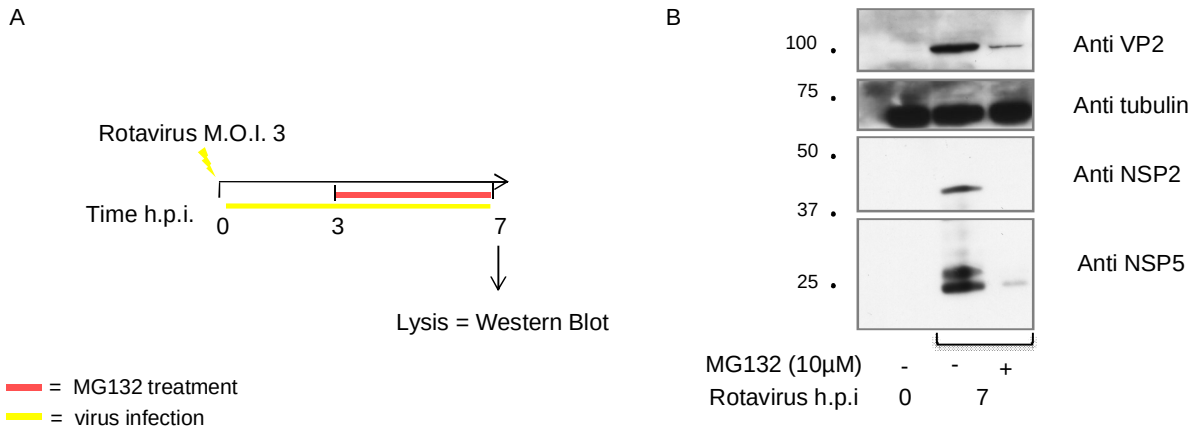

Figure 30: Effect of MG132 added at 3 hours post Rotavirus infection. A) Schematic representation of the experimental steps. **B)** Western blot analysis of extracts of treated and untreated infected cells. Upon MG132 treatment there is a decrease in both structural e non structural viral proteins production.

The effect of MG132 was evident in different rotavirus strains. Indeed we performed the same analysis using the porcine rotavirus strain OSU and the monkey strain SA11 and we observed that both strains had their infection impaired when treated with MG132 since the amount of rotaviral proteins was reduced compared to the controls (Fig.31B). In particular, OSU strain appeared to be more sensitive to MG132 treatment than SA11 strain.

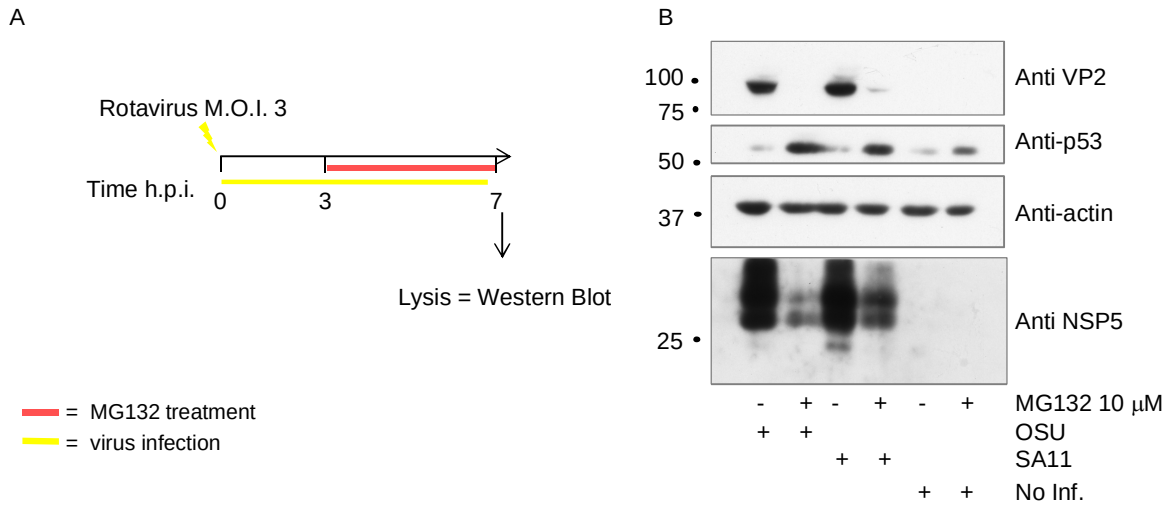

Figure 31: Effect of MG132 on different Rotavirus strains. A) Schematic representation on experimental steps. **B)** Western blot analysis of the extracts of cells infected with different Rotavirus strains, or not infected, and treated or not with MG132. OSU strains seems more sensitive to the treatment respect to SA11 strain.

In order to characterize the effect of MG132 on Rotavirus infection from the early time post infection, we treated infected cells with different concentrations of the drug. MA104 cells were infected with Rotavirus (OSU strain) for one hour, then MG132 at different concentrations was added, and western blot analysis was performed at 7 h.p.i. (Fig32A). Figure 32B clearly shows that the accumulation of viral proteins was dependent on MG132 concentration; in particular, with increasing concentrations of the inhibitor there is a decrease in the level of viral proteins, that is appreciable in NSP5 profile. Furthermore, the addition of the drug soon after the removal of the virus, indicated that the effect, observed in the previous experiments, was not due to the inhibition of the entry and the uncoating of the virus. Since MG132 is a widely used proteasome inhibitor, this observation suggests that rotavirus infection depends in some way on the functionality of the proteasome machinery.

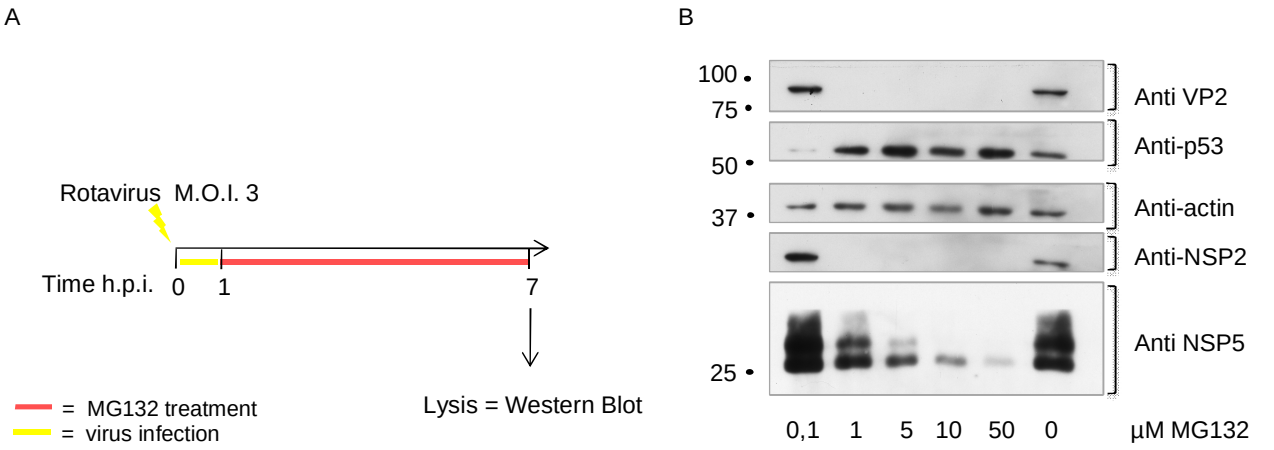

Figure 32: OSU strain treated with different concentration of MG132. A) Schematic representation of the treatment. **B)** Western blot analysis of infected cells treated with different concentration of MG132. Increasing the concentration of the drug induce a concomitant decrease on viral protein accumulation, in a inverse proportion way.

We then measured the amount of viral RNA accumulated upon proteasome inhibition treatment in the first hours post infection. Cells were infected for one hour, and then proteasome inhibitor MG132 (10 µM) was added at one or three hours post infection till seven hours. At the end of the treatment, we performed RT-PCR with primers specific for gene 11 (that correspond to the NSP5), and the levels of viral RNAs (both mRNA and dsRNA), were normalized to the amount present at 1 h.p.i.. In MG132-treated samples, the amount of viral RNAs was lower respect to that in the control (DMSO-treated) and is comparable to that at the beginning of each treatment (Fig.33). Thus, the impairment of proteasome activity affects viral infection both at RNA and protein level.

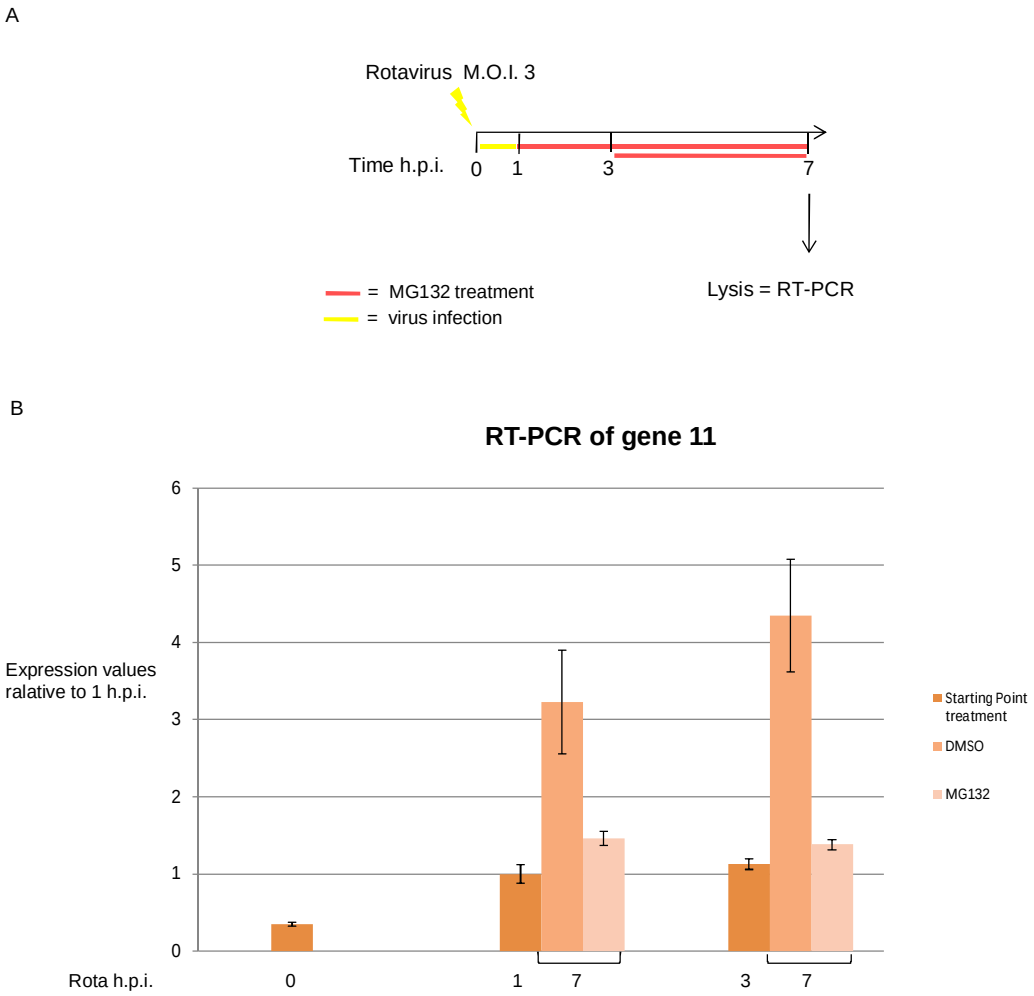

Figure 33: Effect of MG132 on viral RNA. A) Scheme of the experimental procedure. **B)** Total viral RNAs isolated from infected cells after treatment with MG132, were subjected to a real time RT-PCR analysis on NSP5 RNA. The data were normalized to the RNA level present at 1 hour post infection. The graphic shows the impaired viral RNA production in the present of MG132. Graphs report ±SEM in each column

The direct implication of the reduction of viral protein and RNAs accumulation is the impairment of the production of infective viral particles (as described below in paragraph 6.6, page 111), that correspond to a reduction of viral replication.

6.3 Proteasome activity is involved in Rotavirus infection

In order to investigate whether the effect of MG132 on Rotavirus infection was due to inhibition of the proteasome activity, we treated infected cells with other proteasome inhibitors: Bortezomib, and Epoxomycin.

Bortezomib (PS341) is a reversible inhibitor of proteasome activity, as MG132, but is selective towards the proteasome over common proteases. It was approved by FDA as an anti-cancer drug. Its structure and mechanism of action is different from MG132, and is

more active and generally used at concentrations as low as 100 nM. Epoxomycin belongs to the class of irreversible non-aldehydic peptide inhibitors, highly selective and potent with a distinct mechanism of action, with respect to MG132 (130).

Infected cells were treated with different concentration of MG132, Bortezomib, and Epoxomycin, after one hour of virus absorption, and the biochemical analysis was performed at 7 h.p.i. (Fig.34A). All the proteasome inhibitors tested affected the accumulation of viral proteins, while inducing a strong inhibition of the proteasome activity as revealed by the accumulation of p53. Among the three inhibitors, MG132 and Bortezomib have the stronger effect on virus infection. Already at a concentration of 1 μM, there was an effect, which was almost complete at 10 μM. Epoxomycin showed a reduced effect on the amounts of viral proteins at a concentration of 10 μM, which was nevertheless very effective in inducing accumulation of p53 (Fig 34B). This analysis confirmed that when the proteasome was strongly inhibited, Rotavirus infection was effectively compromised.

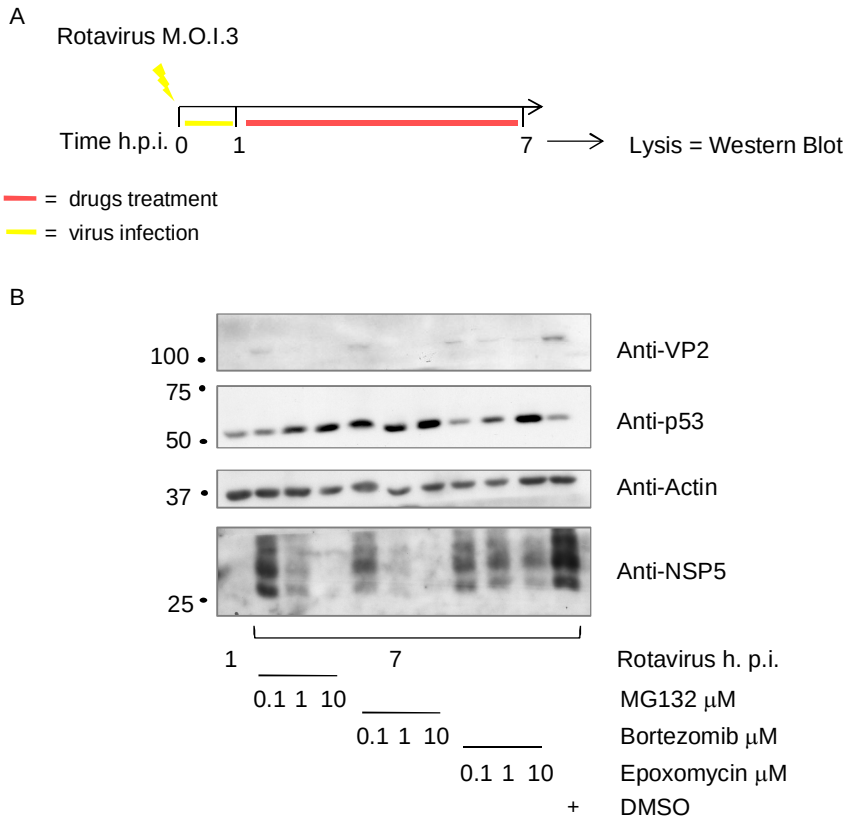

Figure 34: Rotavirus infection depends on proteasome activity. A) Schematic representation of the experimental procedure. **B)** Western blot analysis of extracts of infected cells treated with different concentration (0,1; 1; 10 μM) of different proteasome inhibitors (MG132, Bortezomib, Epoxomycin). The effect on Rotavirus infection is proteasome dependent.

Since we have excluded that proteasome inhibition affects the phases of virus entry and uncoating (Fig.31,32), we performed different kinetic experiments in order to better define the time window in which the drug impairs the viral cycle.

We let the virus infect the cell for one hour, then, after washing with serum free medium, the cells were treated or not with MG132 or Bortezomib for 4 hours at different time points post infection (Fig.35 A). The western blot analysis performed at the end of the treatments confirms that proteasome activity is important for viral proteins production primarly at early time points post infection, since its inhibition from the very beginning of infection causes a more clear arrest on viral protein accumulation (Fig.35 B). The effect is less evident at 5 hr post infection, as evidenced in the experiment of panel C (Fig.35, left panel), suggesting that the viral mechanism sensitive to proteasome activity takes place in the first five hours of infection. Indeed, when the drug was added at later time points post infection, hour 7 to 10, the inhibition is almost null. (Fig 35C right blot).

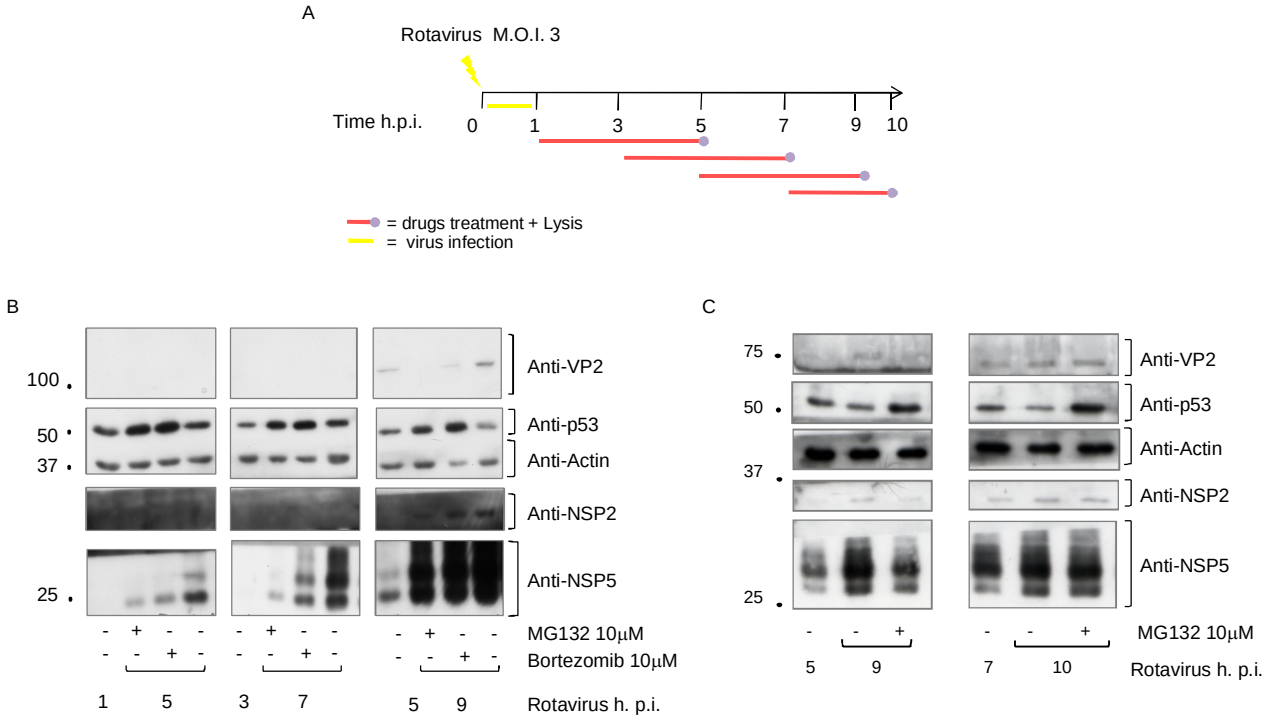

Figure 35: Time-windows treatments with proteasome inhibitors. A) Schematic representation of the kinetic. **B),C)** Western blot analysis of the cell lysates of treated and untreated infected cells as indicated in A). Treatment in the first five hours of infection affects virus proteins production.

6.4 Proteasome inhibition affects viroplasms formation

These results suggest that the effect is stronger in the phase when viroplasms are formed and expanded in size and number. We therefore performed immunofluorescence analysis

to characterize the effect of proteasome inhibition on viroplasms formation during Rotavirus infection. For this purpose, kinetic experiments, were performed using the NSP5-EGFP stable cell line (previously described).

NSP5-EGFP cells were infected for one hour and then, at different times post infection, were treated with MG132 or bortezomib at an effective concentration of 10μM. At 9 h.p.i viroplasm formation was evaluated with confocal microscopy. As shown in figure 36B, addition of proteasome inhibitors from 1 to 5 h.p.i induces an arrest on formation of viroplasms that appear in reduced number and look smaller, with respect to those in untreated cells (DMSO-treated). On the contrary the addition of proteasome inhibitors at 7 h.p.i did not show any effect on viroplasms which were comparable in number and dimension, confirming that the early/middle phases of expansion of viroplasms are the ones more susceptible to proteasome inhibition. The immunofluorescence analysis confirmed the previous observations, with a strong reduction in the number of viroplasms without preventing virus entry or uncoating. Moreover we confirm the observations of the previous kinetic analysis, since in treated infected cells the viroplasms appear smaller and even less in number with respect to the control cells.

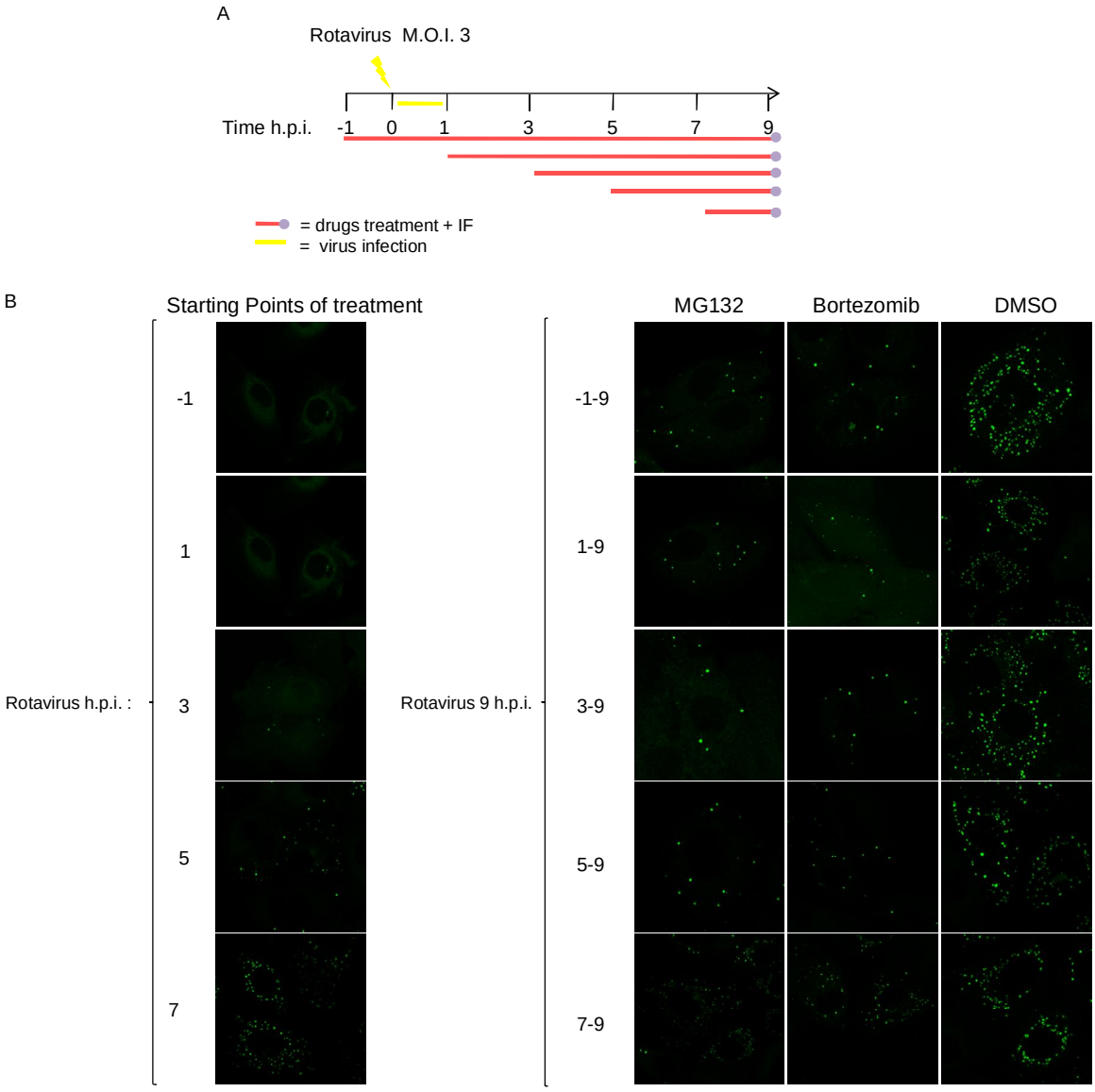

Figure 36: A) Scheme of the kinetic. **B)** Immunofluorescence analysis of NSP5-EGFP cell line infected with Rotavirus 3 M.O.I and treated, or not, with proteasome inhibitors (10 μM) at different time pre and post infection. Inhibition of proteasome activity induces the formation of small and less numerous viroplasms.

6.5 Proteasome inhibition affects viroplasms growth

According to these observations, we performed time-windows kinetic as well, to quantify the effect of proteasome inhibition on viroplasms formation.

The quantification was made with an automated microscope able to identify and quantify defined structures in the cytoplasm of cells, such as viroplasms upon infection of the NSP5-EGFP stable cell line. Initial experiments were performed on untreated cells to follow the kinetics of viroplasms accumulation during infection at M.O.I. 3 (as shown in the graphic in figure 37).

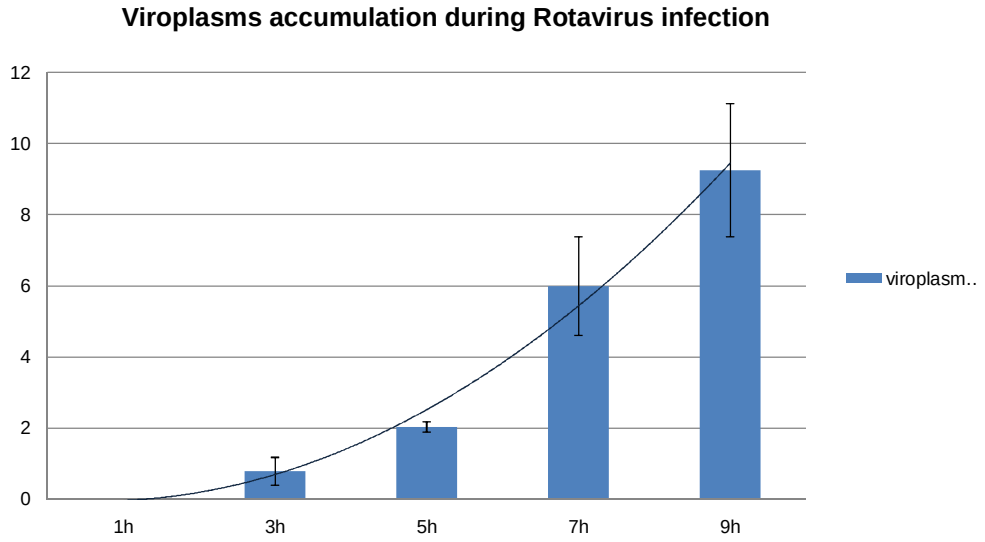

Figure 37: Viroplasms accumulation during viral infection. Viroplasms per cell were quantified during a typical Rotaviral infection with an automated high content microscope (as describe in material and methods). Graphs report ±SEM in each column.

MA104 NSP5EGFP were plated on a 96 multiwell plate, infected for one hour and, at different times post infection, MG132 or Bortezomib, or DMSO as control, were added for four hours. Each time windows was performed in triplicates, and the graphic 2 shows the mean of the measurements relative to the number of viroplasms per cell obtained with the quantification analysis. Treatment with MG132 or Bortezomib affects viroplasms formation when added both at the beginning of infection (starting point SP), and at 5 hours of virus infection. The number of viroplasms per cells in MG132 or Bortezomib treated cells is almost the same to that found in cells fixed at the beginning of each treatment, strongly suggesting that inhibition of proteasome activity affects the assembly of new viroplasm and their growth.(Fig 38)

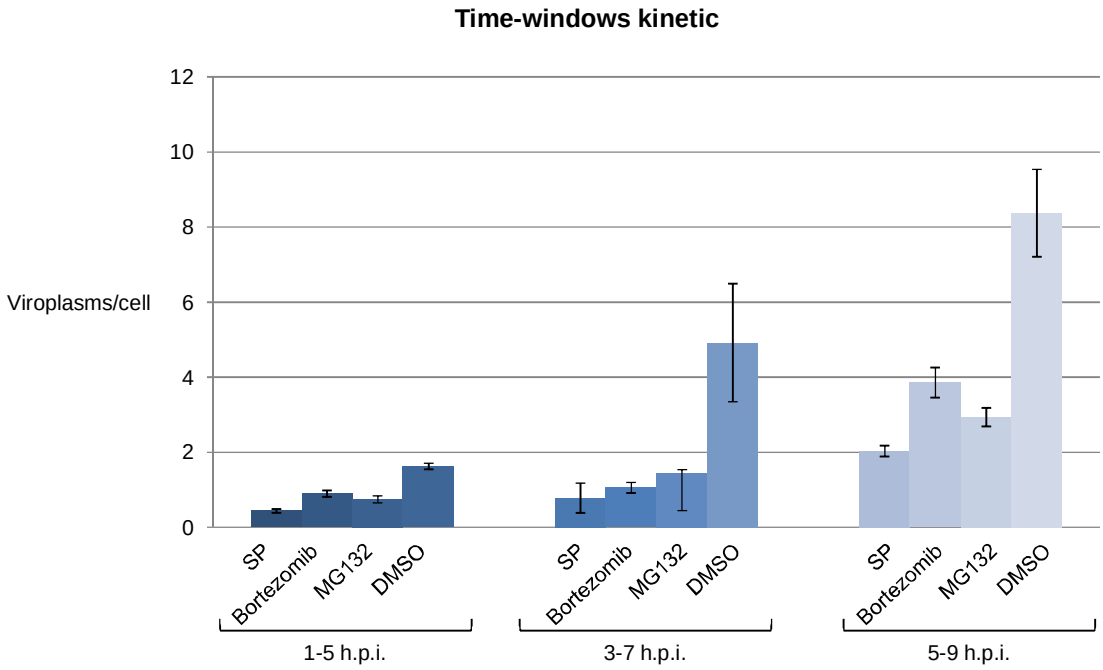

Figure 38: Time-windows treatment of NSP5-EGFP cells. Quantification of viroplasms accumulation within infected cells (M.O.I. 3) in a time-windows treatment with MG132 and Bortezomib at 10 μM concentration. The graphic shows the mean of viroplasms/cell of one exemplificative experiment. Graphs report ±SEM in each column

6.6 Proteasome inhibition affects production of viral particles

Since inhibition of proteasome activity induces arrest of viral protein synthesis and viroplasms growth, we expect a decrease in the production of new viral particles. To address this point we analysed the viral progeny from treated or untreated infected cells titrating by IF the yield of infective particles produced. Trypsin activated particles were used to infect the NSP5-EGFP cell line, at different dilutions. The amount of green cells and viroplasms per cells, after seven hours of infection, was determined with the same automated microscope. As shown in the graphic of figure 39B, cells treated with proteasome inhibitors showed a strong reduction in viral titers. While a reduction of 75% of virus was observed when considering the number of cells with viroplasms (Fig 39C), a reduction of more than 90% was obtained considering the number of viroplasms per cell.(Fig 39B)

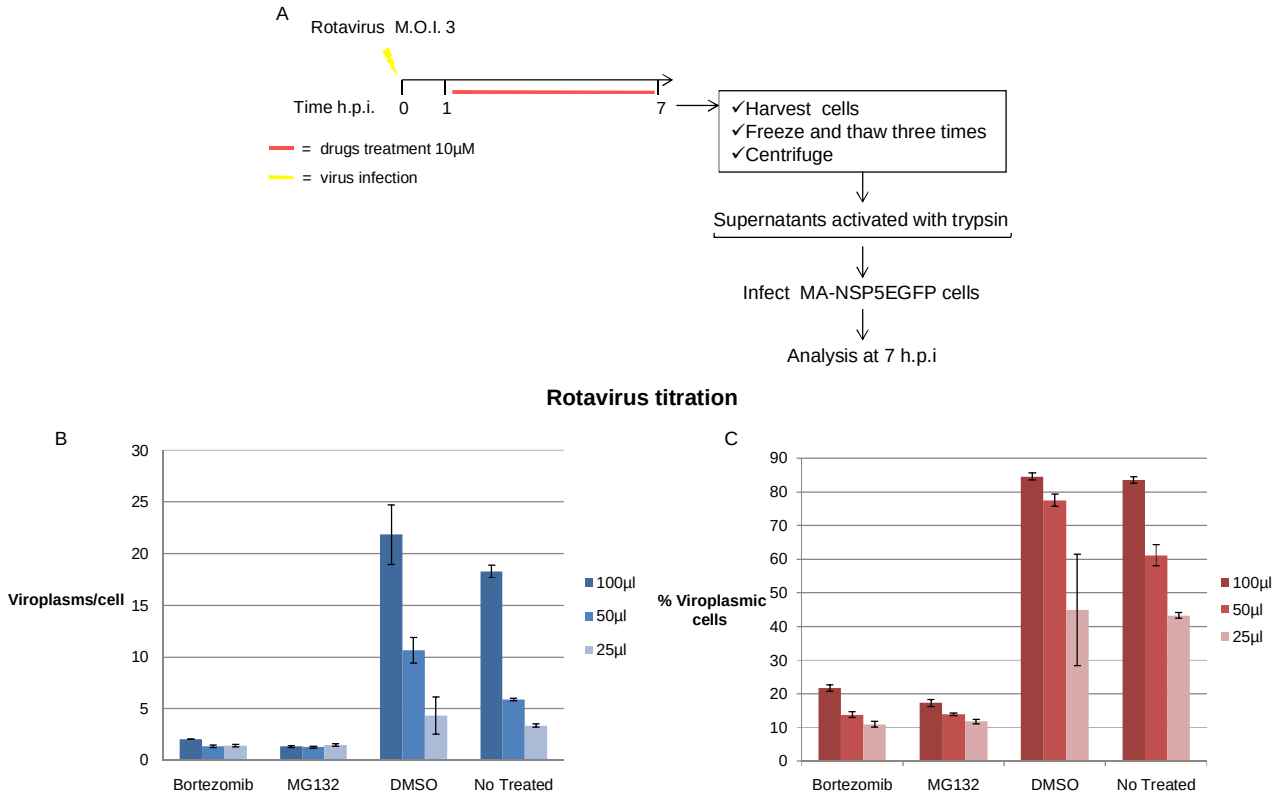

Figure 39: Titration of Rotavirus obtained from treated cells. A) Scheme of experimental procedure. **B)** Graphics show the mean of the viroplasms per cell (left) and of the percentage of cells with viroplasms (right) of NSP5-EGFP cells infected (M.O.I. 3) with different amounts of supernatants derived from MA104 infected cells treated or un treated with proteasome inhibitors (10µM). Graphs report ±SEM in each column

6.7 Viral proteins expression is not affected by proteasome inhibition

The effect of proteasome inhibition upon infection could be due to a direct involvement of proteasome activity on the expression of viral proteins. Following our studies on NSP5 and its modifications induced by the interaction with NSP2 and VP2, we investigated if these proteins changed their expression when proteasome functionality was impaired. For these purpose we transfected the cells with NSP5, NSP2, and VP2 alone or in different combinations and then treated with MG132 at high concentration (50 µM) for two hours. The Western blot analysis of cell extracts reveals that there is not differences on NSP5, or NSP2 or VP2 expression between treated or not treated cells, as it happens for the irrelevant transfected protein EGFP (Fig.40). Furthermore, in the presence of MG132, NSP5 modifications in the presence of VP2 or NSP2 do not change. These observations suggest that proteasome activity is not directly involved in modulating the expression of these proteins that, are fundamental for virus replication (27), (180), (141),. Moreover it is

not involved either in controlling hyperphosphorylation of NSP5 induced both by VP2 or NSP2.

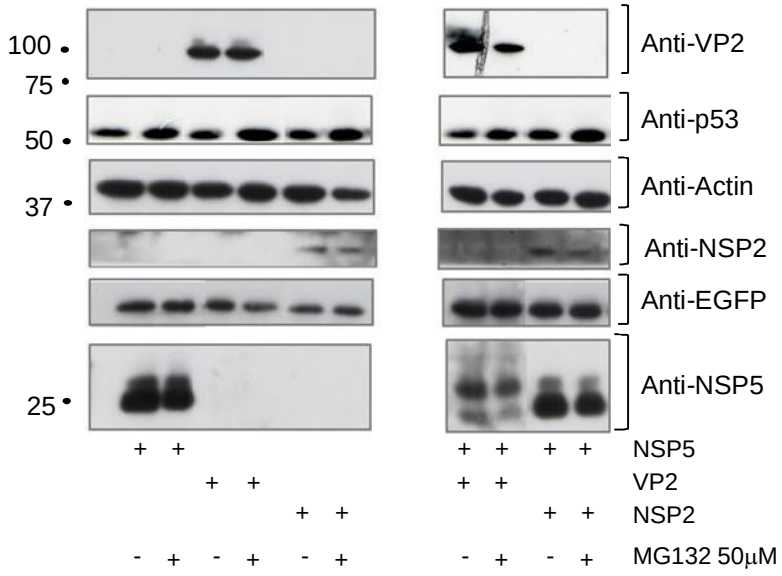

Figure 40: Proteasome inhibition does not affect viral protein expression. Western blot analysis of cells transfected with NSP5, NSP2, VP2 alone and in different combinations, in treated or untreated conditions.(MG132 50μM). Proteasome inhibition does not arrest viral protein expression.

We also investigated the cytoplasmic distribution of these proteins upon treatment with MG132. As previously described, NSP5 forms VLS in the presence of NSP2 or VP2, thus we performed immunofluorescence assays, in NSP5-EGFP cell line, to look at VLS formation in cells transfected with these proteins, and treated or not with the proteasome inhibitors. Figure 41 shows that under these conditions, treatment with MG132 does not impair VLS formation, either those formed by VP2 (VLS (VP2i)) or by NSP2 (VLS (NSP2i)) or by both VLS(VP2/NSP2i).

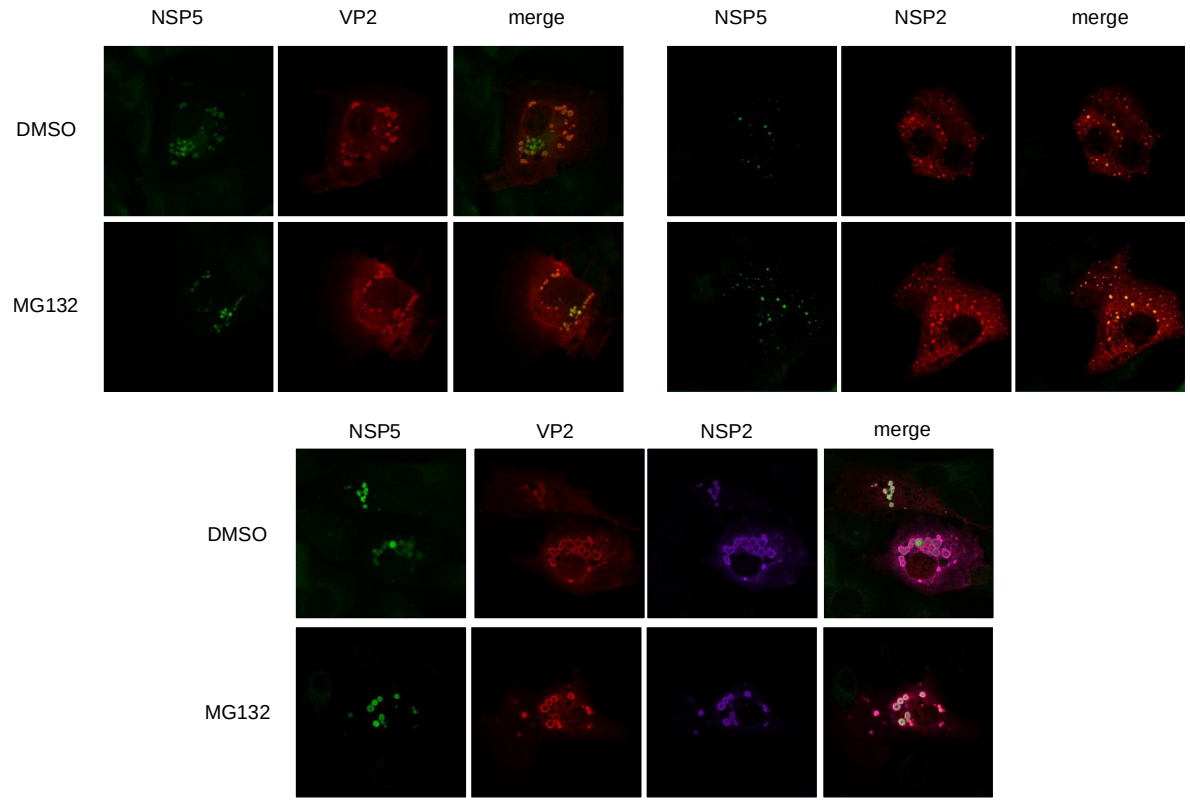

Figure 41: VLS formation is not impaired by proteasome inhibition. Immunofluorescence analysis of NSP5-EGFP cells transfected with VP2, or NSP2, or both in the presence of proteasome inhibitor MG132, 50 µM, for 2 hours before the cell lysis. VLS formation is not affected when proteasome activity is inhibited.

Together these observations suggest that the effect observed on Rotavirus replication upon proteasome inhibition is not due to an effect regulating expression of NSP5, NSP2, VP2, nor to their capacity to interact (co-localising in VLS) and to induce NSP5 hyperphosphorylation. Rather, this indicate that there are essential host factor(s) needed to be properly removed through degradation by the proteasome to allow the assembly of viroplasms.

6.8 Proteasome inhibition does not impaired viral polymerase activities

Alternatively, the block in viroplasms formation could be due to a direct, yet improbable, effect of the proteasome inhibitors on the viral polymerase activity.

To test this hypothesis we analysed both the transcriptase and replicase activity of VP1 in the presence of MG132.

Transcriptase activation was performed on purified DLPs which are well-known to have only trascriptase (and not replicase) activity when incubated *in vitro* in appropriate conditions. To monitor synthesis of mRNA, DLPs incubations were carried out with [^{32}P]-

αUTP, in the presence or not of MG132, and the products precipitated by TCA10% and radioactivity counted on a scintillator counter (count per minute, CPM). An additional control was conducted incubating DLPs without nucleotide GTP to validate the occurrence of transcription. Measurements were performed in triplicate and non treated sample was considered as the standard. The CPM mean values relative to the standard condition, of four independent experiments are plotted in figure 42.

The results clearly indicate that VP1 transcriptase activity was totally unaffected by MG132; suggesting that the effect in vivo on virus replication is not due to a direct inhibition of trascription.

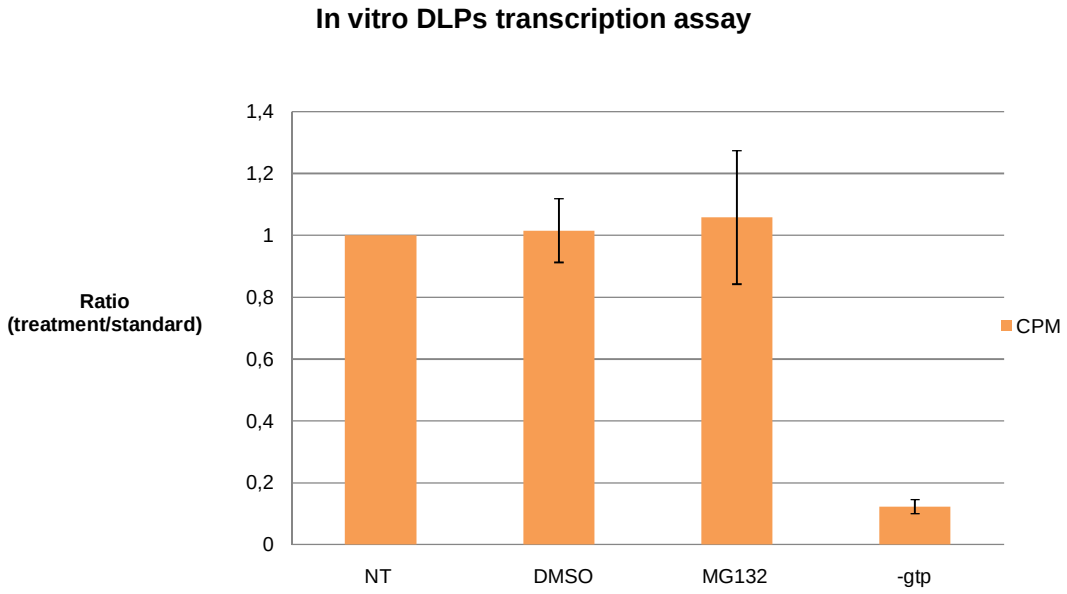

Figure 42: In vitro transcription assay. Graphic of the mean of four different in vitro transcription assays. Non treated (NT) condition is considered as the standard, treated conditions (DMSO, MG132) measurements are relative to NT, -gtp is the control of the transcription assays. Graphs report ±SEM in each column

To test the replicase activity we performed in vivo labeling in cell infected for five hours and then incubated with ^{32}P with or without MG132 for one hour. At five hours post infection the VP1 replicase activity is quite high, and therefore the addition of the proteasome inhibitor (in this case MG132) at this phase would reveal if it directly affects the VP1 polymerase activity. The level of replication was visualized by purification of viral dsRNA and analysed by PAGE as shown in figure 43. These preliminary results suggest that also the activity of the polymerase is not compromised by inhibition of the proteasome. Taken together these observations strongly suggest that it is indeed some

stage of viroplasm assembly that proteasome activity is required for efficient virus replication.

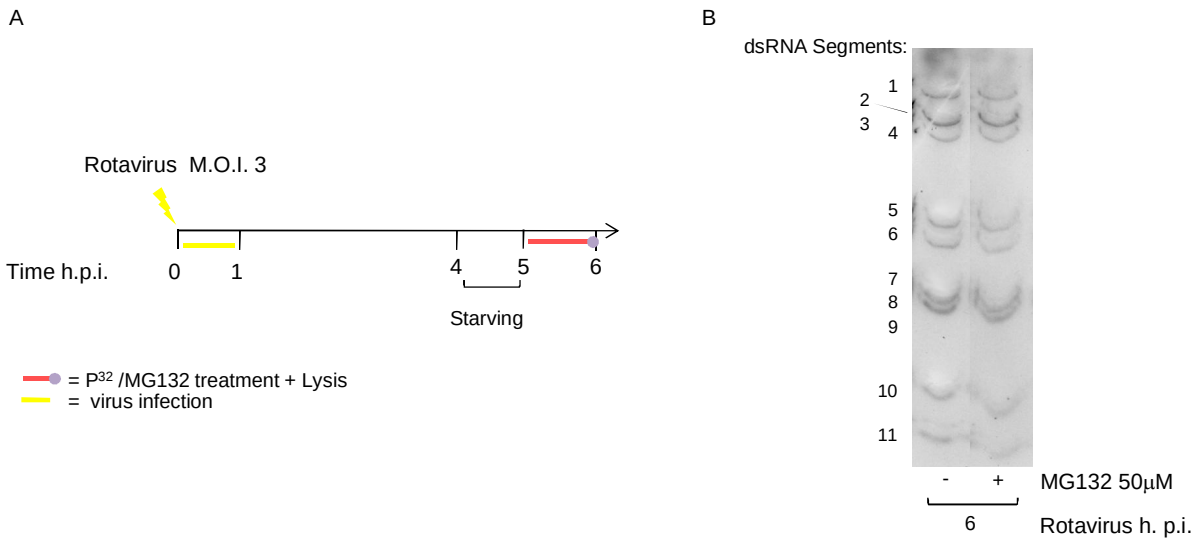

Figure 43: Replicase activity assay. A) Scheme of the experimental procedure. **B)** SDS-PAGE of radiolabeled dsRNA from treated and untreated infected cells. Treatment with proteasome inhibitor does not impaired viral dsRNA production of the VP1 polymerase.

6.9 Viral infection affected by proteasome inhibitor is not due to IRF3 amounts

As already described in the introduction(1) (page 32), NSP1 is involved in the evasion of cellular antiviral response, by inducing the proteasomal degradation of IRF3 and, in this way, preventing the activation of interferon-β response (13). Moreover, according to recent observations, IRF3 disactivation by Rotavirus NSP1 is dependent on both Rotavirus strain and host cell (177). In particular, the porcine Rotavirus strain OSU does not induce the degradation of IRF3, whereas the SA11 strain does induce proteasome-mediated degradation of IRF3 (177),(13). To investigate if the effect of MG132 on viral proteins was related to the accumulation of IRF3, due to the proteasome inhibition, we performed Western blot analysis of extracts of non infected and infected cells with both OSU and SA11 Rotavirus strains, treated or not with MG132. By biochemical analysis we confirmed that OSU strain does not induce degradation of IRF3, and that the effect of proteasome inhibition shown on viral protein expression is independent of IRF3 amount (lane 1 and 2 fig.44). On the contrary, SA11 causes an almost complete degradation of IRF3 factor, that is poorly recovered by the addition of MG132 (lane 3 and 4, fig.44). All

these data support the hypothesis that, even if from the last observation we cannot exclude that, in SA11 strain, it is the little amount of IRF3 that affects viral protein accumulation, the accumulation of IRF3 is not related to the decreased amount of viral proteins observed in the presence of MG132. This is further supported by the evidence that in OSU strain where IRF3 amount does not change, the effect of MG132 on viral protein accumulation is stronger. Basal IRF3 expression itself is not affected by the inhibition of the proteasome as it is shown in non infected cells (fig.44 lane 5, 6).

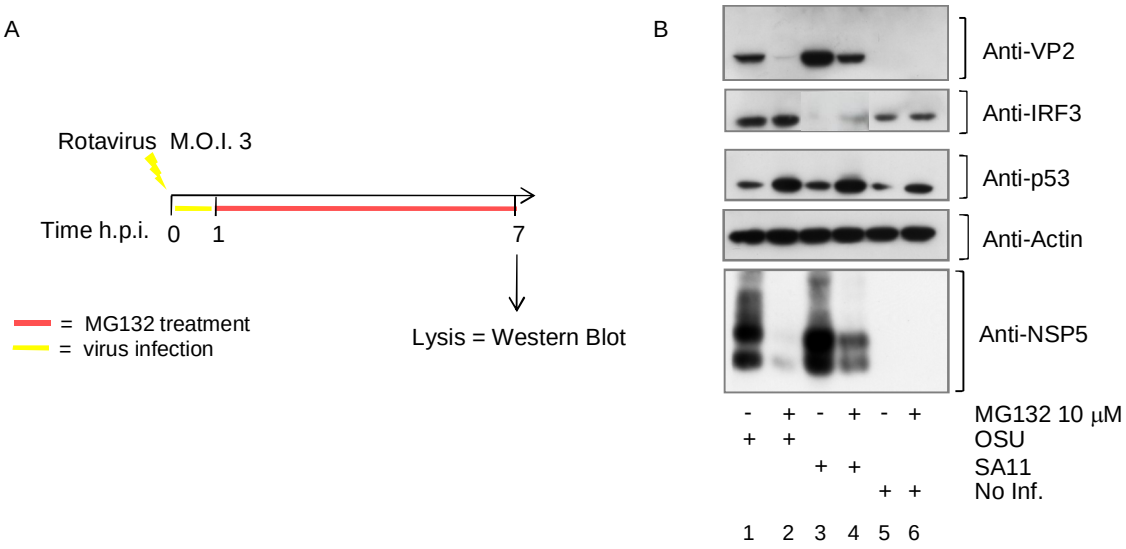

Figure 44: IRF3 amount is not related to inhibition of infection. A) Scheme of the experimental procedure. **B)** Western blot analysis of exctrats of infected cells treated or not with MG132 (10μM). IRF3 is degraded upon infection with SA11, but not with OSU strain, however the amount of viral protein is strong affected in both cases.

7 DISCUSSION (2)

Proteasomal degradation is involved in different cellular functions like transcription factor regulation, gene expression, cell differentiation, regulation of the newly synthesized proteins (ERAD), cell cycle regulation, immune response. In particular, it is the central machinery for the production of peptides to load on the MHC class I molecules for the antigen presentation. Viral proteins, as well as misfolded ones, are ubiquitinated, processed by proteasome, and the obtained peptides are presented on cell surface through MHC class I, in order to induce the cytotoxic T lymphocytes activation, that start the elimination of the infected cells (93),(80).

Viruses have been shown to manipulate the ubiquitin-proteasome pathway at different stages of the virus life-cycle, to enhance viral activities and to escape the viral cellular response. For example, influenza virus has been shown to utilize the UPS for efficient trafficking to the late endosome/lysosome stages of virus entry (99), mouse hepatitis virus (a coronavirus) or minute virus (a parvovirus) have been shown to use the proteasome machinery for their trafficking in the cytoplasm (212) or to the nucleus, (167) respectively. Retroviruses, like HIV, need a functional UPS for the release of mature viral particles. Indeed, this process involves ubiquitylation of some components of the complex that drive the exit of the virus from the cells, and an alteration of the store of free ubiquitin, induced by proteasome inhibition, prevents the budding of the virus (176),(86). Multiple members of the *Herpesviridae* family have developed different strategies to manipulate UPS, encoding ubiquitin ligase like proteins (39), or targeting to degradation specific host proteins (39), (161), (100).

In this work we characterized the effect of proteasome inhibition on Rotavirus infection. Indeed, we observed that the inhibition of proteasome activity, induced mainly with two different proteasome inhibitors (MG132 and Bortezomib), affects Rotavirus replication, indicating that functional proteasome is needed during its replicative cycle.

We first observed a decrease in the amount of both structural and non-structural viral proteins accumulated in virus infected cells in the presence of the MG132 inhibitor (fig.29) and this effect is also evident when the inhibitor is added at 3 hours post infection (fig.30). Moreover, the effect is appreciable in two different Rotavirus strains, a porcine OSU and a simian SA11 strain, in particular OSU strain results more sensitive to proteasome inhibition respect to the SA11, using comparable M.O.I. (Fig.31). This first indications suggest that

entry and uncoating of the virus were not the steps affected by proteasome inhibition. The timing of the Rotavirus life cycle is not well established, however, the processes of virus entry and uncoating likely occur in the first hour of infection (97). Thus the treatment of infected cells with MG132 performed one hour after the absorption of the virus on the cells would discriminate these first steps from the other later viral processes (transcription, replication, morphogenesis) (Fig.32A). Indeed, after one hour the viral particles have already entered the cell, and uncoated DLPs are producing mRNAs. Addition of MG132 one hours post viral absorption still affects viral proteins production, confirming the hypothesis that the entry and uncoating of virus are not the processes impaired by proteasome inhibition (Fig.32B). Moreover, the addition of MG132 till 5 hours post infection, cause a moderate/appreciable decrease on the amount of viral proteins, whereas the treatment at later time point post infection, from 7 h.p.i. until 10, does not affect viral protein accumulation at all (Fig.35C). Therefore, a functional proteasome machinery is needed principally in the early phases of virus infection in order to allow Rotavirus replication into the host cells.

The inhibition observed in the accumulation of viral proteins amount was dependent on the concentration of the drugs used, this is clearly demonstrated in figure 32, where increasing MG132 concentrations corresponded to an almost proportional decrease in viral proteins, visible in NSP5 profile (Fig.32B). But it is also evident when other different proteasome inhibitors at different concentrations were used (Fig.34). MG132, Bortezomib and Epoxomycin induce accumulation of p53 protein, demonstrating the effective inhibition of the proteasome activity, furthermore they inhibit viral protein production, strongly confirming the necessity of a functional proteasome during viral infection.

The impaired viral proteins production is probably due to the concomitant impairment of viral RNA accumulation. RT-PCR analysis revealed that the amount of total viral RNAs (both mRNA and dsRNA) decreases upon treatment with MG132 at different hour post infection (Fig 33). However, with this technique it was not possible to discriminate the viral transcribed RNA (mRNA), that is continuously produced from newly synthesized DLPs and is source for viral proteins, from the replicated RNA (dsRNA); but, in addition to the previous observations, it gives indications that different viral functions are compromised when proteasome activity is impaired.

An important characteristic in Rotavirus infection is the formation of viroplasms, that, as previously described, are cytoplasmic structures where viral replication and new DLPs assembly occur. Proteasome inhibition causes a reduction on viroplasms formation, as

well. Immunofluorescence analysis revealed that the addition of proteasome inhibitors from 1 till 5 hours post infection induced a decrease in viroplasms formation and their growth. On the contrary when the drugs were added at 7 hours post infection this effect was not any longer appreciable, in agreement with the observations of the biochemical analysis (Fig.36). The quantification analysis of this reduction was performed with an automated microscope, and confirms the decreased number of viroplasms per cell upon inhibition of proteasome. In particular the number of viroplasms measured at the beginning of the treatment with proteasome inhibitors is very similar to that find at the end, suggesting that the process of viroplasms formation is like frozen at the moment of drug addition and the early phase of viroplasms assembly is more susceptible to proteasome inhibition, as expected from the previous biochemical analysis (Fig.38). Since the mechanism of viroplasm formation are still obscure, even their composition and function have been differently characterized (55), (56),(60),(127),(180),(178), and the involvement of cellular components within viroplasm are under investigation, we can propose, according to these observations, that proteasome regulate the early step of viroplasms formation and growth, controlling either viral or cellular mechanisms.

The final consequence of the proteasome inhibition is the reduction of viral particles production. Indeed, the treatment from 1 till 7 hour post infection allowed the recovery of particles that are yet functional and infective, following activation with trypsin; however the yield was extremely reduced since, when cells were infected with these particles for 7 hours, only the 25% of infected cells presented viroplasms. Moreover, the amount of viroplasms per cells is very low and the reduction is quantified at around the 90% compared to the control cells (Fig 39).

The transient expression, alone and in different combinations, of viral proteins like NSP5, NSP2, VP2, that have been demonstrated to be essential for viral replication (180),(27),(141), seemed not to be affected by proteasome inhibitor treatment (Fig.40). Moreover, the NSP5 profile of hyperphosphorylation induced by NSP2 or VP2 does not change in the presence of MG132. Nevertheless, this is only a first indication since, due to technical problems, the treatment was performed in a short time window, 2h, and the effect of proteasome inhibition, evaluated with the accumulation of p53, is not easily appreciated in treated sample. Further experiments are underway to improve proteasome inhibition and to investigate what happen to the viral proteins expression.

As described in the first part of this thesis, transient expression of NSP5 with NSP2 or VP2, induces the formation of VLS in the cytosol. The structural changes and the

interactions that permit the formation of VLS are still under investigation, however VLS formation seems not to be affected by proteasome inhibition (for this assay it was possible to peformed the treatment 4h after the transfection, for 2h, and any differences in VLS formation were appreciated, not shown), first indicating that this event does not depend on proteasome activity, as well (Fig.41). Furthermore, the co-localization of viral proteins into VLS was not altered, suggesting that the interactions that allow VLS formation, take place even when the proteasome is inhibited.

Since VLS are considered the model that better resembles viroplasms, the different sensitivity of these two structures to the proteasome inhibition would suggest that the similarity between them is mainly structural. Therefore, these observations would confirmed our previous hypothesis that, during infection, an unidentified host/viral mechanism/factor (different from NSP5, NSP2, VP2) rather-dependent on proteasome activity, is needed in order to maintain viroplasms function and growth and consequently viral replication; moreover the same factor is not activated by induction on VLS formation probably due to the lack of other different viral components. However, functional assays with VLS, containing also VP1 VP6 and VP3, and viral mRNAs are underway and would eventually lead to a better functional characterization of VLS.

The improbable direct effect of the inhibitors on polymerase activities has also been investigated. The trascriptase activity was measured by counting the radiolabeled viral mRNA transcribed *in vitro* from DLPs in the presence or not of MG132. The measurements of the radioactivity incorporated into mRNA reveal that, there is no differences in mRNA amount produced in treated and untreated samples, further, no transcription was observed in the absence of GTP nucleotide, confirming that the transcription event is taking place and validating the result obtained (Fig.42). The replicase activity was tested *in vivo* when it reaches the maximal level between 5 and 9 hours post infection (184), through labeling of dsRNA with a pulse of radioactive inorganic phosphate ^{32}P. Treatment with MG132 was performed at 5 hour post infection, for one hour in order to limit its effect upon the whole infection and possibly concentrated it on viral replicase activity. Preliminary result, shown in figure 43, suggests that the replicase activity of VP1 is not impaired by proteasome inhibitor treatment, as well. These experiments exclude the possibility of a direct effect of the drug used on viral polymerase activity, and direct the research towards the cellular of viral mechanism that take place during the infection.

Rotavirus NSP1 has been demonstrated to be related to the UPS, since experimental data and sequence analysis identified a variant of a RING finger motif, similar to E3 ligase,

suggesting a putative function for NSP1 as an E3 ligase. Indeed, NSP1 is able to promote its self-ubiquitinylation and moreover to induce the degradation of different members of IRF family, IRF3, IRF5, IRF7, preventing the activation of IFNβ, proinflammatory cytokine, and IFNα genes, respectively (13, 14). Therefore, like many other viruses, Rotavirus manipulates the proteasome machinery to create an opportune environment for its replication.

According to these observations, inhibition of proteasome activity during infection would cause an accumulation of IRF3 factor with a consequent enhanced IFN-β response that may be responsible of the affected viral infection. Thus, the accumulation of IRF3 has been investigated, to understand if this was the case. The regulation of IRF3 amount through proteasome degradation is virus-strain specific (177). For this reason the analysis has been performed with two different Rotavirus strains.

Upon infection with SA11 strain, IRF3 factor is strongly degraded, and when infected cells are treated with proteasome inhibitor, a very low rescue of this factor was observed, and a strong effect on viral protein production is still visible (Fig.44 lanes 1,2). It is possible that the little amount of IRF3 rescued with MG132 treatment causes a reduction of viral protein accumulation, possibly through IFNβ activation. However, the amount of IFNβ has not been measured and we do not know if at 7 h.p.i, when we performed the analysis, critical amounts of IFNβ are produced that affect viral infection. Evidences of a high gene expression induced by IFNβ production upon Rotavirus infection has been provided by Barro et al. (13) in $FRhL_2$ cells at 10 h.p.i.; however there are not indications to what happens at 7 h.p.i in MA104 cells.

Infection with OSU strain does not induce IRF3 degradation, as already demonstrated (69). When the proteasome is inhibited, despite there is not further accumulation of IRF3, the effect on viral proteins amount is even stronger respect to SA11 (Fig.44 lane 3,4). All together these observations suggest that cytosolic amount IRF3 upon inhibition of proteasome activity is not related to the impairment of Rotaviral infection Moreover, it has been recently observed that OSU strain mediates the proteasome degradation of cellular factors involved in NFκB activation (68). Thus, it would be important for this strain to investigate if impairment of its replication by proteasome inhibition is related to NFκB activation.

NSP1 regulates its own stability through proteasome-mediated degradation, however we could not analyse the amount of this protein due to the lack of a specific NSP1 Ab. It has been demonstrated that NSP1 is not fundamental for Rotavirus infection, since infected

cells treated with an siRNA specific for NSP1 actively support virus replication (180). However, it cannot be ruled out that an accumulation of NSP1 induced by proteasome inhibition interferes with viral infection. Moreover its putative E3 ligase activity would be altered, when proteasome is impaired, affecting and destabilizing virus replication.

The inhibition of viral infection induced by the treatment with proteasome inhibitors has been recently described for other dsRNA viruses like ARV (avian reovirus) (36), and IBDV (infectious bursal desease virus) (113). Even for these viruses, inhibition of the proteasome causes a decrease in viral proteins amount, a reduction in viral progeny production, and a diminished viral transcription. Moreover, in both cases this inhibitory effect is evident at early phases of the infection, suggesting that the UPS is involved in the early steps of viral replication. However, the mechanisms involve in the reduced viruses replication through proteasome inhibition has not been characterized either for ARV or IBDV.

The observations collected for Rotavirus are in line with those of ARV and IBDV, suggesting that, in dsRNA virus infection, there are common mechanisms, that cause the impairment of infections followed by proteasome inhibitors, most likely related to alteration of UPS, or of cellular processes involving key host factors dependent on proteasome activity, rather than to the functions of viral proteins.

BIBLIOGRAPHY

1. **Afrikanova, I., E. Fabbretti, M. C. Miozzo, and O. R. Burrone.** 1998. Rotavirus NSP5 phosphorylation is up-regulated by interaction with NSP2. J Gen Virol **79 (Pt 11):**2679-86.

2. **Afrikanova, I., M. C. Miozzo, S. Giambiagi, and O. Burrone.** 1996. Phosphorylation generates different forms of rotavirus NSP5. J Gen Virol **77 (Pt 9):**2059-65.

3. **Ago, H., T. Adachi, A. Yoshida, M. Yamamoto, N. Habuka, K. Yatsunami, and M. Miyano.** 1999. Crystal structure of the RNA-dependent RNA polymerase of hepatitis C virus. Structure **7:**1417-26.

4. **Aoki, S. T., E. C. Settembre, S. D. Trask, H. B. Greenberg, S. C. Harrison, and P. R. Dormitzer.** 2009. Structure of rotavirus outer-layer protein VP7 bound with a neutralizing Fab. Science **324:**1444-7.

5. **Arias, C. F., P. Isa, C. A. Guerrero, E. Mendez, S. Zarate, T. Lopez, R. Espinosa, P. Romero, and S. Lopez.** 2002. Molecular biology of rotavirus cell entry. Arch Med Res **33:**356-61.

6. **Arnoldi, F., M. Campagna, C. Eichwald, U. Desselberger, and O. R. Burrone.** 2007. Interaction of rotavirus polymerase VP1 with nonstructural protein NSP5 is stronger than that with NSP2. J Virol **81:**2128-37.

7. **Au, K. S., W. K. Chan, J. W. Burns, and M. K. Estes.** 1989. Receptor activity of rotavirus nonstructural glycoprotein NS28. J Virol **63:**4553-62.

8. **Au, K. S., N. M. Mattion, and M. K. Estes.** 1993. A subviral particle binding domain on the rotavirus nonstructural glycoprotein NS28. Virology **194:**665-73.

9. **Au, W. C., P. A. Moore, D. W. LaFleur, B. Tombal, and P. M. Pitha.** 1998. Characterization of the interferon regulatory factor-7 and its potential role in the transcription activation of interferon A genes. J Biol Chem **273:**29210-7.

10. **Au, W. C., P. A. Moore, W. Lowther, Y. T. Juang, and P. M. Pitha.** 1995. Identification of a member of the interferon regulatory factor family that binds to the interferon-stimulated response element and activates expression of interferon-induced genes. Proc Natl Acad Sci U S A **92:**11657-61.

11. **Ball, J. M., P. Tian, C. Q. Zeng, A. P. Morris, and M. K. Estes.** 1996. Age-dependent diarrhea induced by a rotaviral nonstructural glycoprotein. Science **272:**101-4.

12. **Bar-Magen, T., E. Spencer, and J. T. Patton.** 2007. An ATPase activity associated with the rotavirus phosphoprotein NSP5. Virology **369:**389-99.

13. **Barro, M., and J. T. Patton.** 2005. Rotavirus nonstructural protein 1 subverts innate immune response by inducing degradation of IFN regulatory factor 3. Proc Natl Acad Sci U S A **102:**4114-9.

14. **Barro, M., and J. T. Patton.** 2007. Rotavirus NSP1 inhibits expression of type I interferon by antagonizing the function of interferon regulatory factors IRF3, IRF5, and IRF7. J Virol **81:**4473-81.

15. **Bass, D. M., M. R. Baylor, C. Chen, E. M. Mackow, M. Bremont, and H. B. Greenberg.** 1992. Liposome-mediated transfection of intact viral particles reveals that plasma membrane penetration determines permissivity of tissue culture cells to rotavirus. J Clin Invest **90:**2313-20.

16. **Bergmann, C. C., D. Maass, M. S. Poruchynsky, P. H. Atkinson, and A. R. Bellamy.** 1989. Topology of the non-structural rotavirus receptor glycoprotein NS28 in the rough endoplasmic reticulum. Embo J **8:**1695-703.

17. **Berkova, Z., S. E. Crawford, S. E. Blutt, A. P. Morris, and M. K. Estes.** 2007. Expression of rotavirus NSP4 alters the actin network organization through the actin remodeling protein cofilin. J Virol **81:**3545-53.

18. **Berois, M., C. Sapin, I. Erk, D. Poncet, and J. Cohen.** 2003. Rotavirus nonstructural protein NSP5 interacts with major core protein VP2. J Virol **77:**1757-63.

19. **Bishop, R. F., G. P. Davidson, I. H. Holmes, and B. J. Ruck.** 1973. Virus particles in epithelial cells of duodenal mucosa from children with acute non-bacterial gastroenteritis. Lancet **2:**1281-3.

20. **Blackhall, J., M. Munoz, A. Fuentes, and G. Magnusson.** 1998. Analysis of rotavirus nonstructural protein NSP5 phosphorylation. J Virol **72:**6398-405.

21. **Boutell, C., S. Sadis, and R. D. Everett.** 2002. Herpes simplex virus type 1 immediate-early protein ICP0 and is isolated RING finger domain act as ubiquitin E3 ligases in vitro. J Virol **76:**841-50.

22. **Boyce, M., C. C. Celma, and P. Roy.** 2008. Development of reverse genetics systems for bluetongue virus: recovery of infectious virus from synthetic RNA transcripts. J Virol **82:**8339-48.

23. **Boyce, M., and P. Roy.** 2007. Recovery of infectious bluetongue virus from RNA. J Virol **81:**2179-86.

24. **Brunet, J. P., J. Cotte-Laffitte, C. Linxe, A. M. Quero, M. Geniteau-Legendre, and A. Servin.** 2000. Rotavirus infection induces an increase in intracellular calcium concentration in human intestinal epithelial cells: role in microvillar actin alteration. J Virol **74:**2323-32.

25. **Butcher, S. J., J. M. Grimes, E. V. Makeyev, D. H. Bamford, and D. I. Stuart.** 2001. A mechanism for initiating RNA-dependent RNA polymerization. Nature **410:**235-40.

26. **Campagna, M., M. Budini, F. Arnoldi, U. Desselberger, J. E. Allende, and O. R. Burrone.** 2007. Impaired hyperphosphorylation of rotavirus NSP5 in cells depleted of casein kinase 1alpha is associated with the formation of viroplasms with altered morphology and a moderate decrease in virus replication. J Gen Virol **88:**2800-10.

27. **Campagna, M., C. Eichwald, F. Vascotto, and O. R. Burrone.** 2005. RNA interference of rotavirus segment 11 mRNA reveals the essential role of NSP5 in the virus replicative cycle. J Gen Virol **86:**1481-7.

28. **Carpio, R. V., F. D. Gonzalez-Nilo, H. Jayaram, E. Spencer, B. V. Prasad, J. T. Patton, and Z. F. Taraporewala.** 2004. Role of the histidine triad-like motif in nucleotide hydrolysis by the rotavirus RNA-packaging protein NSP2. J Biol Chem **279:**10624-33.

29. **Charpilienne, A., J. Lepault, F. Rey, and J. Cohen.** 2002. Identification of rotavirus VP6 residues located at the interface with VP2 that are essential for capsid assembly and transcriptase activity. J Virol **76:**7822-31.

30. **Chen, D., M. Barros, E. Spencer, and J. T. Patton.** 2001. Features of the 3'-consensus sequence of rotavirus mRNAs critical to minus strand synthesis. Virology **282:**221-9.

31. **Chen, D., C. L. Luongo, M. L. Nibert, and J. T. Patton.** 1999. Rotavirus open cores catalyze 5'-capping and methylation of exogenous RNA: evidence that VP3 is a methyltransferase. Virology **265:**120-30.

32. **Chen, D., and J. T. Patton.** 2000. De novo synthesis of minus strand RNA by the rotavirus RNA polymerase in a cell-free system involves a novel mechanism of initiation. Rna **6:**1455-67.

33. **Chen, D., and J. T. Patton.** 1998. Rotavirus RNA replication requires a single-stranded 3' end for efficient minus-strand synthesis. J Virol **72:**7387-96.

34. **Chen, D., C. Q. Zeng, M. J. Wentz, M. Gorziglia, M. K. Estes, and R. F. Ramig.** 1994. Template-dependent, in vitro replication of rotavirus RNA. J Virol **68:**7030-9.

35. **Chen, J. Z., E. C. Settembre, S. T. Aoki, X. Zhang, A. R. Bellamy, P. R. Dormitzer, S. C. Harrison, and N. Grigorieff.** 2009. Molecular interactions in rotavirus assembly and uncoating seen by high-resolution cryo-EM. Proc Natl Acad Sci U S A **106:**10644-8.

36. **Chen, Y. T., C. H. Lin, W. T. Ji, S. K. Li, and H. J. Liu.** 2008. Proteasome inhibition reduces avian reovirus replication and apoptosis induction in cultured cells. J Virol Methods **151:**95-100.

37. **Ciarlet, M., and M. K. Estes.** 1999. Human and most animal rotavirus strains do not require the presence of sialic acid on the cell surface for efficient infectivity. J Gen Virol **80 (Pt 4):**943-8.

38. **Cohen, J., J. Laporte, A. Charpilienne, and R. Scherrer.** 1979. Activation of rotavirus RNA polymerase by calcium chelation. Arch Virol **60:**177-86.

39. **Coscoy, L., D. J. Sanchez, and D. Ganem.** 2001. A novel class of herpesvirus-encoded membrane-bound E3 ubiquitin ligases regulates endocytosis of proteins involved in immune recognition. J Cell Biol **155:**1265-73.

40. **Cuadras, M. A., C. F. Arias, and S. Lopez.** 1997. Rotaviruses induce an early membrane permeabilization of MA104 cells and do not require a low intracellular Ca2+ concentration to initiate their replication cycle. J Virol **71:**9065-74.

41. **Cuadras, M. A., B. B. Bordier, J. L. Zambrano, J. E. Ludert, and H. B. Greenberg.** 2006. Dissecting rotavirus particle-raft interaction with small interfering RNAs: insights into rotavirus transit through the secretory pathway. J Virol **80:**3935-46.

42. **Cuadras, M. A., and H. B. Greenberg.** 2003. Rotavirus infectious particles use lipid rafts during replication for transport to the cell surface in vitro and in vivo. Virology **313:**308-21.

43. **Dector, M. A., P. Romero, S. Lopez, and C. F. Arias.** 2002. Rotavirus gene silencing by small interfering RNAs. EMBO Rep **3:**1175-80.

44. **Deepa, R., C. Durga Rao, and K. Suguna.** 2007. Structure of the extended diarrhea-inducing domain of rotavirus enterotoxigenic protein NSP4. Arch Virol **152:**847-59.

45. **Delmas, O., M. Breton, C. Sapin, A. Le Bivic, O. Colard, and G. Trugnan.** 2007. Heterogeneity of Raft-type membrane microdomains associated with VP4, the rotavirus spike protein, in Caco-2 and MA 104 cells. J Virol **81:**1610-8.

46. **Delmas, O., A. M. Durand-Schneider, J. Cohen, O. Colard, and G. Trugnan.** 2004. Spike protein VP4 assembly with maturing rotavirus requires a postendoplasmic reticulum event in polarized caco-2 cells. J Virol **78:**10987-94.

47. **Dennehy, P. H.** 2008. Rotavirus vaccines: an overview. Clin Microbiol Rev **21:**198-208.

48. **Deo, R. C., C. M. Groft, K. R. Rajashankar, and S. K. Burley.** 2002. Recognition of the rotavirus mRNA 3' consensus by an asymmetric NSP3 homodimer. Cell **108:**71-81.

49. **Desselberger, U., and M. A. McCrae.** 1994. The rotavirus genome. Curr Top Microbiol Immunol **185:**31-66.

50. **Dong, Y., C. Q. Zeng, J. M. Ball, M. K. Estes, and A. P. Morris.** 1997. The rotavirus enterotoxin NSP4 mobilizes intracellular calcium in human intestinal cells by stimulating phospholipase C-mediated inositol 1,4,5-trisphosphate production. Proc Natl Acad Sci U S A **94:**3960-5.

51. **Dormitzer, P. R., H. B. Greenberg, and S. C. Harrison.** 2000. Purified recombinant rotavirus VP7 forms soluble, calcium-dependent trimers. Virology **277:**420-8.

52. **Dormitzer, P. R., E. B. Nason, B. V. Prasad, and S. C. Harrison.** 2004. Structural rearrangements in the membrane penetration protein of a non-enveloped virus. Nature **430:**1053-8.

53. **Dormitzer, P. R., Z. Y. Sun, G. Wagner, and S. C. Harrison.** 2002. The rhesus rotavirus VP4 sialic acid binding domain has a galectin fold with a novel carbohydrate binding site. Embo J **21:**885-97.

54. **Eichwald, C., G. Jacob, B. Muszynski, J. E. Allende, and O. R. Burrone.** 2004. Uncoupling substrate and activation functions of rotavirus NSP5: phosphorylation of Ser-67 by casein kinase 1 is essential for hyperphosphorylation. Proc Natl Acad Sci U S A **101:**16304-9.

55. **Eichwald, C., J. F. Rodriguez, and O. R. Burrone.** 2004. Characterisation of rotavirus NSP2/NSP5 interaction and dynamics of viroplasms formation. J Gen Virol **85:**625-634.

56. **Eichwald, C., F. Vascotto, E. Fabbretti, and O. R. Burrone.** 2002. Rotavirus NSP5: mapping phosphorylation sites and kinase activation and viroplasm localization domains. J Virol **76:**3461-70.

57. **Estes, M.** 2001. Rotaviruses and their replication, p. 1747-1785. *In* D. Knipe and P. Howley (ed.), Fields Virology, fourth ed, vol. 2. Lippincott Williams and Wilkins, New York.

58. **Estes, M., Kapikian, A.** 2007. Rotaviruses, p. 1917-1974. *In* P. H. DM Knipe, et al (ed.), Fields Virology, 5th ed. Wolters Kluwer Health/Lippincott Williams & Wilkins, Philadelphia.

59. **Estes, M. K., D. Y. Graham, C. P. Gerba, and E. M. Smith.** 1979. Simian rotavirus SA11 replication in cell cultures. J Virol **31:**810-5.

60. **Fabbretti, E., I. Afrikanova, F. Vascotto, and O. R. Burrone.** 1999. Two non-structural rotavirus proteins, NSP2 and NSP5, form viroplasm-like structures in vivo. J Gen Virol **80 (Pt 2):**333-9.

61. **Ferrell, K., C. R. Wilkinson, W. Dubiel, and C. Gordon.** 2000. Regulatory subunit interactions of the 26S proteasome, a complex problem. Trends Biochem Sci **25:**83-8.

62. **Finley, D.** 2009. Recognition and processing of ubiquitin-protein conjugates by the proteasome. Annu Rev Biochem **78:**477-513.

63. **Fuerst, T. R., E. G. Niles, F. W. Studier, and B. Moss.** 1986. Eukaryotic transient-expression system based on recombinant vaccinia virus that synthesizes bacteriophage T7 RNA polymerase. Proc Natl Acad Sci U S A **83:**8122-6.

64. **Gallegos, C. O., and J. T. Patton.** 1989. Characterization of rotavirus replication intermediates: a model for the assembly of single-shelled particles. Virology **172:**616-27.

65. **Gardet, A., M. Breton, P. Fontanges, G. Trugnan, and S. Chwetzoff.** 2006. Rotavirus spike protein VP4 binds to and remodels actin bundles of the epithelial brush border into actin bodies. J Virol **80:**3947-56.

66. **Gonzalez, R. A., R. Espinosa, P. Romero, S. Lopez, and C. F. Arias.** 2000. Relative localization of viroplasmic and endoplasmic reticulum-resident rotavirus proteins in infected cells. Arch Virol **145:**1963-73.

67. **Gonzalez, S. A., and O. R. Burrone.** 1991. Rotavirus NS26 is modified by addition of single O-linked residues of N-acetylglucosamine. Virology **182:**8-16.

68. **Graff, J. W., K. Ettayebi, and M. E. Hardy.** 2009. Rotavirus NSP1 inhibits NFkappaB activation by inducing proteasome-dependent degradation of beta-TrCP: a novel mechanism of IFN antagonism. PLoS Pathog **5:**e1000280.

69. **Graff, J. W., J. Ewen, K. Ettayebi, and M. E. Hardy.** 2007. Zinc-binding domain of rotavirus NSP1 is required for proteasome-dependent degradation of IRF3 and autoregulatory NSP1 stability. J Gen Virol **88:**613-20.

70. **Graff, J. W., D. N. Mitzel, C. M. Weisend, M. L. Flenniken, and M. E. Hardy.** 2002. Interferon regulatory factor 3 is a cellular partner of rotavirus NSP1. J Virol **76:**9545-50.

71. **Graham, A., G. Kudesia, A. M. Allen, and U. Desselberger.** 1987. Reassortment of human rotavirus possessing genome rearrangements with bovine rotavirus: evidence for host cell selection. J Gen Virol **68 (Pt 1):**115-22.

72. **Graham, K. L., F. E. Fleming, P. Halasz, M. J. Hewish, H. S. Nagesha, I. H. Holmes, Y. Takada, and B. S. Coulson.** 2005. Rotaviruses interact with alpha4beta7 and alpha4beta1 integrins by binding the same integrin domains as natural ligands. J Gen Virol **86:**3397-408.

73. **Graham, K. L., P. Halasz, Y. Tan, M. J. Hewish, Y. Takada, E. R. Mackow, M. K. Robinson, and B. S. Coulson.** 2003. Integrin-using rotaviruses bind alpha2beta1 integrin alpha2 I domain via VP4 DGE sequence and recognize alphaXbeta2 and alphaVbeta3 by using VP7 during cell entry. J Virol **77:**9969-78.

74. **Graham, K. L., W. Zeng, Y. Takada, D. C. Jackson, and B. S. Coulson.** 2004. Effects on rotavirus cell binding and infection of monomeric and polymeric peptides containing alpha2beta1 and alphaxbeta2 integrin ligand sequences. J Virol **78:**11786-97.

75. **Greenberg, H. B., and M. K. Estes.** 2009. Rotaviruses: from pathogenesis to vaccination. Gastroenterology **136:**1939-51.

76. **Guerrero, C. A., D. Bouyssounade, S. Zarate, P. Isa, T. Lopez, R. Espinosa, P. Romero, E. Mendez, S. Lopez, and C. F. Arias.** 2002. Heat shock cognate protein 70 is involved in rotavirus cell entry. J Virol **76:**4096-102.

77. **Guerrero, C. A., E. Mendez, S. Zarate, P. Isa, S. Lopez, and C. F. Arias.** 2000. Integrin alpha(v)beta(3) mediates rotavirus cell entry. Proc Natl Acad Sci U S A **97:**14644-9.

78. **Guerrero, C. A., S. Zarate, G. Corkidi, S. Lopez, and C. F. Arias.** 2000. Biochemical characterization of rotavirus receptors in MA104 cells. J Virol **74:**9362-71.

79. **Guo, C. T., O. Nakagomi, M. Mochizuki, H. Ishida, M. Kiso, Y. Ohta, T. Suzuki, D. Miyamoto, K. I. Hidari, and Y. Suzuki.** 1999. Ganglioside GM(1a) on the cell surface is involved in the infection by human rotavirus KUN and MO strains. J Biochem (Tokyo) **126:**683-8.

80. **Hansen, T. H., and M. Bouvier.** 2009. MHC class I antigen presentation: learning from viral evasion strategies. Nat Rev Immunol **9:**503-13.

81. **Honda, K., H. Yanai, H. Negishi, M. Asagiri, M. Sato, T. Mizutani, N. Shimada, Y. Ohba, A. Takaoka, N. Yoshida, and T. Taniguchi.** 2005. IRF-7 is the master regulator of type-I interferon-dependent immune responses. Nature **434:**772-7.

82. **Hua, J., X. Chen, and J. T. Patton.** 1994. Deletion mapping of the rotavirus metalloprotein NS53 (NSP1): the conserved cysteine-rich region is essential for virus-specific RNA binding. J Virol **68:**3990-4000.

83. **Huang, Y. W., L. Li, and L. Yu.** 2004. [The reverse genetics systems for human and animal RNA viruses]. Sheng Wu Gong Cheng Xue Bao **20:**311-8.

84. **Hwang, L. N., N. Englund, T. Das, A. K. Banerjee, and A. K. Pattnaik.** 1999. Optimal replication activity of vesicular stomatitis virus RNA polymerase requires phosphorylation of a residue(s) at carboxy-terminal domain II of its accessory subunit, phosphoprotein P. J Virol **73:**5613-20.

85. **Isa, P., M. Realpe, P. Romero, S. Lopez, and C. F. Arias.** 2004. Rotavirus RRV associates with lipid membrane microdomains during cell entry. Virology **322:**370-81.

86. **Isaacson, M. K., and H. L. Ploegh.** 2009. Ubiquitination, ubiquitin-like modifiers, and deubiquitination in viral infection. Cell Host Microbe **5:**559-70.

87. **Iturriza-Gomara, M., J. Green, D. W. Brown, U. Desselberger, and J. J. Gray.** 1999. Comparison of specific and random priming in the reverse transcriptase polymerase chain reaction for genotyping group A rotaviruses. J Virol Methods **78:**93-103.

88. **Jagannath, M. R., M. M. Kesavulu, R. Deepa, P. N. Sastri, S. S. Kumar, K. Suguna, and C. D. Rao.** 2006. N- and C-terminal cooperation in rotavirus enterotoxin: novel mechanism of modulation of the properties of a multifunctional protein by a structurally and functionally overlapping conformational domain. J Virol **80:**412-25.

89. **Jayaram, H., M. K. Estes, and B. V. Prasad.** 2004. Emerging themes in rotavirus cell entry, genome organization, transcription and replication. Virus Res **101:**67-81.

90. **Jayaram, H., Z. Taraporewala, J. T. Patton, and B. V. Prasad.** 2002. Rotavirus protein involved in genome replication and packaging exhibits a HIT-like fold. Nature **417:**311-5.

91. **Jiang, X., H. Jayaram, M. Kumar, S. J. Ludtke, M. K. Estes, and B. V. Prasad.** 2006. Cryoelectron microscopy structures of rotavirus NSP2-NSP5 and NSP2-RNA complexes: implications for genome replication. J Virol **80:**10829-35.

92. **Jourdan, N., M. Maurice, D. Delautier, A. M. Quero, A. L. Servin, and G. Trugnan.** 1997. Rotavirus is released from the apical surface of cultured human intestinal cells through nonconventional vesicular transport that bypasses the Golgi apparatus. J Virol **71:**8268-78.

93. **Jung, T., B. Catalgol, and T. Grune.** 2009. The proteasomal system. Mol Aspects Med **30:**191-296.

94. **Kaljot, K. T., R. D. Shaw, D. H. Rubin, and H. B. Greenberg.** 1988. Infectious rotavirus enters cells by direct cell membrane penetration, not by endocytosis. J Virol **62:**1136-44.

95. **Kar, A. K., M. Ghosh, and P. Roy.** 2004. Mapping the assembly pathway of Bluetongue virus scaffolding protein VP3. Virology **324:**387-99.

96. **Kattoura, M. D., X. Chen, and J. T. Patton.** 1994. The rotavirus RNA-binding protein NS35 (NSP2) forms 10S multimers and interacts with the viral RNA polymerase. Virology **202:**803-13.

97. **Keljo, D. J., and A. K. Smith.** 1988. Characterization of binding of simian rotavirus SA-11 to cultured epithelial cells. J Pediatr Gastroenterol Nutr **7:**249-56.

98. **Kenniston, J. A., T. A. Baker, J. M. Fernandez, and R. T. Sauer.** 2003. Linkage between ATP consumption and mechanical unfolding during the protein processing reactions of an AAA+ degradation machine. Cell **114:**511-20.

99. **Khor, R., L. J. McElroy, and G. R. Whittaker.** 2003. The ubiquitin-vacuolar protein sorting system is selectively required during entry of influenza virus into host cells. Traffic **4:**857-68.

100. **Kikkert, M., G. Hassink, M. Barel, C. Hirsch, F. J. van der Wal, and E. Wiertz.** 2001. Ubiquitination is essential for human cytomegalovirus US11-mediated dislocation of MHC class I molecules from the endoplasmic reticulum to the cytosol. Biochem J **358:**369-77.

101. **Kobayashi, T., A. A. Antar, K. W. Boehme, P. Danthi, E. A. Eby, K. M. Guglielmi, G. H. Holm, E. M. Johnson, M. S. Maginnis, S. Naik, W. B. Skelton, J. D. Wetzel, G. J. Wilson, J. D. Chappell, and T. S. Dermody.** 2007. A plasmid-based reverse genetics system for animal double-stranded RNA viruses. Cell Host Microbe **1:**147-57.

102. **Komoto, S., M. Kugita, J. Sasaki, and K. Taniguchi.** 2008. Generation of recombinant rotavirus with an antigenic mosaic of cross-reactive neutralization epitopes on VP4. J Virol **82:**6753-7.

103. **Kraut, D. A., S. Prakash, and A. Matouschek.** 2007. To degrade or release: ubiquitin-chain remodeling. Trends Cell Biol **17:**419-21.

104. **Kumar, M., H. Jayaram, R. Vasquez-Del Carpio, X. Jiang, Z. F. Taraporewala, R. H. Jacobson, J. T. Patton, and B. V. Prasad.** 2007. Crystallographic and biochemical analysis of rotavirus NSP2 with nucleotides reveals a nucleoside diphosphate kinase-like activity. J Virol **81:**12272-84.

105. **Labbe, M., P. Baudoux, A. Charpilienne, D. Poncet, and J. Cohen.** 1994. Identification of the nucleic acid binding domain of the rotavirus VP2 protein. J Gen Virol **75 (Pt 12):**3423-30.

106. **LaMonica, R., S. S. Kocer, J. Nazarova, W. Dowling, E. Geimonen, R. D. Shaw, and E. R. Mackow.** 2001. VP4 differentially regulates TRAF2 signaling, disengaging JNK activation while directing NF-kappa B to effect rotavirus-specific cellular responses. J Biol Chem **276:**19889-96.

107. **Lawton, J. A., M. K. Estes, and B. V. Prasad.** 1999. Comparative structural analysis of transcriptionally competent and incompetent rotavirus-antibody complexes. Proc Natl Acad Sci U S A **96:**5428-33.

108. **Lawton, J. A., M. K. Estes, and B. V. Prasad.** 2001. Identification and characterization of a transcription pause site in rotavirus. J Virol **75:**1632-42.

109. **Lawton, J. A., C. Q. Zeng, S. K. Mukherjee, J. Cohen, M. K. Estes, and B. V. Prasad.** 1997. Three-dimensional structural analysis of recombinant rotavirus-like particles with intact and amino-terminal-deleted VP2: implications for the architecture of the VP2 capsid layer. J Virol **71:**7353-60.

110. **Le, H., R. L. Tanguay, M. L. Balasta, C. C. Wei, K. S. Browning, A. M. Metz, D. J. Goss, and D. R. Gallie.** 1997. Translation initiation factors eIF-iso4G and eIF-4B interact with the poly(A)-binding protein and increase its RNA binding activity. J Biol Chem **272:**16247-55.

111. **Lee, D. H., and A. L. Goldberg.** 1998. Proteasome inhibitors: valuable new tools for cell biologists. Trends Cell Biol **8:**397-403.

112. **Li, Z., M. L. Baker, W. Jiang, M. K. Estes, and B. V. Prasad.** 2009. Rotavirus architecture at subnanometer resolution. J Virol **83:**1754-66.

113. **Liu, J., L. Wei, T. Jiang, L. Shi, and J. Wang.** 2007. Reduction of infectious bursal disease virus replication in cultured cells by proteasome inhibitors. Virus Genes **35:**719-27.

114. **Liu, M., N. M. Mattion, and M. K. Estes.** 1992. Rotavirus VP3 expressed in insect cells possesses guanylyltransferase activity. Virology **188:**77-84.

115. **Lopez, S., and C. F. Arias.** 2006. Early steps in rotavirus cell entry. Curr Top Microbiol Immunol **309:**39-66.

116. **Lopez, S., and C. F. Arias.** 2004. Multistep entry of rotavirus into cells: a Versaillesque dance. Trends Microbiol **12:**271-8.

117. **Lopez, T., M. Camacho, M. Zayas, R. Najera, R. Sanchez, C. F. Arias, and S. Lopez.** 2005. Silencing the morphogenesis of rotavirus. J Virol **79:**184-92.

118. **Lu, X., S. M. McDonald, M. A. Tortorici, Y. J. Tao, R. Vasquez-Del Carpio, M. L. Nibert, J. T. Patton, and S. C. Harrison.** 2008. Mechanism for coordinated RNA packaging and genome replication by rotavirus polymerase VP1. Structure **16:**1678-88.

119. **Lundgren, O., A. T. Peregrin, K. Persson, S. Kordasti, I. Uhnoo, and L. Svensson.** 2000. Role of the enteric nervous system in the fluid and electrolyte secretion of rotavirus diarrhea. Science **287:**491-5.

120. **Maass, D. R., and P. H. Atkinson.** 1990. Rotavirus proteins VP7, NS28, and VP4 form oligomeric structures. J Virol **64:**2632-41.

121. **Mansell, E. A., and J. T. Patton.** 1990. Rotavirus RNA replication: VP2, but not VP6, is necessary for viral replicase activity. J Virol **64:**4988-96.

122. **Matthijnssens, J., M. Ciarlet, E. Heiman, I. Arijs, T. Delbeke, S. M. McDonald, E. A. Palombo, M. Iturriza-Gomara, P. Maes, J. T. Patton, M. Rahman, and M. Van Ranst.** 2008. Full Genome-Based Classification of Rotaviruses Reveals Common Origin between Human Wa-like and Porcine rotavirus strains and Human DS-1-like and Bovine Rotavirus strains. J Virol.

123. **Michelangeli, F., F. Liprandi, M. E. Chemello, M. Ciarlet, and M. C. Ruiz.** 1995. Selective depletion of stored calcium by thapsigargin blocks rotavirus maturation but not the cytopathic effect. J Virol **69:**3838-47.

124. **Mir, K. D., R. D. Parr, F. Schroeder, and J. M. Ball.** 2007. Rotavirus NSP4 interacts with both the amino- and carboxyl-termini of caveolin-1. Virus Res **126:**106-15.

125. **Mirazimi, A., M. Nilsson, and L. Svensson.** 1998. The molecular chaperone calnexin interacts with the NSP4 enterotoxin of rotavirus in vivo and in vitro. J Virol **72:**8705-9.

126. **Mitchell, D. B., and G. W. Both.** 1990. Completion of the genomic sequence of the simian rotavirus SA11: nucleotide sequences of segments 1, 2, and 3. Virology **177:**324-31.

127. **Mohan, K. V., J. Muller, and C. D. Atreya.** 2003. The N- and C-terminal regions of rotavirus NSP5 are the critical determinants for the formation of viroplasm-like structures independent of NSP2. J Virol **77:**12184-92.

128. **Montero, H., C. F. Arias, and S. Lopez.** 2006. Rotavirus Nonstructural Protein NSP3 is not required for viral protein synthesis. J Virol **80:**9031-8.

129. **Montero, H., M. Rojas, C. F. Arias, and S. Lopez.** 2008. Rotavirus infection induces the phosphorylation of eIF2alpha but prevents the formation of stress granules. J Virol **82:**1496-504.

130. **Moore, B. S., A. S. Eustaquio, and R. P. McGlinchey.** 2008. Advances in and applications of proteasome inhibitors. Curr Opin Chem Biol **12:**434-40.

131. **Morris, A. P., J. K. Scott, J. M. Ball, C. Q. Zeng, W. K. O'Neal, and M. K. Estes.** 1999. NSP4 elicits age-dependent diarrhea and Ca(2+)mediated I(-) influx into intestinal crypts of CF mice. Am J Physiol **277:**G431-44.

132. **Nandi, P., A. Charpilienne, and J. Cohen.** 1992. Interaction of rotavirus particles with liposomes. J Virol **66:**3363-7.

133. **Navon, A., and A. L. Goldberg.** 2001. Proteins are unfolded on the surface of the ATPase ring before transport into the proteasome. Mol Cell **8:**1339-49.

134. **Parr, R. D., S. M. Storey, D. M. Mitchell, A. L. McIntosh, M. Zhou, K. D. Mir, and J. M. Ball.** 2006. The rotavirus enterotoxin NSP4 directly interacts with the caveolar structural protein caveolin-1. J Virol **80:**2842-54.

135. **Patton, J., V. Chizhikov, Z. Taraporewala, and D.Y. Chen.** 2000. Virus replication. Rotaviruses. Methods and Protocols (J.Gray and U. Desselberger, Eds.). Humana Press, Totowa, NJ.**:**33-66.

136. **Patton, J. T.** 1996. Rotavirus VP1 alone specifically binds to the 3' end of viral mRNA, but the interaction is not sufficient to initiate minus-strand synthesis. J Virol **70:**7940-7.

137. **Patton, J. T.** 1986. Synthesis of simian rotavirus SA11 double-stranded RNA in a cell-free system. Virus Res **6:**217-33.

138. **Patton, J. T., and D. Chen.** 1999. RNA-binding and capping activities of proteins in rotavirus open cores. J Virol **73:**1382-91.

139. **Patton, J. T., and C. O. Gallegos.** 1990. Rotavirus RNA replication: single-stranded RNA extends from the replicase particle. J Gen Virol **71 (Pt 5):**1087-94.

140. **Patton, J. T., and C. O. Gallegos.** 1988. Structure and protein composition of the rotavirus replicase particle. Virology **166:**358-65.

141. **Patton, J. T., M. T. Jones, A. N. Kalbach, Y. W. He, and J. Xiaobo.** 1997. Rotavirus RNA polymerase requires the core shell protein to synthesize the double-stranded RNA genome. J Virol **71:**9618-26.

142. **Patton, J. T., and E. Spencer.** 2000. Genome replication and packaging of segmented double-stranded RNA viruses. Virology **277:**217-25.

143. **Patton, J. T., Z. Taraporewala, D. Chen, V. Chizhikov, M. Jones, A. Elhelu, M. Collins, K. Kearney, M. Wagner, Y. Hoshino, and V. Gouvea.** 2001. Effect of intragenic rearrangement and changes in the 3' consensus sequence on NSP1 expression and rotavirus replication. J Virol **75:**2076-86.

144. **Patton, J. T., R. Vasquez-Del Carpio, M. A. Tortorici, and Z. F. Taraporewala.** 2007. Coupling of rotavirus genome replication and capsid assembly. Adv Virus Res **69:**167-201.

145. **Patton, J. T., M. Wentz, J. Xiaobo, and R. F. Ramig.** 1996. cis-Acting signals that promote genome replication in rotavirus mRNA. J Virol **70:**3961-71.

146. **Petrie, B. L., D. Y. Graham, H. Hanssen, and M. K. Estes.** 1982. Localization of rotavirus antigens in infected cells by ultrastructural immunocytochemistry. J Gen Virol **63:**457-67.

147. **Petrie, B. L., H. B. Greenberg, D. Y. Graham, and M. K. Estes.** 1984. Ultrastructural localization of rotavirus antigens using colloidal gold. Virus Res **1:**133-52.

148. **Pim, D., P. Massimi, S. M. Dilworth, and L. Banks.** 2005. Activation of the protein kinase B pathway by the HPV-16 E7 oncoprotein occurs through a mechanism involving interaction with PP2A. Oncogene **24:**7830-8.

149. **Pina-Vazquez, C., M. De Nova-Ocampo, S. Guzman-Leon, and L. Padilla-Noriega.** 2007. Post-translational regulation of rotavirus protein NSP1 expression in mammalian cells. Arch Virol **152:**345-68.

150. **Pinto, R. M., J. M. Diez, and A. Bosch.** 1994. Use of the colonic carcinoma cell line CaCo-2 for in vivo amplification and detection of enteric viruses. J Med Virol **44:**310-5.

151. **Piron, M., T. Delaunay, J. Grosclaude, and D. Poncet.** 1999. Identification of the RNA-binding, dimerization, and eIF4GI-binding domains of rotavirus nonstructural protein NSP3. J Virol **73:**5411-21.

152. **Piron, M., P. Vende, J. Cohen, and D. Poncet.** 1998. Rotavirus RNA-binding protein NSP3 interacts with eIF4GI and evicts the poly(A) binding protein from eIF4F. Embo J **17:**5811-21.

153. **Pizarro, J. L., A. M. Sandino, J. M. Pizarro, J. Fernandez, and E. Spencer.** 1991. Characterization of rotavirus guanylyltransferase activity associated with polypeptide VP3. J Gen Virol **72 (Pt 2):**325-32.

154. **Poncet, D., C. Aponte, and J. Cohen.** 1993. Rotavirus protein NSP3 (NS34) is bound to the 3' end consensus sequence of viral mRNAs in infected cells. J Virol **67:**3159-65.

155. **Poncet, D., S. Laurent, and J. Cohen.** 1994. Four nucleotides are the minimal requirement for RNA recognition by rotavirus non-structural protein NSP3. Embo J **13:**4165-73.

156. **Poruchynsky, M. S., and P. H. Atkinson.** 1991. Rotavirus protein rearrangements in purified membrane-enveloped intermediate particles. J Virol **65:**4720-7.

157. **Poruchynsky, M. S., D. R. Maass, and P. H. Atkinson.** 1991. Calcium depletion blocks the maturation of rotavirus by altering the oligomerization of virus-encoded proteins in the ER. J Cell Biol **114:**651-6.

158. **Prasad, B. V., J. W. Burns, E. Marietta, M. K. Estes, and W. Chiu.** 1990. Localization of VP4 neutralization sites in rotavirus by three-dimensional cryo-electron microscopy. Nature **343:**476-9.

159. **Prasad, B. V., R. Rothnagel, C. Q. Zeng, J. Jakana, J. A. Lawton, W. Chiu, and M. K. Estes.** 1996. Visualization of ordered genomic RNA and localization of transcriptional complexes in rotavirus. Nature **382:**471-3.

160. **Prasad, B. V., G. J. Wang, J. P. Clerx, and W. Chiu.** 1988. Three-dimensional structure of rotavirus. J Mol Biol **199:**269-75.

161. **Prosch, S., C. Priemer, C. Hoflich, C. Liebenthaf, N. Babel, D. H. Kruger, and H. D. Volk.** 2003. Proteasome inhibitors: a novel tool to suppress human cytomegalovirus replication and virus-induced immune modulation. Antivir Ther **8:**555-67.

162. **Querido, E., P. Blanchette, Q. Yan, T. Kamura, M. Morrison, D. Boivin, W. G. Kaelin, R. C. Conaway, J. W. Conaway, and P. E. Branton.** 2001. Degradation of p53 by adenovirus E4orf6 and E1B55K proteins occurs via a novel mechanism involving a Cullin-containing complex. Genes Dev **15:**3104-17.

163. **Rainsford, E. W., and M. A. McCrae.** 2007. Characterization of the NSP6 protein product of rotavirus gene 11. Virus Res **130:**193-201.

164. **Randall, R. E., and S. Goodbourn.** 2008. Interferons and viruses: an interplay between induction, signalling, antiviral responses and virus countermeasures. J Gen Virol **89:**1-47.

165. **Randow, F., and P. J. Lehner.** 2009. Viral avoidance and exploitation of the ubiquitin system. Nat Cell Biol **11:**527-34.

166. **Rolsma, M. D., T. B. Kuhlenschmidt, H. B. Gelberg, and M. S. Kuhlenschmidt.** 1998. Structure and function of a ganglioside receptor for porcine rotavirus. J Virol **72:**9079-91.

167. **Ros, C., and C. Kempf.** 2004. The ubiquitin-proteasome machinery is essential for nuclear translocation of incoming minute virus of mice. Virology **324:**350-60.

168. **Rosenzweig, R., P. A. Osmulski, M. Gaczynska, and M. H. Glickman.** 2008. The central unit within the 19S regulatory particle of the proteasome. Nat Struct Mol Biol **15:**573-80.

169. **Ruiz, M. C., M. J. Abad, A. Charpilienne, J. Cohen, and F. Michelangeli.** 1997. Cell lines susceptible to infection are permeabilized by cleaved and solubilized outer layer proteins of rotavirus. J Gen Virol **78 (Pt 11):**2883-93.

170. **Ruiz, M. C., A. Charpilienne, F. Liprandi, R. Gajardo, F. Michelangeli, and J. Cohen.** 1996. The concentration of Ca2+ that solubilizes outer capsid proteins from rotavirus particles is dependent on the strain. J Virol **70:**4877-83.

171. **Sanchez-San Martin, C., T. Lopez, C. F. Arias, and S. Lopez.** 2004. Characterization of rotavirus cell entry. J Virol **78:**2310-8.

172. **Sapin, C., O. Colard, O. Delmas, C. Tessier, M. Breton, V. Enouf, S. Chwetzoff, J. Ouanich, J. Cohen, C. Wolf, and G. Trugnan.** 2002. Rafts promote assembly

and atypical targeting of a nonenveloped virus, rotavirus, in Caco-2 cells. J Virol **76:**4591-602.

173. **Scheffner, M., B. A. Werness, J. M. Huibregtse, A. J. Levine, and P. M. Howley.** 1990. The E6 oncoprotein encoded by human papillomavirus types 16 and 18 promotes the degradation of p53. Cell **63:**1129-36.

174. **Schmid, S., D. Mayer, U. Schneider, and M. Schwemmle.** 2007. Functional characterization of the major and minor phosphorylation sites of the P protein of Borna disease virus. J Virol **81:**5497-507.

175. **Schubert, U., L. C. Anton, I. Bacik, J. H. Cox, S. Bour, J. R. Bennink, M. Orlowski, K. Strebel, and J. W. Yewdell.** 1998. CD4 glycoprotein degradation induced by human immunodeficiency virus type 1 Vpu protein requires the function of proteasomes and the ubiquitin-conjugating pathway. J Virol **72:**2280-8.

176. **Schubert, U., D. E. Ott, E. N. Chertova, R. Welker, U. Tessmer, M. F. Princiotta, J. R. Bennink, H. G. Krausslich, and J. W. Yewdell.** 2000. Proteasome inhibition interferes with gag polyprotein processing, release, and maturation of HIV-1 and HIV-2. Proc Natl Acad Sci U S A **97:**13057-62.

177. **Sen, A., N. Feng, K. Ettayebi, M. E. Hardy, and H. B. Greenberg.** 2009. IRF3 inhibition by rotavirus NSP1 is host cell and virus strain dependent but independent of NSP1 proteasomal degradation. J Virol **83:**10322-35.

178. **Sen, A., N. Sen, and E. R. Mackow.** 2007. The formation of viroplasm-like structures by the rotavirus NSP5 protein is calcium regulated and directed by a C-terminal helical domain. J Virol **81:**11758-67.

179. **Seo, N. S., C. Q. Zeng, J. M. Hyser, B. Utama, S. E. Crawford, K. J. Kim, M. Hook, and M. K. Estes.** 2008. Inaugural article: integrins alpha1beta1 and alpha2beta1 are receptors for the rotavirus enterotoxin. Proc Natl Acad Sci U S A **105:**8811-8.

180. **Silvestri, L. S., Z. F. Taraporewala, and J. T. Patton.** 2004. Rotavirus replication: plus-sense templates for double-stranded RNA synthesis are made in viroplasms. J Virol **78:**7763-74.

181. **Silvestri, L. S., M. A. Tortorici, R. Vasquez-Del Carpio, and J. T. Patton.** 2005. Rotavirus glycoprotein NSP4 is a modulator of viral transcription in the infected cell. J Virol **79:**15165-74.

182. **Smith, D. M., S. C. Chang, S. Park, D. Finley, Y. Cheng, and A. L. Goldberg.** 2007. Docking of the proteasomal ATPases' carboxyl termini in the 20S proteasome's alpha ring opens the gate for substrate entry. Mol Cell **27:**731-44.

183. **Spencer, E., and M. L. Arias.** 1981. In vitro transcription catalyzed by heat-treated human rotavirus. J Virol **40:**1-10.

184. **Stacy-Phipps, S., and J. T. Patton.** 1987. Synthesis of plus- and minus-strand RNA in rotavirus-infected cells. J Virol **61:**3479-84.

185. **Storey, S. M., T. F. Gibbons, C. V. Williams, R. D. Parr, F. Schroeder, and J. M. Ball.** 2007. Full-length, glycosylated NSP4 is localized to plasma membrane caveolae by a novel raft isolation technique. J Virol **81:**5472-83.

186. **Tanaka, K.** 2009. The proteasome: overview of structure and functions. Proc Jpn Acad Ser B Phys Biol Sci **85:**12-36.

187. **Tao, Y., D. L. Farsetta, M. L. Nibert, and S. C. Harrison.** 2002. RNA synthesis in a cage--structural studies of reovirus polymerase lambda3. Cell **111:**733-45.

188. **Taraporewala, Z., D. Chen, and J. T. Patton.** 1999. Multimers formed by the rotavirus nonstructural protein NSP2 bind to RNA and have nucleoside triphosphatase activity. J Virol **73:**9934-43.

189. **Taraporewala, Z. F., X. Jiang, R. Vasquez-Del Carpio, H. Jayaram, B. V. Prasad, and J. T. Patton.** 2006. Structure-function analysis of rotavirus NSP2 octamer by using a novel complementation system. J Virol **80:**7984-94.

190. **Taraporewala, Z. F., and J. T. Patton.** 2001. Identification and characterization of the helix-destabilizing activity of rotavirus nonstructural protein NSP2. J Virol **75:**4519-27.

191. **Taraporewala, Z. F., and J. T. Patton.** 2004. Nonstructural proteins involved in genome packaging and replication of rotaviruses and other members of the Reoviridae. Virus Res **101:**57-66.

192. **Thouvenin, E., G. Schoehn, F. Rey, I. Petitpas, M. Mathieu, M. C. Vaney, J. Cohen, E. Kohli, P. Pothier, and E. Hewat.** 2001. Antibody inhibition of the transcriptase activity of the rotavirus DLP: a structural view. J Mol Biol **307:**161-72.

193. **Tian, P., J. M. Ball, C. Q. Zeng, and M. K. Estes.** 1996. The rotavirus nonstructural glycoprotein NSP4 possesses membrane destabilization activity. J Virol **70:**6973-81.

194. **Tian, P., Y. Hu, W. P. Schilling, D. A. Lindsay, J. Eiden, and M. K. Estes.** 1994. The nonstructural glycoprotein of rotavirus affects intracellular calcium levels. J Virol **68:**251-7.

195. **Torres-Vega, M. A., R. A. Gonzalez, M. Duarte, D. Poncet, S. Lopez, and C. F. Arias.** 2000. The C-terminal domain of rotavirus NSP5 is essential for its multimerization, hyperphosphorylation and interaction with NSP6. J Gen Virol **81:**821-30.

196. **Tortorici, M. A., T. J. Broering, M. L. Nibert, and J. T. Patton.** 2003. Template recognition and formation of initiation complexes by the replicase of a segmented double-stranded RNA virus. J Biol Chem **278:**32673-82.

197. **Tortorici, M. A., B. A. Shapiro, and J. T. Patton.** 2006. A base-specific recognition signal in the 5' consensus sequence of rotavirus plus-strand RNAs promotes replication of the double-stranded RNA genome segments. Rna **12:**133-46.

198. **Trask, S. D., and P. R. Dormitzer.** 2006. Assembly of highly infectious rotavirus particles recoated with recombinant outer capsid proteins. J Virol **80:**11293-304.

199. **Unno, M., T. Mizushima, Y. Morimoto, Y. Tomisugi, K. Tanaka, N. Yasuoka, and T. Tsukihara.** 2002. The structure of the mammalian 20S proteasome at 2.75 A resolution. Structure **10:**609-18.

200. **Vasquez-Del Carpio, R., F. D. Gonzalez-Nilo, G. Riadi, Z. F. Taraporewala, and J. T. Patton.** 2006. Histidine triad-like motif of the rotavirus NSP2 octamer mediates both RTPase and NTPase activities. J Mol Biol **362:**539-54.

201. **Vasquez, M., A. M. Sandino, J. M. Pizarro, J. Fernandez, S. Valenzuela, and E. Spencer.** 1993. Function of rotavirus VP3 polypeptide in viral morphogenesis. J Gen Virol **74 (Pt 5):**937-41.

202. **Vende, P., Z. F. Taraporewala, and J. T. Patton.** 2002. RNA-binding activity of the rotavirus phosphoprotein NSP5 includes affinity for double-stranded RNA. J Virol **76:**5291-9.

203. **Vende, P., M. A. Tortorici, Z. F. Taraporewala, and J. T. Patton.** 2003. Rotavirus NSP2 interferes with the core lattice protein VP2 in initiation of minus-strand synthesis. Virology **313:**261-73.

204. **Wang, Y., P. H. Dennehy, H. L. Keyserling, K. Tang, J. R. Gentsch, R. I. Glass, and B. Jiang.** 2007. Rotavirus infection alters peripheral T-cell homeostasis in children with acute diarrhea. J Virol **81:**3904-12.

205. **Whitby, F. G., E. I. Masters, L. Kramer, J. R. Knowlton, Y. Yao, C. C. Wang, and C. P. Hill.** 2000. Structural basis for the activation of 20S proteasomes by 11S regulators. Nature **408:**115-20.

206. **Wiertz, E. J., T. R. Jones, L. Sun, M. Bogyo, H. J. Geuze, and H. L. Ploegh.** 1996. The human cytomegalovirus US11 gene product dislocates MHC class I heavy chains from the endoplasmic reticulum to the cytosol. Cell **84:**769-79.

207. **Xu, A., A. R. Bellamy, and J. A. Taylor.** 2000. Immobilization of the early secretory pathway by a virus glycoprotein that binds to microtubules. Embo J **19:**6465-74.

208. **Xu, P., D. M. Duong, N. T. Seyfried, D. Cheng, Y. Xie, J. Robert, J. Rush, M. Hochstrasser, D. Finley, and J. Peng.** 2009. Quantitative proteomics reveals the function of unconventional ubiquitin chains in proteasomal degradation. Cell **137:**133-45.

209. **Yeager, M., J. A. Berriman, T. S. Baker, and A. R. Bellamy.** 1994. Three-dimensional structure of the rotavirus haemagglutinin VP4 by cryo-electron microscopy and difference map analysis. Embo J **13:**1011-8.

210. **Yeager, M., K. A. Dryden, N. H. Olson, H. B. Greenberg, and T. S. Baker.** 1990. Three-dimensional structure of rhesus rotavirus by cryoelectron microscopy and image reconstruction. J Cell Biol **110:**2133-44.

211. **Yoder, J. D., and P. R. Dormitzer.** 2006. Alternative intermolecular contacts underlie the rotavirus VP5* two- to three-fold rearrangement. Embo J **25:**1559-68.

212. **Yu, G. Y., and M. M. Lai.** 2005. The ubiquitin-proteasome system facilitates the transfer of murine coronavirus from endosome to cytoplasm during virus entry. J Virol **79:**644-8.

213. **Yu, X., Y. Yu, B. Liu, K. Luo, W. Kong, P. Mao, and X. F. Yu.** 2003. Induction of APOBEC3G ubiquitination and degradation by an HIV-1 Vif-Cul5-SCF complex. Science **302:**1056-60.

214. **Zeng, C. Q., M. J. Wentz, J. Cohen, M. K. Estes, and R. F. Ramig.** 1996. Characterization and replicase activity of double-layered and single-layered rotavirus-like particles expressed from baculovirus recombinants. J Virol **70:**2736-42.

215. **Zhang, M., C. Q. Zeng, Y. Dong, J. M. Ball, L. J. Saif, A. P. Morris, and M. K. Estes.** 1998. Mutations in rotavirus nonstructural glycoprotein NSP4 are associated with altered virus virulence. J Virol **72:**3666-72.

216. **Zhang, M., C. Q. Zeng, A. P. Morris, and M. K. Estes.** 2000. A functional NSP4 enterotoxin peptide secreted from rotavirus-infected cells. J Virol **74:**11663-70.